NASA CR-159525
PWA-5512-35

NASA

PERFORMANCE DETERIORATION
BASED ON IN-SERVICE ENGINE DATA

JT9D JET ENGINE DIAGNOSTICS PROGRAM

G. P. Sallee

UNITED TECHNOLOGIES CORPORATION
Pratt & Whitney Aircraft Group
Commercial Products Division

Prepared for

NATIONAL AERONAUTICS AND SPACE ADMINISTRATION

Lewis Research Center
Cleveland, Ohio 44135

Contract NAS3-20632

PREFACE

The requirements of NASA Policy Directive
NPD 2220.4 (September 14, 1970) regarding
the use of SI Units have been waived in ac-
cordance with the provisions of paragraph
5d of that Directive by the Director of
Lewis Research Center.

PRATT & WHITNEY AIRCRAFT GROUP

Commercial Products Division

East Hartford, Connecticut 06108

In reply please refer to:
GPS:EG:1585G - Eng. 3NJ
Ref. No. PWA-5512-35B

June 23, 1980

To: National Aeronautics and Space Administration
                Lewis Research Center
                21000 Brookpark Road
                Cleveland, Ohio   44135

Attention: Mr. Joseph A. Ziemianski, Project Manager, MS 301-4

Subject: Submittal of Approved Report on "Performance
                Deterioration Based on In-Service Engine Data";
                JT9D Jet Engine Diagnostics Program, Task II;
                Report No. CR-159525 (PWA-5512-35)

References: (A) NASA Letter of Approval, Ref. 2312, dated May
                    29, 1980; J. A. Ziemianski to G. P. Sallee

                (B) Contract NAS3-20632

Gentlemen:

Enclosed herewith are three copies of the subject report which has
been modified according to instructions in the Reference (A) letter.
All other distribution is being made in accordance with NASA
instructions previously received by Pratt & Whitney Aircraft. The
subject report presents the results of studies of in-service JT9D
engine performance deterioration conducted under Task II of the
Reference (B) contract and completes the activity related to this
phase of the program.

Sincerely yours,

UNITED TECHNOLOGIES CORPORATION
Pratt & Whitney Aircraft Group
Commercial Products Division

G. P. Sallee
Program Manager

cc: Administrative Contracting Officer (letter only)
      Air Force Plant Representative Office
      UTC/Pratt & Whitney Aircraft Group
      East Hartford, Connecticut 06108

**UNITED
TECHNOLOGIES**

TABLE OF CONTENTS

TABLE OF CONTENTS (Cont'd.)

TABLE OF CONTENTS (Cont'd.)

LIST OF ILLUSTRATIONS

LIST OF ILLUSTRATIONS (Continued)

LIST OF ILLUSTRATIONS (Continued)

LIST OF ILLUSTRATIONS (Continued)

LIST OF ILLUSTRATIONS (Continued)

LIST OF TABLES

SECTION 1.0

SUMMARY

This report presents the results of an investigation conducted from February 1977 to February 1979 of in-service JT9D engine performance deterioration under the NASA JT9D Jet Engine Diagnostics Program. The primary purpose of this effort was to generate new data under known conditions to permit a more accurate definition of JT9D engine performance deterioration trends and levels. The in-service fleet of 32 JT9D engines utilized in Pan American's fleet of 747 Special Performance aircraft was selected for this purpose. The selection of this engine fleet provided the opportunity of obtaining engine performance data starting before the first flight and continuing through initial service such that the trend and levels of engine deterioration related to both short- and long-term deterioration could be more carefully defined. The performance data collected and analyzed included flight, special ground test using a Plug-In Console (PIC), and test stand prerepair and postrepair performance calibrations. The results of the analyses of these data were used to:

    o   Refine preliminary models of performance deterioration, established in an earlier study conducted under the NASA JT9D Engine Diagnostics Program by filling in gaps and augmenting previously obtained historical data,

    o   Establish an understanding of the relationships between ground and altitude performance deterioration trends,

    o   Refine preliminary recommendations concerning means to reduce and control deterioration, and

    o   Identify areas where additional effort is required to develop an understanding of complex deterioration mechanisms.

The engine performance deterioration levels and trends were primarily determined from two data sources. Short-term trends were obtained from the analyses of the Plug-In Console (PIC) test results which closely monitored four engines from first flight to beyond 500 (cycles). The longer term deterioration was established from sea level facility tests of engines with 700 to 2100 flight cycles before and after engine repair (overhaul). These data showed that the prerepair performance deterioration increased from 1.0 percent loss in TSFC* at 50 flight

---

*——Throughout this report, performance values in Thrust Specific Fuel Consumption (TSFC) and Exhaust Gas Temperature (EGT) are referenced to sea level static conditions. Engine Condition Monitoring (ECM) data in Fuel Flow (Wf) and EGT are referenced to altitude conditions.

1

cycles to 3.0 percent at 1000 cycles and 3.8 percent at 2000 cycles. The corresponding increase in average EGT was 5 to 33°C. The postrepair performance deterioration increased from 2.2 percent at 1000 cycles to 2.8 percent at 2000 cycles. Corresponding increases in EGT were 11 to 21°C.

Models of performance-deterioration were derived for the fan, low- and high-pressure compressor, and high- and low-pressure turbine modules. These models include both module efficiency and flow capacity changes.

The TSFC deterioration at 1500 flight cycles as predicted from the module deterioration models were: fan, 0.2 percent; low-pressure compressor, 0.6 percent; high-pressure compressor, 0.6 percent; high-pressure turbine, 1.2 percent; and low-pressure turbine, 0.8 percent. The summation of 3.4 percent engine TSFC deterioration is slightly below the average JT9D-7A(SP) measured deterioration.

The effect of airplane acceptance testing on early engine performance deterioration was evaluated from four sets of data, each of which compared airplane-delivered engines (which were flight tested) and spare engines (which were not flight tested). No noticable differences in early revenue performance or deterioration trends were observed.

SECTION 2.0

INTRODUCTION

The rapid rise in the cost of oil since the OPEC oil embargo in 1973 has resulted in a national effort to increase the availability of domestic oil, develop alternate sources of energy, and develop near- and long-term means to reduce fuel consumption. To counteract the adverse impact of the world wide fuel crisis on the aviation industry, NASA has initiated the Aircraft Energy Efficiency (ACEE) program. Included in this program are major propulsion projects which are addressing both near-term and long-term goals. The long-term activities are directed toward developing propulsion technology to reduce fuel consumption by at least 12 percent in the late 1980's and an additional 15 percent in the early 1990's. the near-term activities are a part of the Engine Component Improvement (ECI) Project which is directed toward improving the fuel consumption of selected current high bypass ratio turbofan engines and their derivatives by 5 percent over the life of these engines. The ECI project is divided into two subprojects, (1) Performance Improvement and (2) Engine Diagnostics. Performance Improvement is directed at developing fuel saving component technology for existing engines and their derivatives to be introduced during the 1980 to 1982 time period. Engine Diagnostics is directed toward identifying and quantifying engine performance losses that occur during the engine's service life and developing criteria for minimizing these losses.

The first phase of the Engine Diagnostics project was the gathering, documentation and analysis of historical data. The resulting information was used to establish performance deterioration trends at the overall engine and module level, establish probable causes contributing to performance deterioration, and identify areas and/or components where corrective action could be taken.

That effort was completed in 1978, and the results are reported in Reference 1. The effort reported in this document was directed toward expanding the understanding of engine deterioration by acquiring new in-service engine performance data from a selected sample of JT9D engines. This investigation was conducted during the period from February 1977 to February 1979. The main source of data has been the Pan American World Airways JT9D-7A(SP) engines which are installed in their fleet of 747 Special Performance JT9D-7A(SP) aircraft which were introduced in service in March 1976. Data were obtained from on-the-wing ground tests using expanded engine instrumentation, prerepair and postrepair test stand data, and in-flight cockpit monitored data.

The data analyzed from these sources was then used to fill in and refine the analytical deterioration models for the engine and engine modules established from the earlier effort.

These refinements to the preliminary deterioration models considered, in particular, first, the results of the analysis effort of these studies, and then the models developed during the previous historical studies. It also considers the results of the short-term service engine test, as reported in Reference 2.

The following sections of this report describe the data collection and analytical effort, the results of the analysis, deterioration model refinements, recommendations, and conclusions. Supporting documentation is included in Appendices A through F.

SECTION 3.0

DATA COLLECTION AND ANALYSIS METHODOLOGIES

3.1 DATA COLLECTION

The objective of collecting performance and repair-type engine data was to provide an insight into the trends and levels of performance deterioration with usage.

Engine performance data were collected on 32 Pan American JT9D-7A(SP) ranging from zero to more than 2000 engine flight cycles. These performance data along with the pertinent repair data were used to document the performance history of each engine. These data covered both short- and long-term deterioration.

The data gathered included the following:

o   Engine Condition Monitoring (ECM) Data - These data consisted of the basic cruise flight performance data recorded by the flight crews for every flight. ECM data were gathered for the full 32 engine data base, starting from the first revenue flights.

o   In-Flight Performance Calibrations - These calibrations were additional engine and aircraft flight data, recorded periodically, on specific engines by the Pan American (PA) Engineering Staff, starting with the first flights.

o   Plug-In Console (PIC) Testing - These tests were a series of controlled installed-engine ground tests conducted by Pratt & Whitney Aircraft (P&WA) and Pan American personnel with expanded instrumentation. The PIC tests were conducted concurrently with the in-flight calibrations to achieve ground/flight performance comparisons.

o   Prerepair and Postrepair Test Cell Testing - A series of prerepair and postrepair tests with expanded instrumentation were conducted by Pan American in conjunction with repairs of the sample engines. Engine teardown and repair data were also collected for these engines.

3.1.1 Engine Condition Monitoring Data

The Engine Condition Monitoring (ECM) data for 32 Pan American JT9D-7A(SP) engines in 747SP airplanes were collected from the first

5

revenue flight (when it was first recorded) through the first engine overhaul, or to December 15, 1978 when the data collection was completed.

The ECM data included exhaust gas temperature (EGT), fuel flow (Wf), engine pressure ratio (EPR), low- and high-pressure rotor speeds (N1 and N2), Mach number (Mn), air temperature, bleed valve position, aircraft gross weight, and altitude. The data are recorded by the flight crew on every revenue flight at steady state cruise conditions.

The measured data were compared with a set of engine base-line performance data, and the changes or deterioration in exhaust gas temperature, fuel flow, and high- and low-pressure rotor speeds at the measured engine pressure ratio were determined. These data were plotted as functions of calendar time, and the trends were used by Pan American to monitor any changes in engine performance. This collection of data provided the data base for establishing 747SP fleet and individual airplane in-flight performance deterioration trends. A sample of ECM flight data relative to the base-line performance is shown in Figure 1.

3.1.2 In-Flight Performance Calibrations

In-flight engine performance data were obtained from a series of in-flight calibrations performed by Pan American on selected 747SP flights. These calibrations, which were conducted concurrently with the ground test Plug-In Console program, established: engine initial flight performance, short- and medium-term flight performance deterioration trends, and a relationship between installed flight and ground performance.

The performance calibrations were conducted on each of the four engines in two of the Pan American 747SP airplanes starting with the first flight, the delivery flight, and subsequent revenue flights spaced to establish performance trends. Calibrations were made by Pan American Engineering personnel using normal flight deck instrumentation. Calibration conditions were standardized to the extent possible by conducting them at steady state cruise condition with the fuel heating and anti-icing systems shut off. One or two calibrations were made at altitudes between 35,000 and 41,000 feet. The engine and airplane parameters that were recorded at each calibration point are listed below.

Pressure Altitude	P amb
Inlet air total temperature	Tt2
Inlet air static temperature	Ts2

6

Figure 1 Typical Corrected Engine Condition Monitoring (ECM) Data - The data show changes in exhaust gas temperature, fuel flow, and low- and high-pressure rotor speeds relative to the base-line performance.

| Mach number | Mn |

Low-pressure rotor speed	N1
High-pressure rotor speed	N2
High-pressure turbine exhaust gas temperature	EGT
Fuel flow	Wf

Engine pressure ratio	EPR
Number of air-conditioning packs in use	
Aircraft gross weight	TOGW

A calibration consisted of at least four complete data point sets where EPR on each engine was varied between 1.2 and 1.5. This variation, while holding total average thrust constant, was accomplished by increasing EPR on the inboard engines and decreasing EPR on the outboard engines; after data were recorded at this condition, EPR was again varied by decreasing EPR on the inboard engines and increasing EPR on the outboard engines and repeating the calibration. Steady state conditions were established by watching aircraft and engine instrumentation until stabilization was achieved before manually recording each set of data points. In addition, a fuel sample was taken at the end of the flight to establish the fuel heating value.

The recorded in-flight calibration data and fuel sample were delivered to Pratt & Whitney Aircraft and were processed in the same manner as for the ECM data. Changes were noted for exhaust gas temperature, fuel flow, and high- and low-pressure rotor speeds versus engine pressure ratio at standard conditions with the air-conditioning bleed requirement factored out. Table I presents a sample print-out of the corrected data which were then used in the subsequent analyses.

3.1.3 Plug-In Console Testing

The Plug-In Console (PIC) system was developed and operationally checked out by Pratt & Whitney Aircraft as a quick and accurate system for measuring on-wing installed engine performance. A series of PIC tests, conducted by Pratt & Whitney Aircraft personnel, were performed on two engines of two Pan American 747SP aircraft. The first PIC tests were conducted prior to the first flight of each aircraft. The data from PIC tests combined with in-flight calibration tests were used to establish the initial and early engine performance deterioration.

This PIC system provided high quality data on 15 engine performance parameters. With the exception of engine thrust, the PIC system records all test data that were normally obtained in an engine test stand. The engine performance parameters obtained are shown in Table II.

8

TABLE I

SAMPLE PRINT-OUT OF IN-FLIGHT CALIBRATION CORRECTED DATA

A/C NO.	DATE	FLIGHT CONDITIONS			CORRECTED EPR	RECORDED DATA CORRECTED TO STANDARD CONDITIONS (B747)				REFERENCE PERFORMANCE FLEET				AIR-CONDITIONING CABIN BLEED CORRECTION				Δ PERFORMANCE RELATIVE TO REFERENCE			
		AIR TEMP	FLT LVL	MACH	EPR	CONVERSION TO SEA LEVEL				INSTALLED GAS GENERATOR				BLEED CORRECTION				DEVIATION			
						FF	N1	N2	EGT	FF	N1	N2	EGT	FF	N1	N2	EGT	FF	N1	N2	EGT
TSTE-1	6/ 7	-19.0	354	0.867	1.371	17126.	96.4	94.3	1089.	17434.	94.6	93.0	1097.	-131.	0.0	0.4	-5.	-1.0	1.7	0.9	-3.
-2					1.379	17011.	95.4	94.2	105.	17586.	94.8	93.2	1100.	-132.	0.0	0.4	-5.	-2.4	0.5	0.6	-11.
-3					1.366	17115.	96.0	93.8	1084.	17340.	94.4	93.0	1095.	-130.	0.0	0.4	-5.	-0.4	1.6	0.4	-6.
-4					1.462	17040.	96.0	93.5	1086.	17264.	94.3	92.9	1094.	-129.	0.0	0.4	-5.	-0.4	1.7	0.1	-2.
TSTE-1	6/ 7	-19.0	354	0.868	1.375	17146.	96.4	94.3	1090.	17516.	94.7	93.1	1098.	-131.	0.0	0.4	-5.	-1.2	1.6	0.8	-3.
-2					1.380	17059.	95.5	94.2	1084.	17610.	94.9	93.2	1100.	-132.	0.0	0.4	-5.	-2.2	0.6	0.6	-10.
-3					1.368	17131.	95.9	93.7	1085.	17387.	94.5	93.0	1096.	-130.	0.0	0.4	-5.	-0.6	1.4	0.3	-5.
-4					1.364	17074.	96.0	93.3	1086.	17307.	94.4	93.0	1095.	-130.	0.0	0.4	-5.	-0.6	1.6	0.0	-3.
TSTE-1	6/ 7	-24.0	357	0.813	1.346	16366.	95.5	94.0	1077.	16961.	93.8	92.6	1089.	-127.	0.0	0.4	-5.	-2.6	1.6	1.0	-7.
-2					1.347	16241.	94.2	94.0	1071.	16980.	93.8	92.6	1090.	-127.	0.0	0.4	-5.	-3.6	0.3	0.9	-13.
-3					1.349	16617.	95.3	93.8	1077.	17018.	93.9	92.6	1090.	-128.	0.0	0.4	-5.	-1.6	1.3	0.7	-4.
-4					1.345	16445.	95.1	93.0	1077.	16942.	93.8	92.6	1089.	-127.	0.0	0.4	-5.	-2.2	1.2	0.0	-7.
TSTE-1	6/ 7	-24.0	357	0.815	1.347	16412.	95.3	93.9	1077.	16994.	93.9	92.6	1090.	-127.	0.0	0.4	-5.	-2.6	1.4	0.6	-5.
-4					1.347	16474.	95.2	93.0	1078.	16994.	93.9	92.6	1090.	-127.	0.0	0.4	-5.	-2.2	1.3	0.0	-7.
-2					1.350	16349.	94.3	93.9	1071.	17051.	94.0	92.7	1091.	-128.	0.0	0.4	-5.	-3.2	0.3	0.8	-13.
-3					1.351	16709.	95.4	93.7	1077.	17070.	94.0	92.7	1091.	-128.	0.0	0.4	-5.	-1.2	1.4	0.6	-9.
TSTE-1	6/ 7	-24.0	357	0.818	1.346	16378.	95.4	94.0	1077.	16968.	93.8	92.6	1089.	-127.	0.0	0.4	-5.	-2.6	1.5	0.9	-7.
-2					1.348	16284.	94.3	94.0	1071.	17006.	93.9	92.6	1090.	-128.	0.0	0.4	-5.	-3.4	0.4	0.9	-13.
-3					1.350	16674.	95.4	93.7	1077.	17044.	93.9	92.7	1091.	-128.	0.0	0.4	-5.	-1.4	1.4	0.6	-4.
-4					1.344	16671.	95.1	93.0	1077.	16929.	93.8	92.6	1089.	-127.	0.0	0.4	-5.	-1.8	1.3	0.0	-7.
TSTE-1	6/ 7	-24.0	357	0.821	1.348	16390.	95.3	94.1	1075.	16999.	93.9	92.6	1090.	-127.	0.0	0.4	-5.	-2.6	1.4	1.0	-9.
-2					1.352	16359.	94.2	94.0	1072.	17075.	94.0	92.7	1091.	-128.	0.0	0.4	-5.	-3.4	0.7	0.9	-14.
-3					1.352	16670.	95.4	93.7	1077.	17075.	94.0	92.7	1091.	-128.	0.0	0.4	-5.	-1.6	1.3	0.5	-9.
-4					1.344	16462.	95.1	93.0	1077.	16961.	93.8	92.6	1089.	-127.	0.0	0.4	-5.	-2.2	1.2	0.0	-7.
TSTE-1	6/ 9	-16.0	410	0.848	1.375	17222.	96.1	94.2	1099.	17740.	94.7	93.1	1108.	-133.	0.0	0.5	-5.	-2.0	1.3	0.0	-1.
-2					1.375	16993.	95.3	94.4	1095.	17740.	94.7	93.1	1108.	-133.	0.0	0.5	-5.	-3.4	0.3	0.8	-8.
-3					1.376	17757.	96.1	93.9	1103.	17758.	94.8	93.1	1108.	-133.	0.0	0.5	-5.	0.6	1.3	0.3	0.
-4					1.371	17184.	95.9	93.5	1100.	17665.	94.6	93.0	1107.	-132.	0.0	0.5	-5.	-1.8	1.2	0.0	-1.
TSTE-1	6/ 9	-16.0	410	0.849	1.366	17185.	96.1	94.2	1098.	17552.	94.4	92.9	1105.	-132.	0.0	0.5	-5.	-1.2	1.6	0.7	-1.
-2					1.374	16976.	95.3	94.3	1095.	17702.	94.7	93.1	1107.	-133.	0.0	0.5	-5.	-3.2	0.5	0.7	-7.
-3					1.373	17433.	96.0	93.9	1101.	17683.	94.6	93.1	1107.	-133.	0.0	0.5	-5.	-0.6	1.3	0.3	0.
-4					1.369	17185.	95.8	93.5	1099.	17608.	94.5	93.0	1106.	-132.	0.0	0.5	-5.	-1.6	1.2	0.0	-1.
TSTE-1	6/ 9	-32.0	430	0.852	1.505	20258.	101.1	95.7	1165.	20544.	98.7	94.2	1159.	0.	0.0	0.8	0.	-1.2	2.3	0.6	6.
-2					1.203	13702.	90.4	91.8	1009.	14555.	89.1	90.8	1054.	0.	0.0	0.8	0.	-5.8	-1.2	0.2	-45.
-3					1.201	14117.	91.5	92.2	1025.	14517.	89.0	90.7	1054.	0.	0.0	0.8	0.	-2.6	2.4	0.6	-29.
-4					1.488	20127.	100.0	94.6	1164.	20174.	98.2	94.1	1153.	0.	0.0	0.8	0.	-0.2	1.8	-0.3	11.
TSTE-1	6/ 9	-32.0	430	0.851	1.221	14307.	92.2	92.2	1033.	14896.	89.7	91.0	1060.	0.	0.0	0.8	0.	-3.8	2.4	-0.3	-27.
-2					1.511	20061.	100.0	95.8	1156.	20686.	98.9	94.3	1161.	0.	0.0	0.8	0.	-3.0	1.1	0.6	-5.
-3					1.513	20564.	100.8	95.3	1169.	20731.	98.9	94.3	1162.	0.	0.0	0.8	0.	-0.8	1.8	0.2	7.
-4					1.218	14263.	91.5	91.6	1033.	14839.	89.6	90.9	1059.	0.	0.0	0.8	0.	-3.8	1.8	-0.1	-22.

TABLE II

ENGINE PERFORMANCE PARAMETERS RECORDED BY THE-PLUG-IN-CONSOLE SYSTEM

	Temperatures	Pressures	Other
	T amb	P amb	N1
	Tt3	Ps3	N2
	Tt4	Pt3	Fuel Flow
	Tt6 avg.	Ps4	Vane Angle
	Tt6 indiv. (6)	Ps5	
	Tt7 avg.	Pt7	
	Tt7 indiv. (6)		
Total	5	6	4

15 Total Data Parameters

The PIC system is schematically shown in Figure 2. The system consisted of:

o   an engine interface harness, including electrical cables and tubing to the pressure transducers;

o   a modified trim mast to guide cables and tubing through the fan stream;

o   a temperature-controlled pressure transducer box;

o   a data recording system (data logger); and

o   a Hewlett Packard 9825 minicomputer for reducing the data to engineering units, applying standard day corrections, and calculating preliminary module performance.

The installation of the interface harness is shown on Figure 3. The trim mast, transducer box, and leads into the cabin are shown on Figure 4. The recording system and minicomputer on board the aircraft are shown on Figure 5.

During the PIC testing, all corrected parameters were calculated by the minicomputer and plotted for data validation and compared with data from previous tests. Figures 6 and 7 show a typical data print and plots prepared during a PIC test.
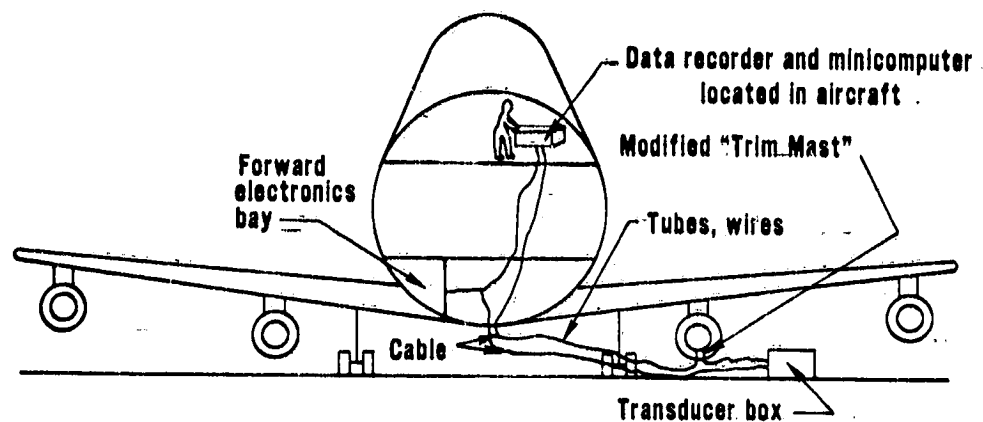
Figure 2 Location of Major Components of the Plug-In Console System --
The instrumentation lines are connected via the modified trim
mast to the transducer box or directly to aircraft to the
special data recording system located inside the aircraft. _____
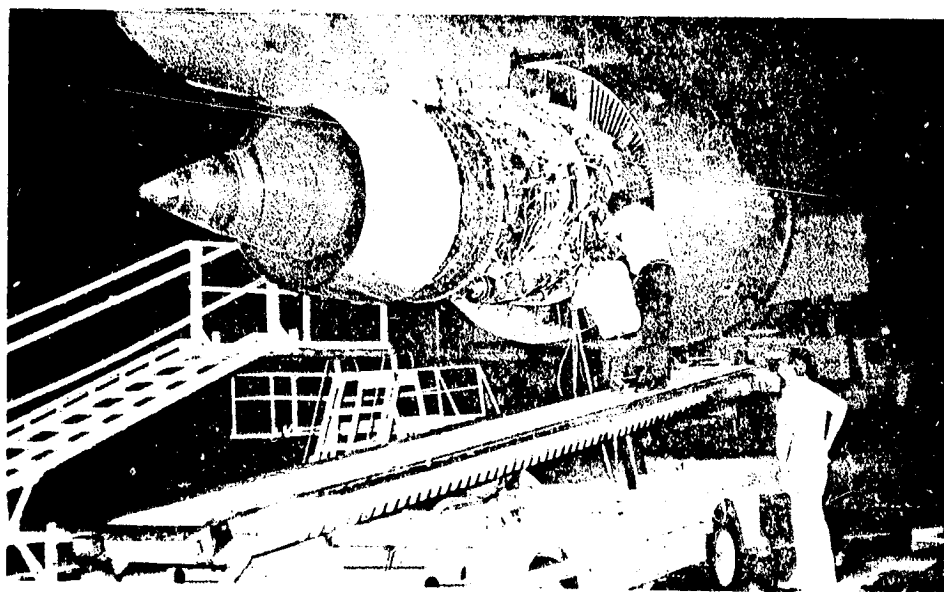
Figure 3 Installation of the PIC System Instrumentation Harness. - The
instrumentation harness was installed prior to each test.
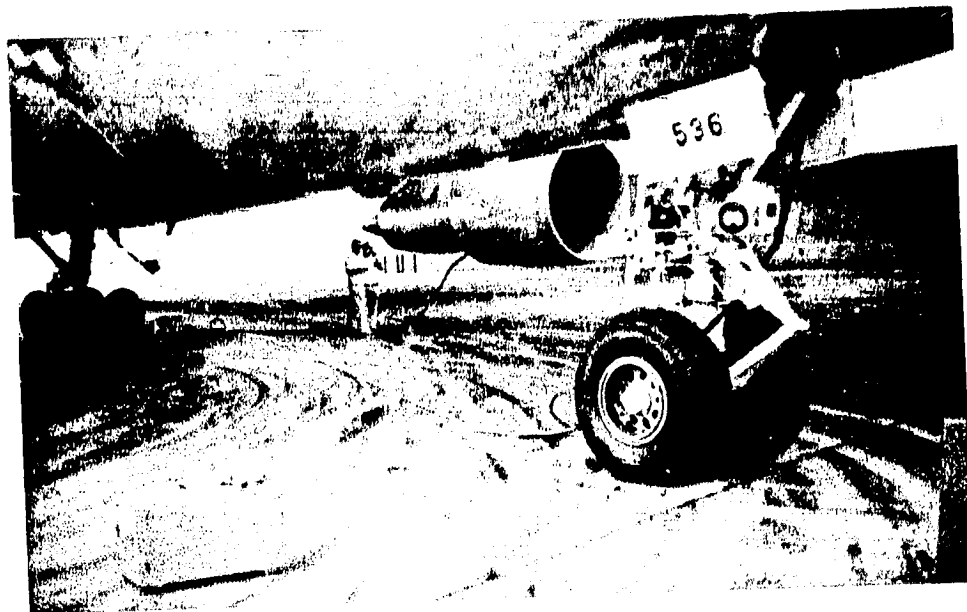
Figure 4 PIC System Instrumentation - The transducer box and instrumentation leads into the cabin are shown.
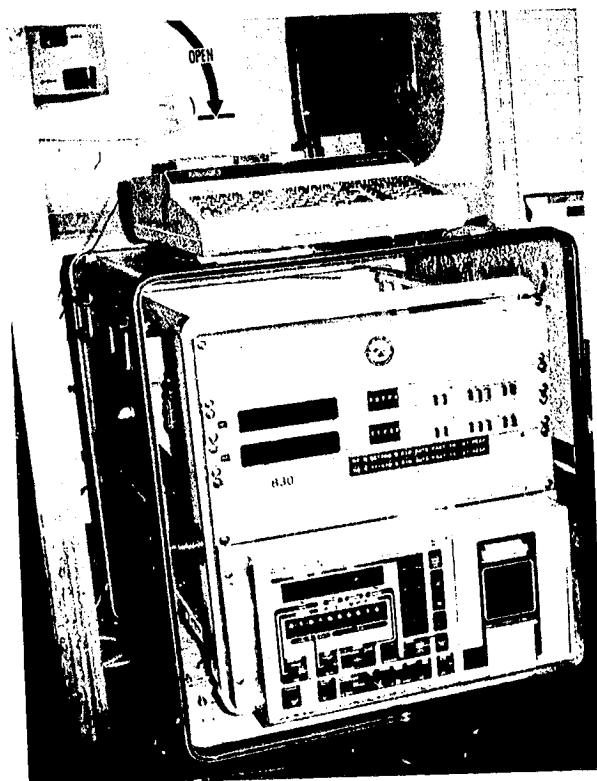
Figure 5 PIC System Data Acquisition Unit - The recording equipment and the HP9825 minicomputer are shown.

12

Observed parameters

Parameters corrected to sea level
static standard day conditions

Baseline data adjusted to current
operating point EPR and constant
EPR parameter changes relative
to the baseline

PRATT
&
WHITNEY
AIRCRAFT

Plug-In Console

Engine N& 695745
Data   07 18/77
Time   05:49:46
Engine Point   4
EPR-   1.424
Eh   1.007

Engineering
Units

N1   3358 R
N2   7429 R
Zero   -0.002
100mV   100.032
Famb   14.717 A
Ps3   26.187 A
Pt3   33.304 A
Ps4   292.874 A
Ps51   203.728 A
Pt7   20.962 A
BV-du   -10.010 V
BV6   4.492 V
BETA   1.1   D
W-rate   4.921 V
Wf   16666 #
Tt5   231.1   F
Tt4.5   930.3   F
Tt6-1   1672.1   F
Tt6-2   1719.9   F
Tt6-3   1648.5   F
Tt6-4   1587.3   F
Tt6-5   1590.0   F
Tt6-6   1599.3   F
Tt6on   1591.9   F
Tt7-1   1100.3   F
Tt7-2   1008.2   F
Tt7-3   1047.1   F
Tt7-4   1056.7   F
Tt7-5   1009.5   F
Tt7-6   1081.9   F
Tt7on   1049.4   F
#3bhr   315.8   F
Tamb   82.3   F
Toven   147.3   F
Toil   96.0   C
#2uren   38.5   C

Corrected to
S.L.S.D. Units

N1 θT2   3388 R
N2 θT2   7725 R
Wf corr   16043 #
Tt3 θ   100.1 F
Tt4.5 θ   874.7 F
Tt6 θ   1511.9 F
Tt7 θ   981.3 F

Calculated
Data

Ps3   11.4696 G
Pt3   18.5869 G
Ps4   278.1564 G
Ps51   189.0110 G
Pt7   6.3450 G
Ps3 Pamb   -1.7793
Pt3 Pamb   2.2629
ΔP3-Pt3   0.2137
Ps4 Pt3   8.7939
Ps51 Pt7   9.7189
Ps4 Pt7   -13.9716
ΔPtco   0.3044
Pt7 Pamb   -1.4243
Tt3 Tt2   1.2759
Tt4-Tt3   2.0165
Tt4-Tt7   0.9261
Tt6-Tt7   1.5682
Woe   240.31 #

Harness Spread
Check

Tt6-1   36F I-ave
Tt6-2   54F I-ave
Tt6-3   12F I-ave
Tt6-4   -49F I-ave
Tt6-5   -46F I-ave
Tt6-6   -37F I-ave
Tt7-1   -50F I-ave
Tt7-2   -42F I-ave
Tt7-3   -4F I-ave
Tt7-4   -6F I-ave
Tt7-5   -41F I-ave
Tt7-6   31F I-ave

Tt6colan 1626.2F
Tt7colan 1050.6F
Tshunt   44.3 F

BASE LINE

DATE   04 21 77
EPR   1.424

Data is
Adjusted to
an Operating
EPR of   1.424

N1 θT2   3313 R
N2 θT2   7325 R
Tt3 θ   205.5 F
Tt4.5 θ   884.8 F
Tt6 θ   1491.3 F
Tt7 θ   978.8 F
Pt3 Pt2   2.2755
Ps4-Pt7   14.1444
Ps4 Pt3   8.8534
Woe   241.33 #
Wf corr   16092 #
Tt3 Tt2   1.2825
Tt4 Tt3   2.0212
Tt4-Tt7   0.9347
Tt6 Tt7   1.3563
BETA   -0.4   d

PARAMETER DELTAS

N1 θT2   -0.84
N2 θT2   0.02
Tt3 θ   -3.46 F
Tt4.5 θ -10.10 F
Tt6 θ   20.49 F
Tt7 θ   2.43 F
Pt3 Pt2   -0.55
Ps4 Pt7   -1.23
Ps4   -0.67
Woe   -0.4
Wf corr   -0.27
Tt3 Tt2   -0.52
Tt4-Tt3   -0.27
Tt4   -0.91
Tt6-Tt7   0.33
BETA   1.4 d

Module
performance
analysis

Figure 6 Typical PIC Data System Print-Out – Tabular data in strip
chart form is output from the minicomputer for plotting and
preliminary analysis.
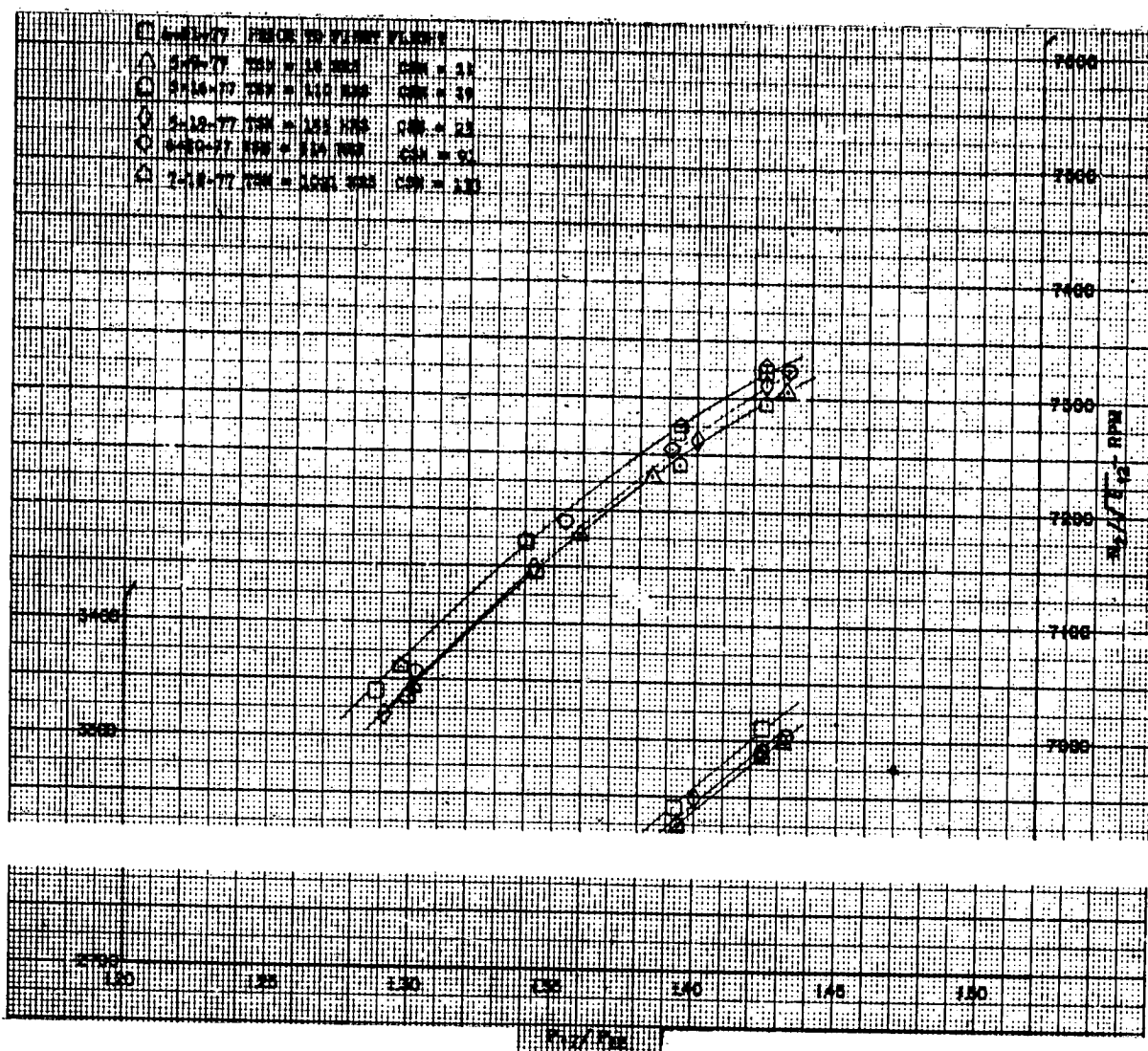
Figure 7 Typical Plot of On-Wing PIC Calibration of JT9D-7(SP) Engine
P-695745 - Plots of the data were made to permit comparison
with previous calibrations and to check on data quality.
(J18859-8)

Ten sets of PIC calibrations were made on the Position 1 and 2 engines
on Pan American 747SP airplane N536PA starting prior to the first
flight. The dates, engine age, and test location are listed on Table
III. Note that engine P-695745 was removed, repaired, and reinstalled
on a different airplane prior to the last test. Six sets of PIC
calibrations were made on the Position 1 and 2 engines on Pan American
747SP airplane N537PA. The dates, engine age, and locations are listed
on Table IV.

14

TABLE III

CHRONOLOGY OF ON-WING PIC TESTING
747SP AIRPLANE N536PA; ENGINES P-695743 AND P-695745

Date	Engine	Hours	Cycles	Test Location
4-21-77	-743, -745	0	0	Boeing - Seattle
5-09-77	-743, -745	18	11	JFK - NY
5-16-77	-743, -745	110	19	JFK - NY
5-19-77	-743, -745	155	23	JFK - NY
6-20-77	-743, -745	614	91	JFK - NY
7-18-77	-743, -745	1021	133	JFK - NY
11-02-77	-743	1081	141	SFO
11-02-77	-745	2486	365	SFO
2-11-78	-743	2473	360	JFK - NY
2-11-89	-745	3878	584	JFK - NY
4-13-78	-743	3415	475	SFO
4-13-78	-745	4820	700	SFO
12-04-78	-743	6903	1078	LAX

TABLE IV

CHRONOLOGY OF ON-WING PIC TESTING
747SP AIRPLANE N537PA; ENGINES P-695760 AND P-695763

Date	Hours	Cycles	Test Location
5-04-78	0	0	TBC
6-07-78	52	15	TBC
6-27-78	297	54	SFO
7-20-78	609	110	LAX
11-05-78	2224	331	JFK - NY
1-04-79	3165	510	SFO

3.1.4. Test Stand Testing

Prerepair and postrepair testing with expanded test instrumentation was conducted on JT9D-7A(SP) engines, from the Pan American 747SP fleet, as they came into the overhaul shop for repair. These tests, for the most part, were conducted by Pan American at their J. F. Kennedy maintenance center. However, for those engines which were repaired by Pratt & Whitney Aircraft, the tests were conducted at the P&WA Middletown test facility.

The engines were tested in a partial Quick Engine Change (QEC) configuration with bellmouth-type inlets, flight nacelles and nozzles. Test data were taken at stabilized steady state operating conditions at a minimum of five power settings between take-off power and idle.

The expanded instrumentation installed for these tests permitted the recording of the parameter data listed below at each engine operating condition:

Bellmouth inlet total pressure	$Pt2$
Low-pressure compressor discharge total temperature	$Tt3$
Low-pressure compressor discharge static pressure	$Ps3c$
Low-pressure compressor discharge total pressure	$Pt3c$
High-pressure compressor discharge total temperature	$Tt4$
Burner static pressure	$Ps4$
High-pressure turbine inlet static pressure	$Ps5$
High-pressure turbine exhaust gas temperature, average	$Tt6$
High-pressure turbine exhaust gas temperature, 6 points	$Tt6$
Low-pressure turbine exhaust gas temperature, 7 points	$Tt7$
Low-pressure turbine exhaust gas temperature, average	$Tt7$
Low-pressure turbine exhaust total pressure	$Pt7$
Net thrust	Fn
Fuel flow	Wf
Low-pressure rotor speed	$N1$
High-pressure rotor speed	$N2$
Variable stator vane bell crank angle	β
Barometric pressure	$P\ bar$
Dry bulb temperature	$T\ db$
Wet bulb temperature	$T\ wb$
Test stand pressure depression, front	$P\ cdf$
Test stand pressure depression, rear	$P\ cdr$

Test data were recorded and transmitted to Pratt & Whitney Aircraft for reduction and preliminary analysis. Adjustments were required to correct the test data from partial QEC engines in both Pan American and Pratt & Whitney Aircraft test stands to permit comparisons with test data from original production bare engines in the P&WA test stands. Data processing flow is illustrated in Figure 8.
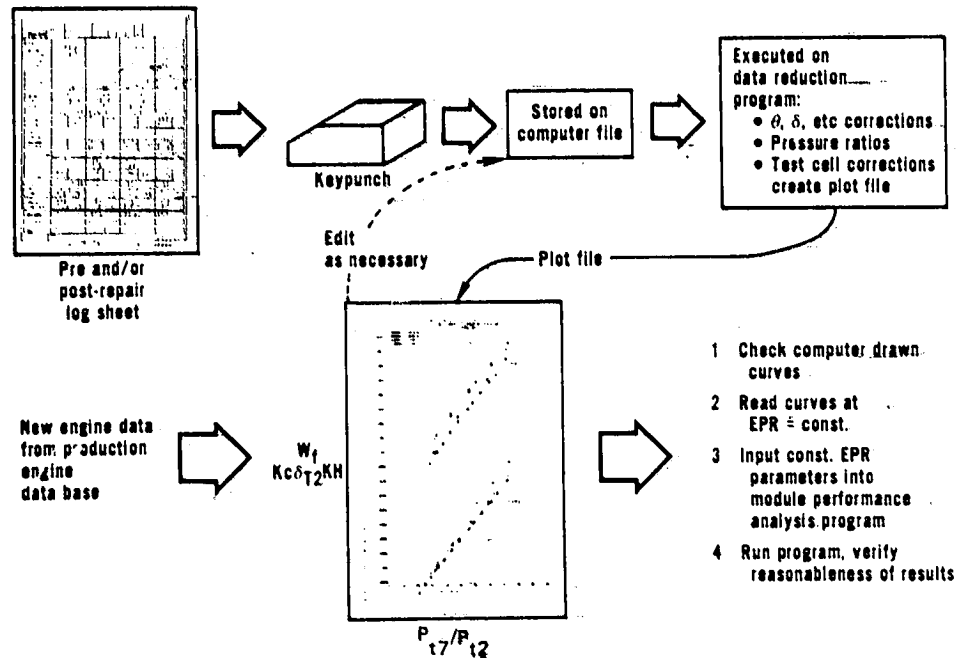
Figure 8 Data Processing Flow for Prerepair and Postrepair Test Stand Testing – The steps in processing test cell data from test log sheets through preliminary module analysis are shown schematically.

Ten sets of prerepair and postrepair tests, two prerepair-only tests, and 12 postrepair-only tests were conducted on 19 JT9D-7A(SP) engines. Table V presents a list of these engines with their removal dates, engine ages in hours and flight cycles, test dates, and test locations. The table also lists the engine prerepair and postrepair changes in TSFC and EGT relative to the new engine acceptance test,

based on the analysis of the test data where both prerepair and postrepair tests were completed. The corrected test data, along with the engine teardown and repair build data (Section 3.3), were then used as input to the detailed top-down analysis (Section 3.4.2).

3.2 PAN AMERICAN TEST STAND INSTRUMENTATION AND TEST DATA UNCERTAINTIES.

3.2.1 Expanded Instrumentation

The Pan American test stand incorporates visual instrumentation, and data was visually acquired and recorded on engine test log sheets by the test stand crew. The parameters normally recorded were limited to those required for production engine performance testing and by the physical dimensions of the instrumentation console. For this program, additional instrumentation was installed in the test stand and control room for the additional engine parameters required. The chromel-alumel temperature system was expanded to include one Tt3, one Tt4, and seven Tt7 readings. All of these temperatures were recorded on the existing Doric Model 400 indicator via ten-channel select switches. Provisions were also made to record eight bellmouth Pt2 and two cell static pressure readings on U-tube manometers with a 30 inches of water capability that were already available on the Pan American test stand.

3.2.2 Test Stand Instrumentation Calibrations

The performance instrumentation on the Pan American test stand was calibrated in-place by the Pan Am Instrumentation personnel. The normal calibration interval for the majority of the instrumentation is six months. However, the calibration of the test stand instrumentation was dependent on the engine test requirements so that the actual time intervals between calibrations varied. Whenever possible, Pratt & Whitney Aircraft Instrumentation personnel were present for the calibrations. The instrumentation and calibration procedures utilized by Pan American were developed in accordance with the accuracies defined by the Pratt & Whitney Aircraft Test Instruction Sheets (T.I.S.). No special modifications were made to either the instrumentation or to the procedures used in conjunction with this program.

The Pan American thrust system (indicator, cable, and load cell) and the fuel flow meters were periodically brought to East Hartford for calibration in the Pratt & Whitney Aircraft Instrumentation Standards Laboratory. The master thrust system was calibrated three times and the flow meters (meter numbers 23275 and 23276) were calibrated twice. The results of the flow meter calibrations were compared to the Pan American results obtained using their Cox Instruments Calibrator. The master thrust system calibrations were compared to the primary calibrations performed by the manufacturer (BLH).

18

TABLE 3.1-V

SUMMARY OF ENGINE PERFORMANCE DATA OBTAINED FROM TEST-STAND TESTING

Engine Serial Number	Removal Number	Removal Date	Total Hours	Total Cycles	Test Date Prerepair	Test Date Postrepair	Test Location	Prerepair Change in TSFC (%)*	Prerepair Change in Tt6 (°C)**	Postrepair Change in TSFC (%)*	Postrepair Change in Tt5 (°C)**
686047	1	11-06-77	7158	1083	11-22-77	12-08-77	PA	+3.7	+7.4	+4.1	+13.8
686048	1	12-21-77	7675	1242	01-01-78	02-15-78	PA	+3.9	+11.6	+2.5	+25.9
686048	2	08-23-78	10447	1642	----	09-15-78	PA			+2.3	+3.2
686049	4	09-21-78	11664	1823	----	01-03-79	PA			+2.0	+11.0
686050	1	05-17-78	9825	1546	05-27-78	08-12-78	PA			+0.04	-31.2
686053	4	09-21-78	11406	1757	----	11-22-78	PA	+4.8	+36.2	+3.0	-0.4
686054	2	05-01-78	9350	1405	----	05-15-78	PA			+3.7	+17.0
686055	2	08-31-78	10925	1639	----	09-19-78	PA			+2.5	-1.6
686060	3	02-09-78	6696	1101	02-22-78	04-25-78	P&WA	+3.1	+17.6	+1.3	+8.2
686060	4	08-01-78	7816	1283	08-07-78	----	PA	+2.9	+17.1		
686068	2	09-12-78	11081	1670	----	11-13-78	PA			+2.1	+2.9
686070	2	05-28-78	10073	1448	----	08-18-78	PA			+2.4	+26.8
686071	3	10-06-78	8706	1258	----	11-08-78	PA			+1.5	+1.3
685083	1	05-17-77	5100	770	05-19-77	06-30-77	PA	+2.0	+24.3	+1.6	+18.4
685083	2	07-12-78	9054	1760	----	08-30-78	PA			+2.3	+9.6
686083	3	11-13-78	10073	1932	11-16-78	11-22-78	PA	+3.1	+22.9	+4.0	-7.1
686097	3	10-08-78	12170	1852	----	10-25-78	PA			+2.8	+2.9
695716	4	07-06-78	10197	1719	----	09-2907-8	PA			+2.8	+7.2
695722	3	10-23-78	12102	2135	10-27-78	01-09-79	PA	+3.2	+31.0	+1.9	-7.0
695727	1	12-13-77	5579	1616	12-17-77	01-06-78	PA	+3.0	+22.6	+3.1	+9.8
695727	2	08-14-78	8514	2056	----	09-16-78	PA			+2.7	-28.1
695732	1	07-10-78	7652	2127	07-11-78	08-31-78	PA	+3.7	+21.4	+2.5	-2.2
695745	1	04-20-78	4845	703	04-29-78	06-13-78	P&WA	+1.4	+31.7	+0.4	-12.8
695743	2	06-18-79	9642	1480	06-20-79	- - -	PA	4.0	+30.0		

* TSFC change at constant thrust;
**Tt6 change at constant EPR.

19

Detailed discussions of the Pan American test stand calibration standards, procedures and results, and of the thrust system calibrations at Pratt & Whitney Aircraft are presented in Appendix D.

3.2.3 Measurement Uncertainties of the Pan American Test Stand Instrumentation

There is a degree of uncertainty in all test stand performance measurements which must be considered in the subsequent analysis of the recorded performance data. This uncertainty is a function of the following: (1) accuracy of the installed instrumentation, (2) thoroughness and frequency of instrumentation calibration, and (3) accuracy of the reference or master instruments. A summary of the Pan American test stand instrumentation uncertainties is listed in Table VI.

TABLE VI

SUMMARY OF TOTAL PARAMETER UNCERTAINTIES

Parameter	Total Uncertainty
Pt2, ιcd (% Reading) *	+0.50
P breather (in. HgG)	∓1.13
Pt7 (in. HgA)	∓0.35
Pt3 (in. HgA)	∓0.48
Ps3 (in. HgA)	∓0.052
Ps5 (in. HgG)	+5.57
Ps4 (in. HgG)	∓3.10
Barometer (in. HgA)	∓0.28
Tt3, Tt4, Tt6, Tt7 (°C)	+6.3 to +13.0
Tt2 (°F)	+2.83
Thrust (lb)	+136.
N1 (rpm)	+5.
N2 (rpm)	+10.
Fuel Flow (% Reading)	+0.46
TSFC (%)	∓0.55

*U-tubes employed for eight bellmouth Pt2 pressures and one Pcd pressure.

A detailed discussion of the factors contributing to and the derivation of the above data uncertainties is presented in Appendix D.

3.2.4 Measurement Uncertainties Due To Data Sampling and Engine Configuration Differences

Analysis of test stand data was subject to other uncertainties in addition to the measurement uncertainties associated with the physical measurement hardware and calibration equipment which have just been discussed. One major source of this type of uncertainty was sampling error. This error referred to differences between measured parameters and true average parameters resulting from a limited number of measurement points in a flow field which had significant circumferential/radial profile variations. This uncertainty has been particularly noticeable in the measured values of Tt6 and Tt7 from prerepair and postrepair data, where repairs involved burner liner replacement. All of the JT9D-7A(SP) engines for which prerepair and postrepair data were available had burner liners replaced during repair, (in most cases by liners of a different design). Comparison of prerepair and postrepair data for these engines showed that while TSFC improved as a result of repairs in nearly all instances, thereby inferring reductions in both Tt6 and Tt7, the measured Tt6 and Tt7 values increased from prerepair to postrepair in several engines. Moreover, individual engines were not consistent in trend, some exhibiting increases in Tt6 but decreases in Tt7 as a result of repair, others with increasing Tt7 but decreasing Tt6, etc. The conclusion is that the burner liner replacement (and possibly other repairs) resulted in a shift in the temperature profiles at both locations. Since Tt6 and Tt7 probes were at different locations both circumferentially and radially, a profile shift could result in changes in magnitude and/or direction of measured values at the two locations (although analysis shows that the average values of the two should change in the same direction and by nearly the same magnitude). As an indication of the magnitude of this uncertainty, differences between thermodynamic (the true average value based on fuel flow) and measured temperatures of 20 to 30°C or more have been observed for individual JT9D-7A (SP) engines, with differences of 10°C or more common. In comparison to the instrumentation accuracies shown in Table VI, it can be seen that the sampling error differences can be quite significant.

Data sampling uncertainties have also been observed with Tt3, Pt3, and Tt4, but to a far lesser extent than with the hot section temperatures. As a result of Tt6 and Tt7 uncertainty, the analysis methodology had to be modified (in most instances) to disregarad the measured values of Tt6 and Tt7. The analysis methodology is discussed in more detail in Section 3.4.2.

There was also a minor area of hardware-related uncertainty where engines have had retrofit part changes after introduction into service (P-686 series of JT9D-7A(SP) engines). Production data for such engines were adjusted to reflect estimated performance changes associated with the part changes. In other words, these engines were treated as though they came off the production line in the retrofit configuration. These retrofit changes may have removed some part deterioration that was present, thereby making the analyzed performance deterioration less than was really the case. This was not a significant problem however, since the retrofit was accomplished on most of these engines early in their service lives. Another uncertainty had to do with production tolerance variations for the retrofit parts; the data adjustment reflected a nominal part configuration. Because of the limited scope of the retrofit changes, this was not believed to be a serious problem.

3.2.5 Test Stand Correlations

It was necessary to apply corrections to the Pan American test stand data in order to make a direct comparison between engine test parameters recorded in Pan American's test stand and parameters recorded at Pratt & Whitney Aircraft during the production test run of a particular engine. Cell-to-cell corrections resulting from back-to-back testing (at Pan American and P&WA) of P-695745 were used. These corrections represent the most recent back-to-back tests and were believed to be the best correlation available.

The uncertainties in airline test stand data analysis were caused primarily by hardware differences between the engine configuration as tested in the PA stand and in the production configuration. Generally, engines in the PA test stand are tested in the partial QEC configuration. The engine is tested with bellmouth inlet and actual flight nacelle rearward of the inlet. For the production test, on the other hand, the engine has a bellmouth inlet and special production nozzles; fan discharge flow is manifolded and discharged through two long ducts with convergent nozzles. QEC corrections were used to correct the data for differences between the two configurations. However, these corrections cannot account for physical jet area differences between different individual flight nozzles and individual production nozzles. These differences can amount to +0.5 percent or more in jet area because of production tolerances. Nozzle area variations of this magnitude can significantly affect measured gas generator parameter and, therefore, the analyzed component performance changes as well as overall performance loss.

22

3.3 MAINTENANCE DATA COLLECTION

The "top down" analyses of engine performance deterioration on both engine and module bases were aided by knowing the extent of changes in gas-path conditions, in each module, that contributed to the performance changes. These conditions include airfoil wear, changes in blade tip-to-seal clearances, and thermal distortion effects. Likewise, the analysis of the postrepair performance restoration was aided by knowing which gas-path components were replaced or rebuilt and the assembled dimensions and clearances in the gas path.

Performance deterioration and restoration analyses were made on the 19 engines listed on Table V. These analyses included 12 prerepair tests and 22 postrepair tests.

The prerepair and postrepair engine condition data and the extent of repair was collected for each engine from Pan American (PA) and P&WA repair records, P&WA Service Representative Reports, and by measurements and observations by P&WA Engineering specialists.

Detailed prerepair inspections were limited to three engines since the Pan American 747 SP engine repair schedule did not permit time for inspection prior to each engine overhaul or repair. The three engines included serial numbers P-686060 and P-695745, which were repaired at the Pratt & Whitney Aircraft (P&WA) Service Center, and P-686049, which was removed after 11,663 hours of continual operation. The teardown inspection of the disassembled modules included:

o   Blade tip to outer air-seal (OAS) clearances and OAS rub depth measurements;

o   Inspection of airfoils and seals in disassembled modules including the extent and type of wear and distortion;

o   Inspection of combustor including wear, distortion, burning, and cracking; and

o   Measurement of sample fan blades from engine P-695745 including surface roughness, wear, and distortion.

23

In addition to the prerepair and/or postrepair test performance data, information was collected for all maintenance actions including the following:

Engine hours and cycles since the last repair;

Causes of current and past engine removals;

Prior repair history;

Comments on condition of disassembled modules

Modules replaced as part of the overhaul with repair history on each replacement module;

Part replacement and repair on engine;

Gas-path measurements and clearances on built-up engine; and

Subsequent changes and repairs if initial repair does not achieve required performance restoration.

The 23 JT9D-7A(SP) engine repairs which were analyzed during the program are summarized in Appendix C. Information in this appendix includes:

Engine removal date, removal cause, who repaired the engine, and the extent of the repair;

Prior operating and repair history;

Identification of the various modules, their operating hours since refurbishment, and which were replaced during this repair;

Documentation of improvements in thrust specific fuel consumption (TSFC) and exhaust gas temperature (EGT) resulting from this overhaul (for engines which received a prerepair and postrepair test); and

Sample teardown and build-up data on one of these 23 engine repairs.

3.4 ANALYSIS TECHNIQUES

3.4.1 Flight Data and Plug-In Console Data

During this investigation the flight data included both Engine Condition Monitoring (ECM) data and in-flight performance calibrations. Plug-In Console (PIC) data were obtained from on-the-wing engine tests at sea level static conditions. These types of data are discussed in the following paragraphs.

The ECM data were corrected to standard day conditions by a computer program. Additional corrections were applied for Reynolds number, Mach number, and aircraft service bleed variations that normally occur in revenue service in order to further normalize the data. No corrections were made for variation in fuel lower heating value since this information was not available. The normalized data were then compared to a set of generalized engine gas generator curves and ten-day averages of the resulting deltas were plotted versus cycles for each engine. Since these trends still exhibited erratic variations in engine performance, smoothed curves were drawn of each curve for comparison of all engines.

The in-flight calibrations taken on two aircraft (serial numbers N536 and N537) were reduced to a usable form similar to the ECM data. However, rather than comparing the data to a set of generalized engine gas generator curves, each engine's data were compared to that engine's first in-flight calibration. Gas generator parameter deltas were then calculated at constant engine pressure ratio (EPR) and plotted versus cycles to establish individual engine trends.

The PIC data taken on-the-wing at sea level static conditions were corrected to standard day conditions with additional corrections applied to correct for variations in fuel lower heating valve and water content of the air. An additional correction was made to the data taken at Boeing to account for the apparent presence of a vortex being ingested into the inlet of the engine. Analysis of the data for all four engines involved in this part of the program exhibited improvements in fan and low-pressure compressor performance between tests at Boeing and subsequent tests elsewhere. These improvements were not expected. Investigation of the manner in which these tests were run revealed that all Boeing tests were conducted with a screen placed in front and partially to the sides of the engines to reduce the possibility of foreign object damage to the engine. Experience at Pratt & Whitney Aircraft has indicated that the presence of such a

device in relatively close proximity to the engine produced a weak vortex that was ingested by the engine. This resulted in losses in fan and low-pressure compressor performance.

The performance deterioration for each of the four engines followed in the PIC program was determined starting with the Production Acceptance Test data and applying corrections to it based on other testing to synthesize the data to an outdoor flight nacelle configuration. These data were compared to the measured deltas between Production Acceptance Test data and on-the-wing PIC data, and a comprehensive gas generator analysis was performed to assess modular performance changes required to close the two sets of data. These losses were then removed for the subsequent data analysis. Each subsequent PIC calibration was compared to the previous calibration, and an assessment of module performance changes based on an analysis of the gas generator parameter changes was made. Finally, the accumulative module performance losses were plotted versus engine cycles to establish the module and overall engine performance deterioration trends relative to the reference base line.

Based on comparisons of the three types of data, it may be concluded that ECM data provided a broad data base, in-flight performance calibrations provided better-controlled flight data, and PIC data provided accurate installed ground data in the same time frame as the in-flight calibrations.

3.4.2 Top Down Analysis of Prerepair and Postrepair Tests

The top down data analysis approach has been previously described in Reference 1, NASA report CR-135448, on historical data studies. To summarize, this approach uses a computer simulation of the JT9D engine which has been modified through the addition of special iteration balances. These iteration balances were used to modify efficiency and flow capacity levels for all components in order to match shifts in measured data parameters relative to the base-line production values for that particular engine. The measured data parameter shifts were obtained after correcting the engine test cell data, first for standard conditions of temperature and humidity, then for airline-to-engine manufacturer test cell differences (test cell corrections). The data were also corrected for differences in test configuration relative to production base-line (such as nozzles), and finally, for any retrofit part changes that have been made to the engine since the original production configuration. The test cell and configuration corrections used represent revisions based on recent P-695745 engine correlation testing and Pratt & Whitney Aircraft back-to-back testing of production and flight nozzles. The result of the analysis was a simulation point for the deteriorated engine,

26

listing all the component performance shifts required to match that particular set of data. The approach reduced the inherent inaccuracies of influence coefficient techniques that had traditionally been employed in performance deterioration analysis and could not properly account for nonlinear sensitivities and component interaction effects. The top down analysis procedure is schematically illustrated in Figure 9.

```
┌──────────────────┐          ┌──────────────────┐
│   Engine test    │          │  Modify computer │
│  data @ X cycles │          │ engine simulation│
├──────────────────┤          ├──────────────────┤
│    % ΔFn         │          │                  │
│    % ΔWf.        │          │    Add special   │
│    % ΔN₁, etc.   │          │ iteration balances│
└──────────────────┘          └──────────────────┘
         │                             │
         ▼                             │
┌──────────────────┐                   │
│  Analyze test    │                   │
│     data         │                   │
├──────────────────┤                   │
│ Iterates to match:│◄─────────────────┘
│    % ΔFn         │
│    % ΔWf         │
│    % ΔN₁, etc.   │
└──────────────────┘
         │
         ▼
┌──────────────────┐
│Component variations│
│   calculated     │
├──────────────────┤
│   Δ η fan        │
│   % Δ fan FC     │
│   Δ η LPC,       │
│   etc.           │
└──────────────────┘
```
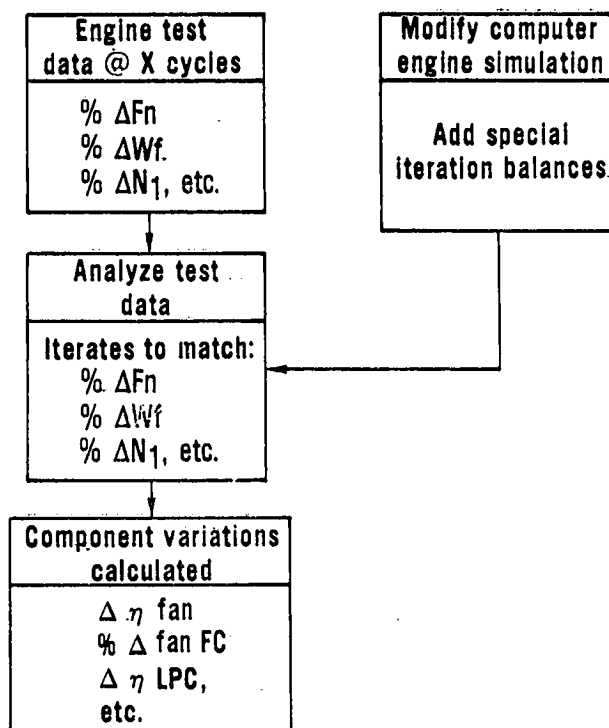
Figure 9 Flow Diagram for "Top Down" Analysis - Top down analysis begins with measured engine performance parameter changes and utilizes the JT9D engine simulation to analyze the module performance losses required to match the performance data.

In general, the test cell data analysis of JT9D-7A(SP) engine performance changes includes measurement of P_{t2}, T_{t2}, P_{t3}, T_{t3}, P_{s4}, T_{t4}, T_{t6}, P_{t7}, T_{t7}, N1, N2, thrust, and fuel flow. In theory, this was a sufficient number of parameters to permit independent determination of efficiency and flow capacity for all five component modules. Table VII illustrates the top down iteration logic required. It should be pointed out that although the iteration balances were specified in

27

terms of variable pairs (for example, vary A6 to converge Tt6), the final solution incorporates all variable interactions (i.e., effect of A5 and other flow capacities and efficiencies on Tt6).

TABLE VII

ENGINE SIMULATION ITERATION LOGIC FOR TOP DOWN APPROACH

Observed Parameter Shifts	Component Variable Iterated
Percent Change in N_1	Percent Change in Fan Flow Capacity
Percent Change in N_2	Percent Change in High-Pressure Compressor Flow Capacity
Percent Change in P_{t3}/P_{t2}	Percent Change in Low-Pressure Compressor Flow Capacity
Percent Change in P_{s4}/P_{t7}	Percent Change in High-Pressure Turbine Inlet Area
Change in T_{t3}	Change in Low-Pressure Compressor Efficiency
Change in T_{t4}	Change in High-Pressure Compressor Efficiency
Change in T_{t6}	Percent Change in Low-Pressure Turbine Inlet Area
Change in T_{t7}	Change in Low-Pressure Turbine Efficiency
Percent Change in Fuel Flow	Change in High-Pressure Turbine Efficiency
Percent Change in Net Thrust	Change in Fan Efficiency

In practice, however, because both Tt6 and Tt7 for individual engines were subject to significant radial and circumferential profile effects which masked, biased, or otherwise distorted the true thermodynamic average temperature at these locations. Therefore, it was generally found to be necessary to "couple" fan efficiency and flow capacity as well as low-pressure turbine efficiency and flow capacity. Table VIII shows the modified top down iteration logic required because of Tt6 and Tt7 accuracy limitations. This iteration logic was used for analysis of

the test data. The concept of coupling was developed in the historical data analysis efforts where the number of parameters measured was not adequate to define the unknowns. Briefly, it involves using a known quantitative relationship between efficiency and flow capacity change for a given component, thus, the term "coupling." was used. Generally, this relationship had been obtained from component rig testing where tip clearance was varied, or from back-to-back testing where modules were "swapped."

TABLE VIII

MODIFIED ENGINE SIMULATION ITERATION LOGIC USED IN ANALYSIS

Observed Parameter Shifts	Component Variable Iterated
Percent Change in N_1	Percent Change in Fan Flow Capacity (Coupled to Fan Efficiency)
Percent Change in N_2	Percent Change in High-Pressure Compressor Flow Capacity
Percent Change in P_{t3}/P_{t2}	Percent Change in Low-Pressure Compressor Flow Capacity
Percent Change in P_{s4}/P_{t7}	Percent Change in High-Pressure Turbine Inlet Area
Change in T_{t3}	Change in Low-Pressure Compressor Efficiency
Change in T_{t4}	Change in High-Pressure Compressor Efficiency
Percent Change in Fuel Flow	Change in High-Pressure Turbine Efficiency
Percent Change in Net Thrust	Change in Low-Pressure Turbine Efficiency (Coupled to Low-Pressure Turbine Inlet Area

The analysis of a single engine test was subject to uncertainty for reasons discussed previously under Section 3.2. Much of the problem involves the inability of the production instrumentation to measure true average conditions as a result of limited instrumentation locations. Shifting profiles as a result of test cell interactions and

part changes during repair served to accentuate this problem. In order to minimize error, an integral part of the data analysis methodology was to perform both prerepair and postrepair testing whenever possible, and obtain records of repairs performed and rebuild clearances, plus any available information on part condition at teardown.

The procedure then used was to vary the tolerances, or closure accuracy, of the computed parameters with the test cell data parameters, so that the differences between prerepair and postrepair analyses reflected the known repairs performed. In particular, those modules on which no repair had been performed should have the same computed performance levels for both prerepair and postrepair analyses, while performance improvements were generally to be expected in those components which had been repaired or replaced. Except for Tt6 and Tt7, the closure tolerances between analysis and the observed data were nearly always well within the instrumentation accuracies discussed for the measured parameters.

An example of how the top down analysis was performed for a particular engine is shown in Tables IX through XIV. The JT9D-7A(SP) engine selected for the example is P-695745. The engine history is shown in Table IX. Following removal for high exhaust gas temperature (EGT), the engine was prerepair tested at Pratt & Whitney Aircraft, and an extensive teardown was performed prior to repair. The engine was then repaired and postrepair tested at Pratt & Whitney Aircraft. The engine was then shipped to Pan American and postrepair tested there. The test data analyzed for this engine is from the prerepair and postrepair testing at Pratt & Whitney Aircraft. Table X presents the results of the teardown inspection following prerepair testing. Fan rub and minor foreign object damage (FOD) was observed, as well as low-pressure compressor rub-strip wear, burner distress, and high-pressure turbine damage. The top-down analysis of the prerepair data is shown in Table XI. When the simulation was run with all iteration balances (Table VII), there was no thermodynamic solution which matched the data with acceptable accuracy. Similarly, when the Tt7 balance was eliminated (low-pressure turbine efficiency iterated on thrust and fan efficiency coupled to fan flow capacity) there was no thermodynamic solution. The iteration balance on Tt6 had to be eliminated to obtain an analysis which gave acceptable closure with the data, because the measured Tt6 differed significantly from the true average value. The resulting analysis showed (1) efficiency and flow capacity losses in the fan and low-pressure compressor, (2) high-pressure turbine efficiency loss and flow capacity increase, and (3) minor low-pressure turbine efficiency loss plus flow capacity increase.

Table XII summarizes repairs performed on the engine. Fan foreign object damage was blended and the rub strip replaced with a different

TABLE IX

HISTORY OF JT9D-7A(SP) ENGINE P-695745

o   Installed on aircraft N536PA, position 1, 11/18/76

o   Removed for high EGT, 4/20/78 with 4845 hours and 703 cycles

o   Returned to P&WA

    o   Prerepair tested 4/29/78

    o   Repaired per JT9D maintenance program instructions

    o   Postrepair tested 6/10 - 6/13/78

o   Delivered to PA

    o   Postrepair tested 6/19 - 6/20/78

    Installed on aircraft N534PA, position 1, 7/7/78

TABLE X

OBSERVATIONS DURING TEARDOWN OF JT9D-7A(SP) ENGINE P-795745

Fan -   Light erosion damage. 2 blades FOD damage. Avg rub depth 0.052".

LPC -   Blades and vanes good. Rubber OAS worn. 0.03" - 0.04" rub depth 3rd stage.

HPC -   Not disassembled. Borescope inspection showed slight feltmetal loss 9th stage. No other discrepancies.

Combustor - Axial cracking in vicinity of 3rd louvers.

HPT -   Slight leading edge blade erosion. Average blade tip erosion 0.010". Slight twist 2nd stage vanes. Rub and some smearing on 1st OAS. Knife edge rubs and microfin damage on 2nd OAS. Avg clearance 0.081" 1st stage; 0.043" 2nd stage.

LPT -   Not disassembled. No observable damage.

31

TABLE XI

DETAILED RESULTS OF PREREPAIR "TOP DOWN" ANALYSIS
JT9D-7A(SP) Engine P-695745 at Sea Level Static
Take-Off Conditions, EPR = 1.455

Parameter	Prerepair Test; 4-29-78; Rel. to Production *	Engine Simulation		
		(All Balances)	(Eliminate TT7 Balance)	(Eliminate TT6 Balance)
$\%\Delta$Fn	-0.8			-0.9
$\%\Delta$Wf	+0.4			+0.7
$\%\Delta$TSFC	+1.2			+1.6
$\%\Delta$N1	-0.4			-0.2
$\%\Delta$N2	+0.07			-0.2
ΔTt3, °C	+0.1	NO SOLUTION	NO SOLUTION	-0.1
ΔTt4, °C	-5.3			-3.5
ΔTt6, °C	+32.0			+8.7
ΔTt7, °C	+11.0			+11.0
$\%\Delta$Pt3/Pt2	-0.4			-0.2
$\%\Delta$Ps4/Pt7	-1.8			-1.7
$\Delta\eta$ Fan, pts				-0.3
$\%\Delta$ Fan, FC				-0.4
$\Delta\eta$ LPC, pts				-0.2
$\%\Delta$ LPC, FC				-0.3
$\Delta\eta$ HPC, pts				--
$\Delta\eta$ HPT, pts				-0.9
$\%\Delta$ A5				+1.4
$\Delta\eta$ LPT, pts				-0.2
$\%\Delta$ A6				+1.5

*Adjusted to remove smoke probe and for +1% PT3/PT2 profile.

TABLE XII

SUMMARY OF REPAIRS ON JT9D-7A(SP) ENGINE P-695745

Module		Repair Performed
Fan	-	OAS replaced with axial skewed groove configuration. Repair FOD. Avg clearance 0.138".
LPC	-	New OAS. Avg. Clearances - 2nd
0.067", 3rd 0.032", 4th 0.043.		
HPC	-	No repair.
Combustor - Replace with mod 2 liners.		
HPT	-	New 1st stage blades and 2nd stage vanes. Replace 2 - 2nd stage blades.
		Rebuild 2nd OAS segments with new
honeycomb.		
		Avg clearance - 1st
stage 0.0675".		
		- 2nd
stage 0.041".		
LPT	-	No repair

TABLE XIII

DETAILED RESULTS OF POSTREPAIR "TOP DOWN" ANALYSIS
JT9D-7A(SP) Engine P-695745 at Sea Level Static Take-Off Conditions, EPR = 1.455

Parameter	Postrepair Test; 6-13-78; Rel. to Production	Engine Simulation			
		(All Balances)	(Eliminate Tt7 Balance)	(Eliminate Tt6 Balance)	(Eliminate Tt6 & Tt7 Balance)
%ΔFn	-0.7		-0.3	-0.7	-0.9
%ΔWf	-0.5		-0.7	-0.5	-0.3
%ΔTSFC	+0.2		-0.3	+0.2	+0.6
%ΔN1	-0.4		-0.4	-0.4	-0.3
%ΔN2	+0.8		+0.8	+0.8	+0.8
ΔTt3, °C	-0.5	N	-0.4	-0.8	-0.2
ΔTt4, °C	--	O	-0.3	-2.2	-1.0
ΔTT6, °C	-13.0		-9.7	+2.7	-2.2
ΔTt7	+16.0	S	-6.9	+16.0	+1.1
%ΔPt3/Pt2	-1.1	O	-1.0	-1.1	-1.1
%ΔPs4/Pt7	-1.5	L	-1.6	-1.5	-1.2
		U			
Δη Fan, pts		T			
%Δ Fan FC		I	+0.06	+6.0	-0.2
Δη LPC, pts		O	+0.1	+0.1	-0.3
		N	-0.2	-0.5	--
%Δ LPC, FC					
Δη HPC, pts			+0.9	-0.8	--
Δη HPT, pts			--	--	-- --
			+2.0	1.0	-- --
%Δ A5					
Δη LPT, pts			+2.5	+0.6	+1.2
%Δ A6			-0.4	-2.9	--
			+2.0	+2.3	±1.5

*Adjusted to remove smoke probe and for +1% Pt3/Pt2 profile.

TABLE XIV

COMPARISON OF PREREPAIR-TO-POSTREPAIR MODULE PERFORMANCE IMPROVEMENTS
JT9D-7A(SP) Engine P-695745

Module	Repair Performed	Change in Module Performance	
		Pts	% FC
Fan	New OAS (axial skewed groove); repair FOD	+0.1 —	+0.1
LPC	New OAS	+0.2	— +0.32
HPC	None	- -- -	- - -
Combustor	Replace Mod 5 liners with Mod 2 —	- -- -	- - --
HPT	New 1st stage blades and 2nd stage vanes. Rebuild 2nd OAS	+0.9—	—0.2
LPT	None	+0.2	- - —

(Burner profile)

type. Low-pressure compressor outer airseals were replaced, the Mod. 5 combustor liners replaced with Mod. 2, and the high-pressure turbine was rebuilt. No repairs were performed to the high-pressure compressor or the low-pressure turbine. The analysis of the postrepair-test data is shown in Table XIII. When all iteration balances are used, there was again no solution to the data with acceptable accuracy. If the Tt7 balance was eliminated, there was a solution as shown. However the solution was not believable since inspection of high-pressure turbine build clearances indicates that efficiency could be at most 0.1 to 0.2 points better than production levels. Also, a low-pressure compressor flow capacity that was significantly better than new was not credible. When the Tt6 iteration balance was eliminated, there was an approximate solution, but the performance levels of the fan and low-pressure turbine are not believable (fan much better than new, and low-pressure turbine considerably worse than prerepair, even though no repairs were performed on that module). In order to obtain an acceptable analysis of this data, both the Tt6 and Tt7 balances had to be eliminated, and the fan efficiency had to be coupled to its flow capacity as previously described. In other words, circumferential/radial profile changes have masked the true average values of both Tt6 and Tt7 in the postrepair data. The resulting final analysis is shown in the right hand column. The fan still showed minor

losses, but low-pressure compressor performance had been improved to the original level. High-pressure turbine efficiency had been recovered, but some flow capacity increase was still shown (a portion of this increase was due to decreased burner pressure loss, as described below). A minor improvement in low-pressure turbine efficiency was noted relative to prerepair; this improvement was explainable in terms of the burner change from Mod. 5 to Mod. 2 (shifted radial temperature profile inward, which resulted in tighter low-pressure turbine clearances). It should be noted that there was a minor improvement in burner pressure loss associated with this change also. In this analysis, and those which follow, any change in burner pressure loss has been combined with the predicted high-pressure turbine flow capacity change as indicated above. Table XIV summarizes by module the repairs performed, together with the analyzed prerepair and postrepair performance changes. Good agreement between the two is shown. The analyses were felt to be credible because they show good agreement with observed part condition and repairs performed, even though some data parameters had to be rejected (Tt6 prerepair, Tt6 and Tt7 postrepair). In general, neither Tt6 nor Tt7 could be used for most of the prerepair and postrepair analyses performed. In a few cases, low-pressure compressor efficiency and flow capacity were coupled (drop Tt3 balance), because of profile effects at Station 3.

SECTION 4.0

RESULTS AND DISCUSSIONS

This section of the report has two primary parts: overall engine performance deterioration, and engine module performance deterioration. The deterioration data were obtained and analyzed over the period from February 1977 to February 1979. Overall engine performance deterioration was acquired from four sources which are described in detail in Section 3.0, Data Acquisition and Analysis Methodology. These sources were Engine Condition Monitoring (ECM), In-Flight Calibration, Prerepair and Postrepair Tests, and Plug-In Console (PIC) Tests. Engine module performance was analyzed from only the Prerepair and Postrepair Tests and the PIC Tests inasmuch as the other data sources did not include the instrumentation necessary to determine module performance. Each of the sources of data covered a range of engine cycles and times. Table XV summarizes the engine cycles/times associated with the data from each source.

TABLE XV

SUMMARY OF ENGINE CYCLES/TIME
FOR EACH SOURCE OF PERFORMANCE DATA

Data Source	Approx. Range of	
	Cycles	Time (hours)
Engine Condition Monitoring	25 - 2300	100 - 12000
In-Flight Calibration	10 - 1000	20 - 6900
Prerepair and Postrepair Tests	700 - 2100	4800 - 12000
Plug-In Console Tests	1 - 1000	0 - 6900

4.1 OVERALL ENGINE PERFORMANCE DETERIORATION RESULTS

The presentation of the overall engine performance deteriortion results are, in general, given in the order of data quality. The ECM and In-Flight Calibration data results are presented first because the data were subject to scatter and variations which precluded any substantive conclusions. Then the Prerepair and Postrepair and PIC Test data, the quality of which is considered very good, are presented.

4.1.1 Engine Condition Monitoring Data

A detailed description of the methods and procedures for obtaining the ECM data is given in Section 3.0. As described in this section, ECM

data for an individual engine required statistical treatment of the data in order that parameter plots, such as fuel flow or EGT versus engine flight cycles, yield reasonably smooth trend variations. Even then, parameter variations with engine cycles is somewhat erratic as shown in Figures 10 and 11 where the changes in fuel flow (Wf) in percent and the changes in exhaust gas temperature (EGT) in $^{\circ}C$ are plotted as functions of engine flight cycles for the 32 747(SP) engines studied and tested during this investigation. The base-line, or zero, value represents the JT9D-7A engine gas generator values obtained from the Boeing Performance Engineers Manual.
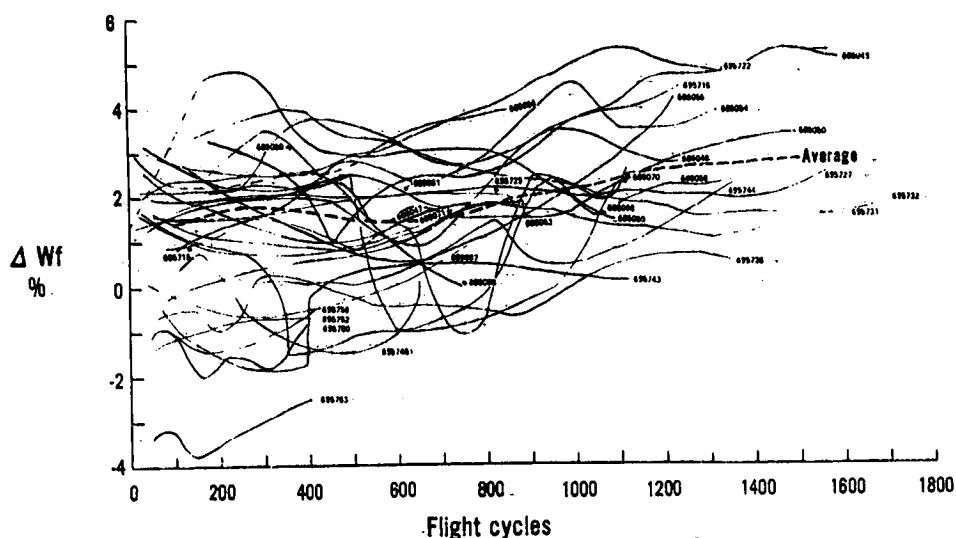
Figure 10   ECM Plot of Change in Fuel Flow with Usage - Data from 32 Pan American JT9D-7A(SP) engines through the first removal results in a relatively constant average fuel flow to about 750 cycles (average does not include the last four engines).

Dashed lines representing the average values are shown on these two figures. These average values show a 1.3 percent and a 20°C increase in fuel flow and exhaust gas temperature, respectively, over the first 1500 cycles (approximately two years) for this particular group of JT9D-7A engines.

Some of the variations shown in Figure 10 and 11 are believed to result from instrument error and nonuniform extraction of engine bleed air among the engines. (A discussion of the nonuniform extraction of engine

38

bleed is given in Appendix A.) Averaging the results from each airplane, which attenuates these individual engine effects, yields the results presented in Figures 12 and 13 where fuel flow change in percent and exhaust gas temperature change in ^{o}C are plotted as functions of engine flight cycles. The reason for the distinct levels, which for example shows airplanes N531, 532, 534, and 658 grouped together, is that changes in the engine configurations over the period of airplane delivery had different levels of performance. In addition, the installation of a Control Differential Transformer (that is, CDX) unit, which caused the indicated engine pressure ratio (EPR) setting at which fuel flow rate was being measured to be greater than the actual EPR, has the effect of reducing the measured fuel flow and exhaust gas temperature. The fewer flight cycles for airplanes N531 and N532 are associated with the time when the engines were removed for their first shop visit.
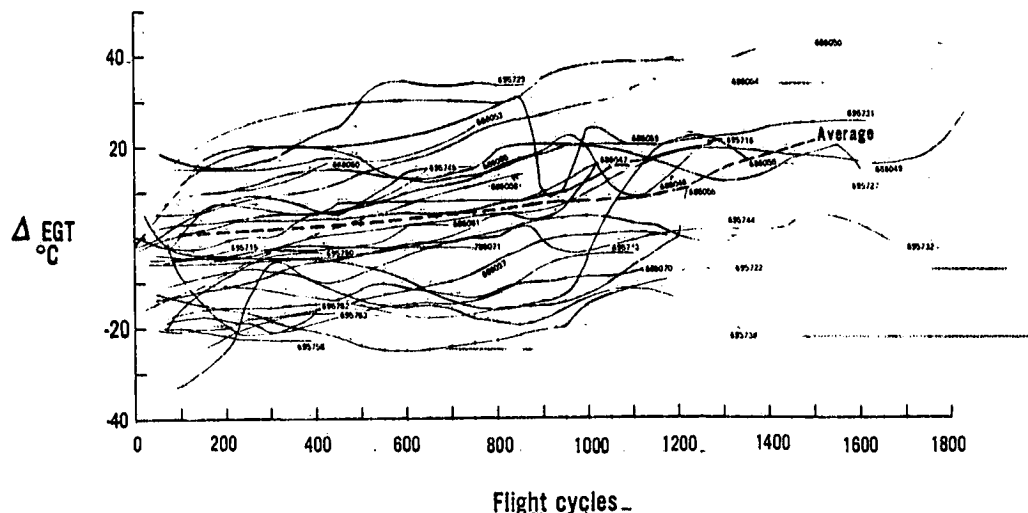
Figure 11   ECM Plot of Change in EGT with Usage -- Data from 32 Pan American JT9D-7A(SP) engines through the first removal results in a slowly increasing average EGT to about 1000 cycles (average does not include the last four engines)

Only data for 28 engines (seven airplanes) are shown in these figures because the other four engines had too few flight cycles to be representative.

One factor which is often thought to have an effect on engine deterioration is the effect of engine location (position) on the airplane. An example of the data examined to see if such an effect were prevalent is shown in Figures 14 and 15 where changes in fuel flow and

39

exhaust gas temperature are plotted as functions of engine flight cycles for each engine on one aircraft. These and similar data (starting at 25 flight cycles and above) did not show any discernible differences in performance deterioration effects between inboard (positions 2 and 3) and outboard (positions 1 and 4) engines.
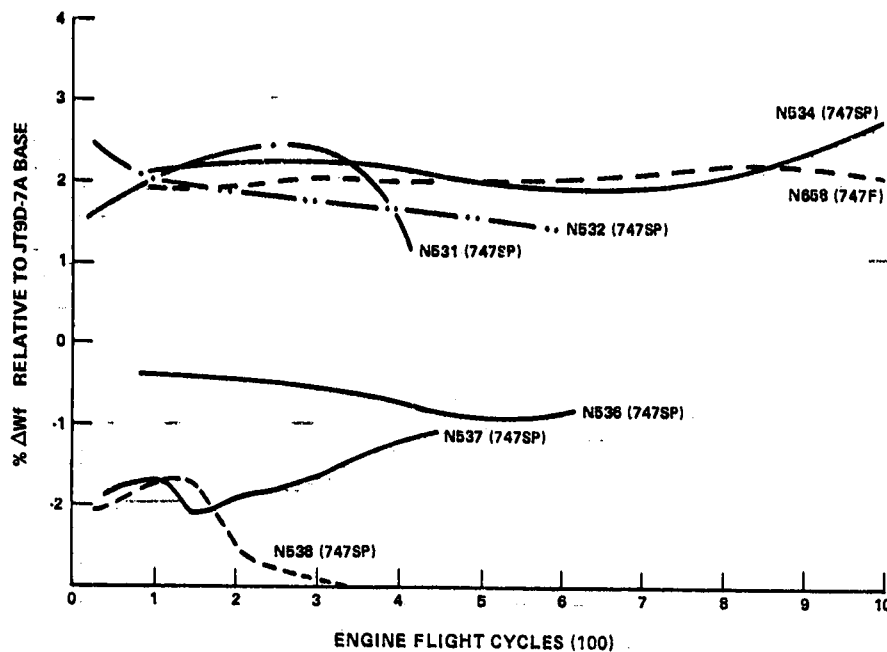
Figure 12   747SP Airplane Average Wf Performance Deterioration Trends Based on ECM Data - The four-engine average change in fuel flow as a function of usage shows little change at constant EPR between 100 and 1000 flights; the later configuration engines in airplanes N536PA and N537PA show better performance.

Another situation, which could contribute to different engine deterioration levels, is whether the engine is installed on the aircraft prior to aircraft acceptance tests or as a spare engine at the beginning or during revenue service. Discussions of the engine deterioration problem have led to the hypothesis that aircraft acceptance tests might have a significant impact on initial (or short-term) performance deterioration. The reason for this is that the acceptance tests are generally believed to be more severe than normal revenue service. The ideal approach would have been to compare a large data sample of spare and aircraft-delivered engines of the same engine model, operating in the same aircraft, and flying the same flight

40

cycles. Since such a data sample did not exist, the following two approaches were used to best compare the available data. In the first approach, the three comparisions shown in Table XVI were made.
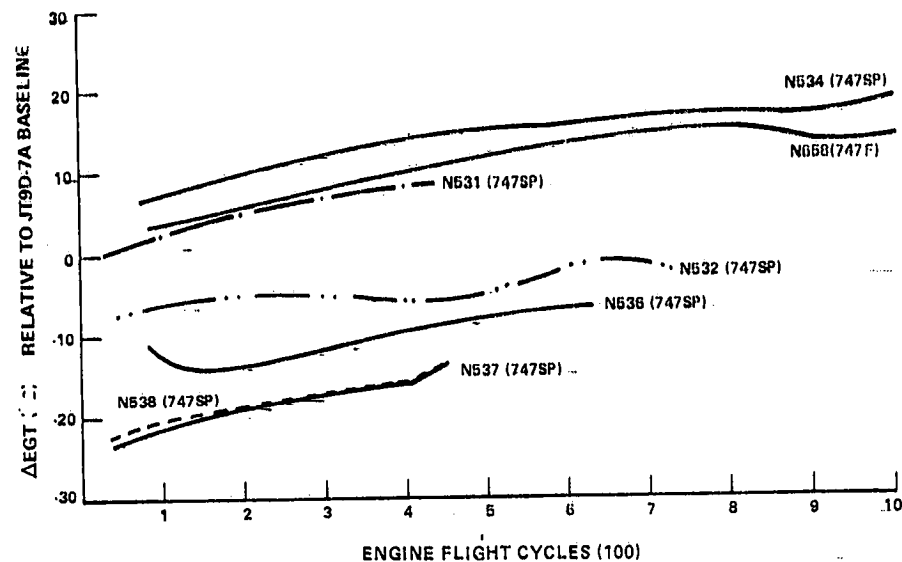
Figure 13   747SP Airplane Average EGT Performance Deterioration Trends Based on ECM Data – The four-engine average change in EGT as a function of usage shows similar trends for the airplanes used in the study.

In each of these cases, the spare engines were operated in the same aircraft, thus on the same route structure as the aircraft-delivered engines. Comparable ECM performance data (changes in fuel flow and exhaust gas temperature) from the earlier recorded revenue flight data out to the 800th engine flight cycle were plotted. In all cases, the data were from the first engine installation and prior to any repair.

Comparative plots of changes in fuel flow and exhaust gas temperature versus flight cycles for the three individual airline comparisons are shown in Figures 16, 17, and 18. The aircraft-delivered engine data are plotted as solid lines and the spare engine data as dashed lines. As with the data of the Pan American 747SP fleet presented in Figures 10 and 11, these data shown wide variations in performance levels and trends. The South African Airways and Iraqi Airlines data show the spare engine performance falling within the performance bands defined by the aircraft-delivered engines. the Northwest Orient Airlines data show the spares to have poorer initial performance but less increase in fuel flow with age.
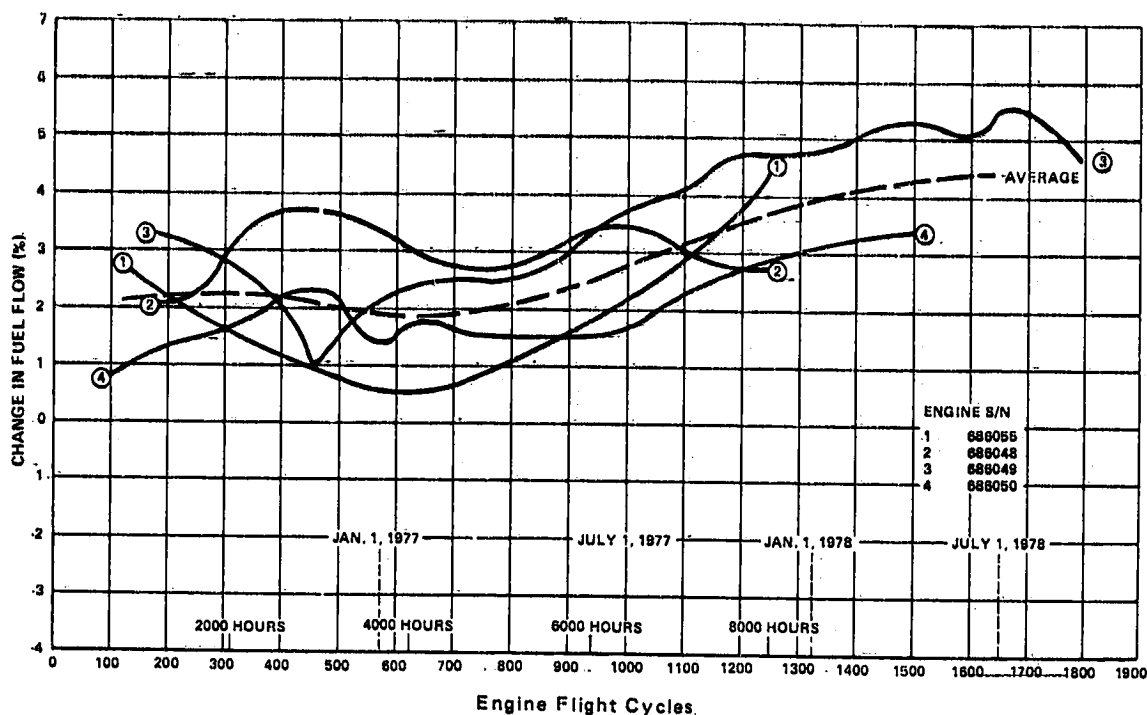
Figure 14   ECM Data from Pan American Airplane N534PA on Change in Fuel Flow with Usage - Early variations in individual trends are believed to be caused by airplane-induced effects; airplane average closely follows the fleet trend.

The second approach compared all of the available spare JT9D-7 engine ECM data with a representative sample of aircraft-delivered JT9D-7 engine ECM data. The advantage in this approach was a large data sample. The disadvantage was that the approach mixed engine models, aircraft, and airlines. Performance of 16 spare engines from eight airlines were compared with the ECM performance records of the first 28 Pan American 747SP aircraft-delivered engines which were collected in this study. In the second approach, the comparative plots for the 16 spare engines and the Pan American 747SP-aircraft-delivered engines are shown in Figures 19 and 20. The plots of change in fuel flow and exhaust gas temperature for the 16 spares generally fall within the bands defined by the 28 Pan American JT9D-7A(SP) engines and exhibit the same average trend with age. These bands were defined by the curves shown in Figures 10 and 11.

42
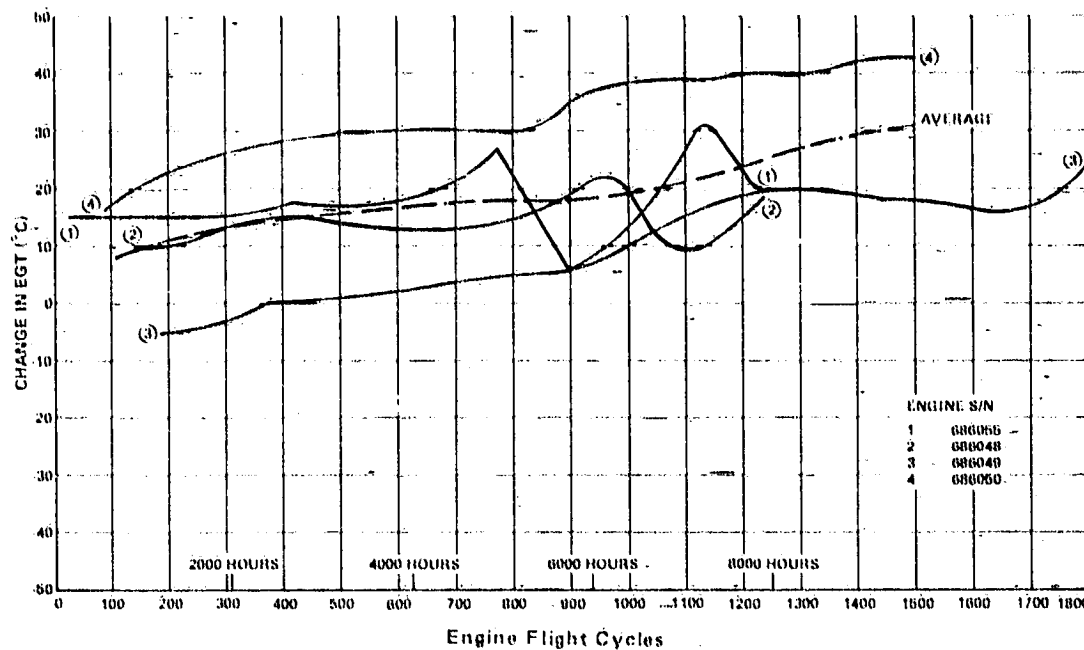
Figure 15   ECM Data from Pan American Airplane N534PA on Change in EGT with Usage - The shift in the EGT trends of engines 1 and 2 coincides with changes in the fuel flow slopes (Figure 14).

TABLE XVI

ENGINE COMPARISONS FOR THE FIRST APPROACH
SPARE VERSUS AIRCRAFT-DELIVERED ENGINES

Airline	Airplane/Engine	Number of Engines	
		Spare	Aircraft-Delivered
South African Airways	747SP/JT9D-7F	2	6
Iraqi Airlines	747/JT9D-7F	3	7
Northwest Orient Airlines	DC10-40/JT9D-20	?	6
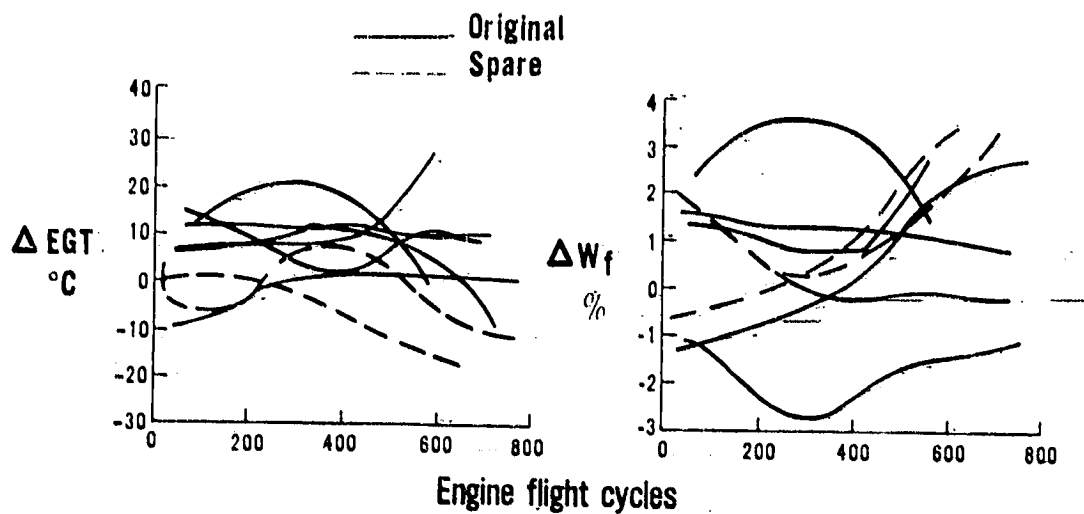
Figure 16 Aircraft-Delivered versus Spare Engine Performance Deterioration for South African Airways JT9D-7F Engines --Based on these data, it would appear that the EGT for the two spare engines improved with usage relative to the six airplane-delivered engines while the fuel flow for the spares increased with usage relative to the airplane-deliveread engines; these apparent trends conflict.
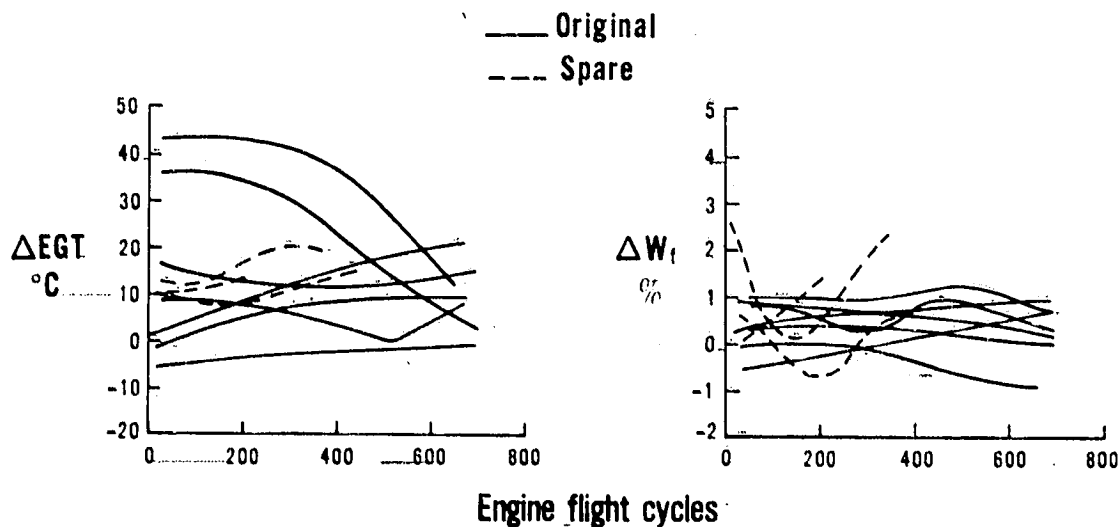
Figure 17 Aircraft-Delivered versus Spare Engine Performance Deterioration for Iraqi Airlines JT9D-7F Engines - The spare engine performance trends generally fall within the trends defined by the airplane-delivered engines; the performance for these spare engines appears to deteriorate slightly more after 150 cycles.

44-
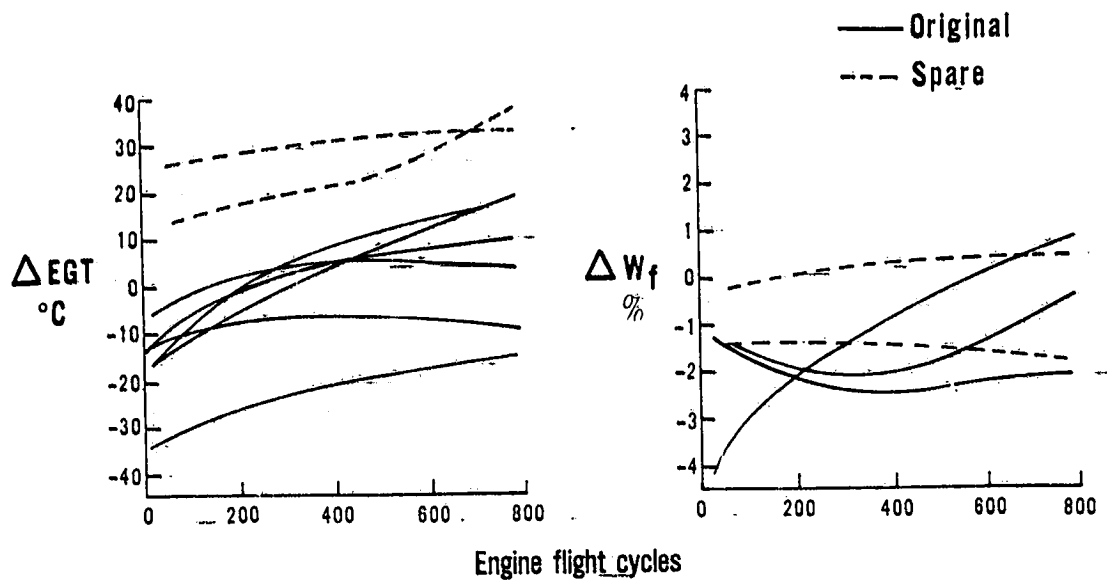
Figure 18. Aircraft-Delivered versus Spare Engine Performance Deterioration for Northwest Orient Airlines JT9D-20 Engines - The spare engines. exhibit poorer initial performance compared to the airplane-delivered engines, but the subsquent fuel flow trends are similar.
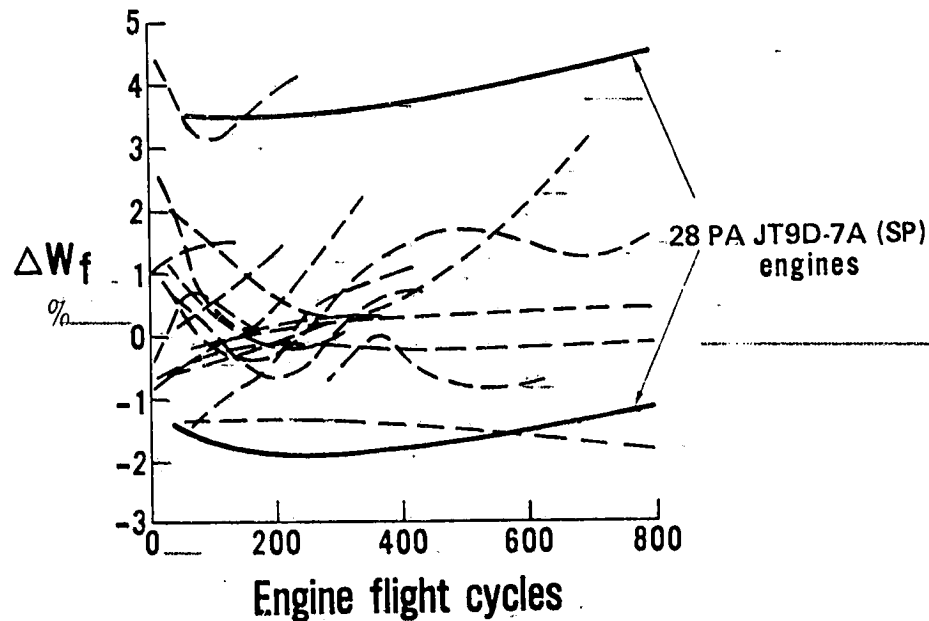
Figure 19 Performance Deterioration for 28 Pan American Airplane-Delivered JT9D-7A(SP) Engines versus 16 Spare Engines from Eight Airlines - The spare engines, operating over different routes and cycles, exhibit a similar band of fuel flow change to that defined by the airplane-delivered engines.

45

40 30 20 10 0 -10 -20 -30 -40

ΔEGT °C

28 PA JT9D-7A (SP) engines ___ ___

0   200   400   600   800

Engine flight cycles
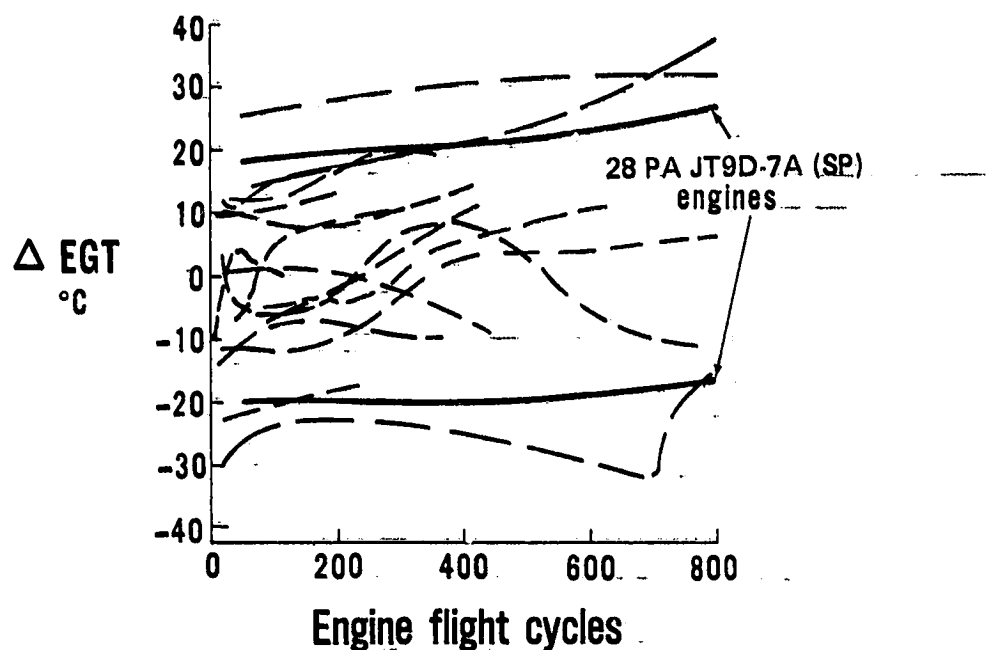
Figure 20.   Performance Deterioration for 28 Pan American Airplane-Delivered JT9D-7A(SP) Engines versus 16 Spare Engines from Eight Airlines - The spare engines, operating over different routes and cycles, exhibit a similar band of EGT change to that defined by the airplane-delivered engines.

The limited amount of data and the variations in the ECM are such that it would not support an accurate comparative performance analysis of spare and aircraft-delivered engines. However, the available data, while limited, shows no noticeable difference in early revenue performance between engines which were and were not part of the aircraft production acceptance testing.

4.1.2   In-Flight Calibration Data

These data were obtained from the same instrumentation as the ECM data. The only significant differences in the two types of data are that the in-flight calibration data were recorded by an observer specifically interested in the results, and that the parameters were treated statistically differently for the two types of data. In the case of the ECM data, the data scatter was handled by amassing large quantities of data. For the in-flight calibration data, engine parameters such as fuel flow, exhaust gas temperature, and low-pressure rotor speed were recorded systematically over a range of power settings and faired values of the engine parameters were then used. Typical data of this type for one engine are presented in Figures 21 and 22 where fuel flow,

46

exhaust gas temperature, and high- and low-pressure rotor corrected speeds are plotted as a functions of engine pressue ratio. Typical data scatter amounts to about $\pm 1/2$ to ± 1 percent for exhaust gas temperature and fuel flow and about ∓ 0.2 percent for high- and low-pressure rotor speeds. Cross plotting data of this type at an engine pressure ratio of 1.40 yielded results similar to those shown in Figures 23 and 24. These figures show the same parameters as a function of flight cycles for engine P-695738 on airplane N536PA. In this instance, the data scatter was at most only slightly greater than the base plots used to generate these figures.

Using data derived by the procedures just described, a comparison of ECM and in-flight calibration data for two airplanes, N536PA and N537PA is made in Figure 25 for the same four gas generator parameters previously discussed. In this instance, the data were averaged for the four engines on each airplane. The data have been normalized such that all parameters for each data source and airplane are equal at 100 cycles. These results show that the ECM and in-flight calibration data exhibit very similar trends. Variations that are evident are within the accuracy and repeatability of the data.

4.1.3 Prerepair and Postrepair Data

Prerepair data for JT9D-7A(SP) engines (12 tests) (see Table V) is presented in Figures 26 and 27. Changes in thrust specific fuel consumption (TSFC) and exhaust gas temperature (EGT) relative to production base-line values of each individual engine are plotted as functions of engine flight cycles. The last three digits of each engine's serial number is shown beside the appropriate data point. TSFC was measured at constant thrust, and EGT at take-off engine pressure ratio (EPR). All engines were tested at Pan American with the exception of P-686060 and P-695745 which were tested and repaired at Pratt & Whitney Aircraft. Fuel flow, thrust, and EGT measured in the test stand have been corrected using standard day, test stand, and configuration corrected factors as described in Section 3.4, Analysis Techniques. Additionally, the data for the P-686 series of engines have been adjusted for a package of engineering retrofit changes incorporated after the engines were flown in the certification flight test program prior to being introduced into commercial service. Data scatter is limited to about ± 1 percent in TSFC, indicating that TSFC deterioration for unrepaired engines should be fairly predictable. The average prerepair TSFC ranges from about 1 percent above production levels at 700 cycles to about +3.8 percent at 2000 cycles.

Figure 27 presents prerepair exhaust gas temperature for the JT9D-7A(SP) engines. Data scatter is partly attributable to the
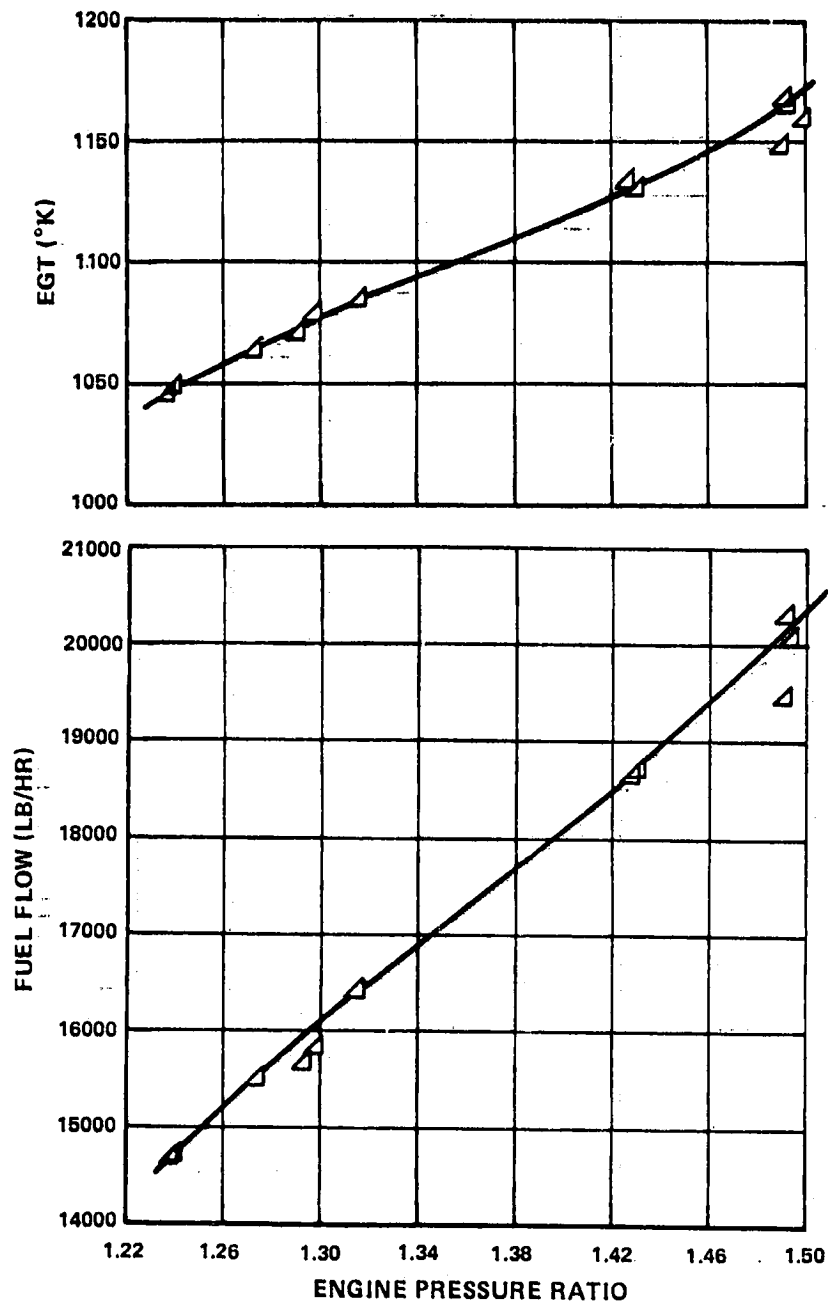
Figure 21   In-Flight Calibration Fuel Flow and Exhaust Gas
             Temperature Data as Functions of Engine Pressure Ratio
             for Engine P-695738 on Airplane N536PA Taken on May 21,
             1977 at 155 Hours/23 Cycles - The data show very little
             scatter over the range of power at which data were
             recorded.

48
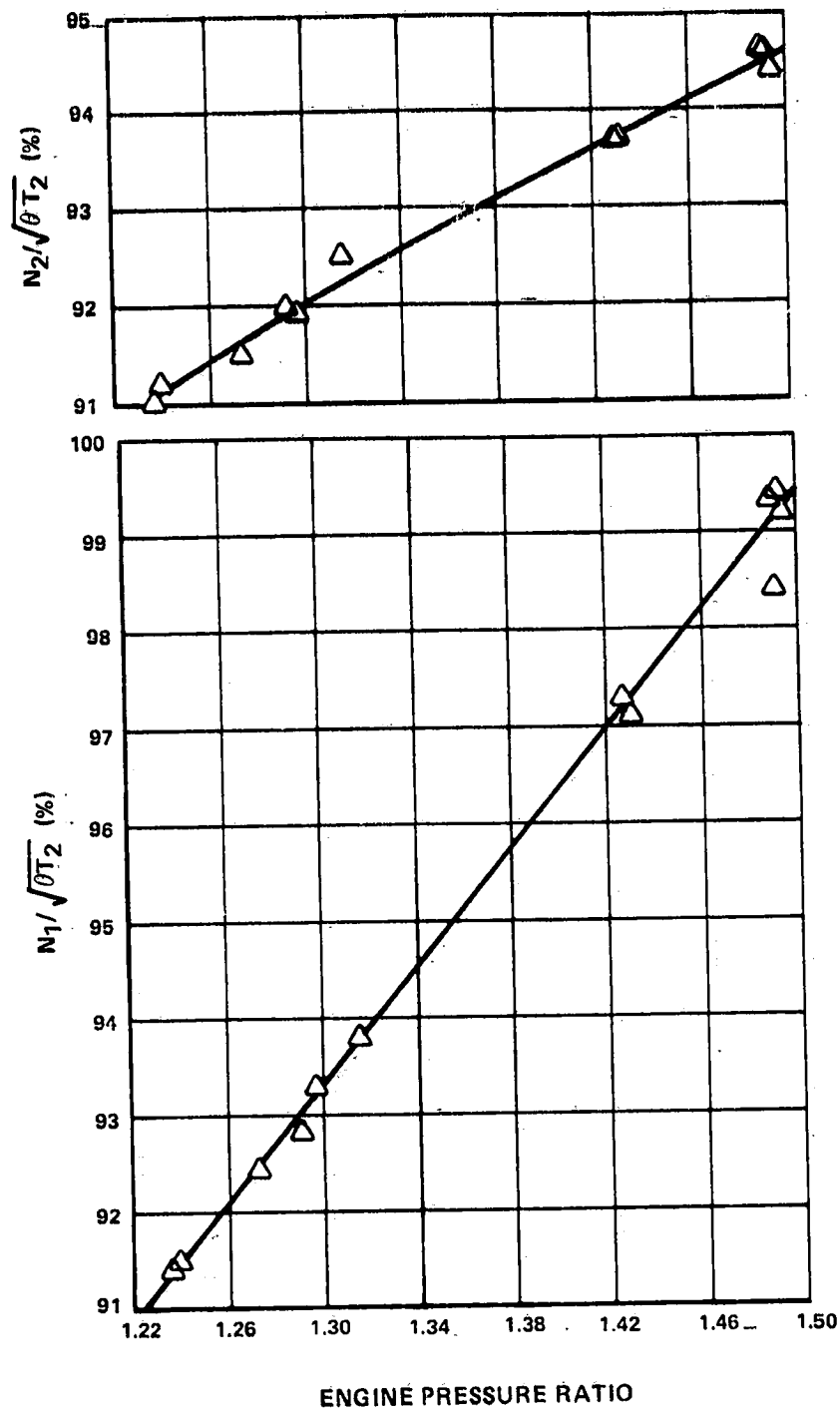
Figure 22   In-Flight Calibration Low- and High-Pressure Rotor Speed Data as Functions of Engine Pressure Ratio for Engine P-695738 on Airplane N536PA Taken on May 21, 1977 at 155 Hours/23 Cylcles - The data show very little scatter over the range of power at which data were recorded.
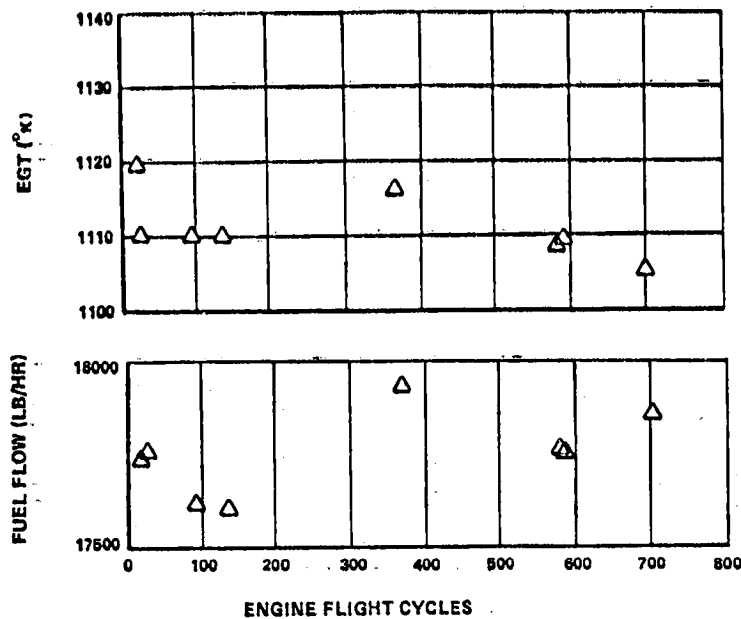
Figure 23 Fuel Flow and Exhaust Gas Temperature Data at EPR of 1.40 as
Functions of Cycles for All In-Flight Calibrations of Engine
P-695738 on Airplane N536PA. - The data scatter is only
slightly greater than the data scatter for individual engine
in-flight calibrations.
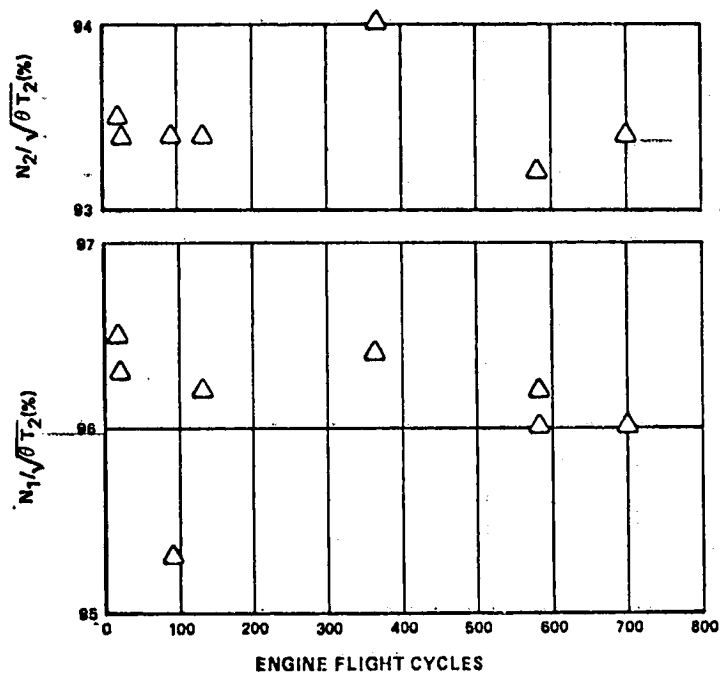
Figure 24 Low- and High-Pressure Rotor Speed Data as Functions of Cycles
for All In-Flight Calibrations of Engine P-695738 on Airplane
N536PA. - The data scatter is only slightly greater than the
data scatter for individual engine in-flight calibrations.

50
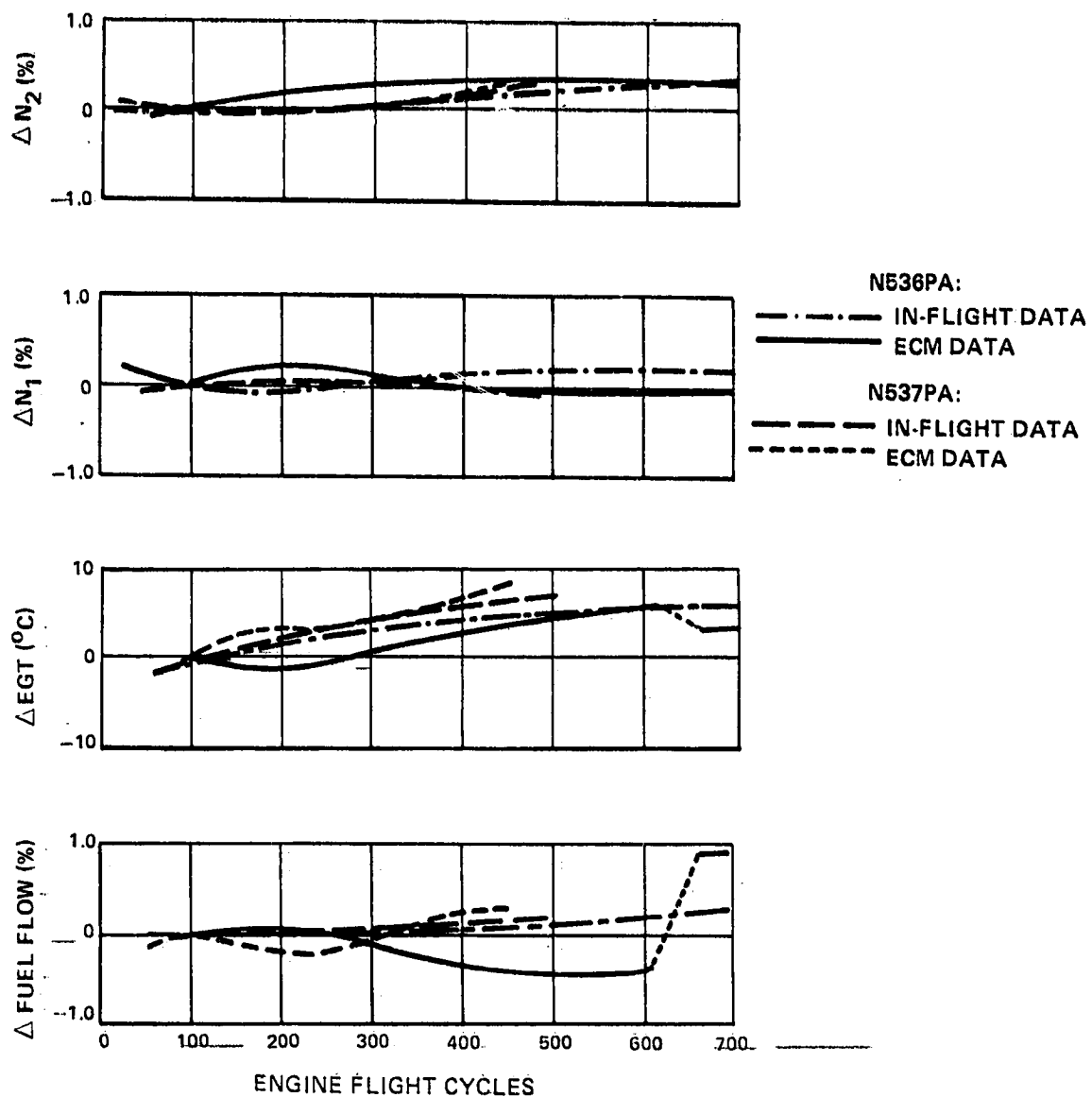
Figure 25   Comparison of Four-Engine Averages of Gas Generator
             Parameters as Functions of Cycles as Determined by
             In-Flight Calibrations and Engine Condition Monitoring of
             Engines on Airplanes N536PA and N537PA - The four-engine
             averages reduce the data scatter and improve the
             agreement between the two data sources.
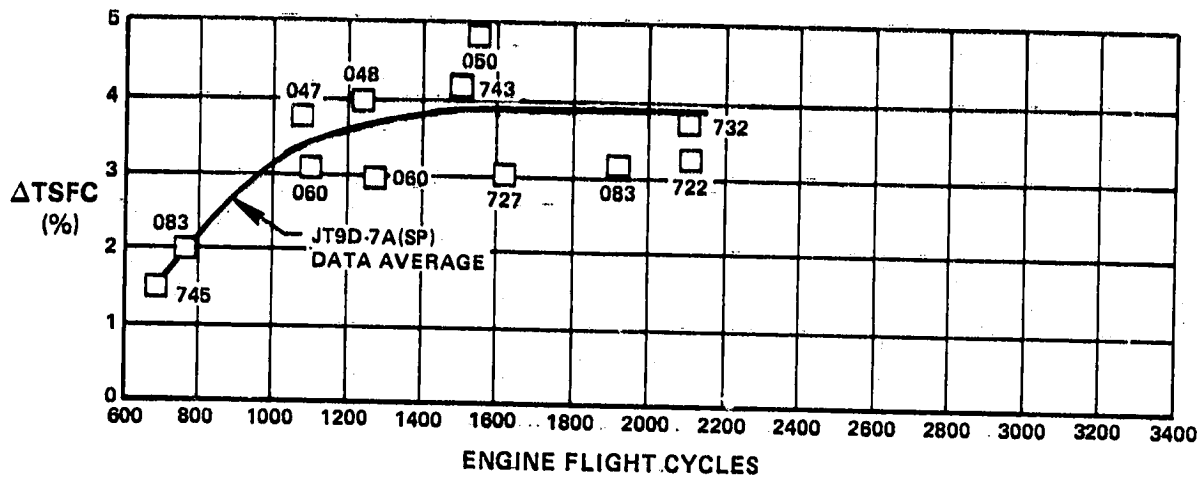
Figure 26   Long-Term Prerepair TSFC Deterioration, Measured at Constant Thrust, as a Function of Flight Cycles - The prerepair data are similar in trend and level to the average of the historical data.
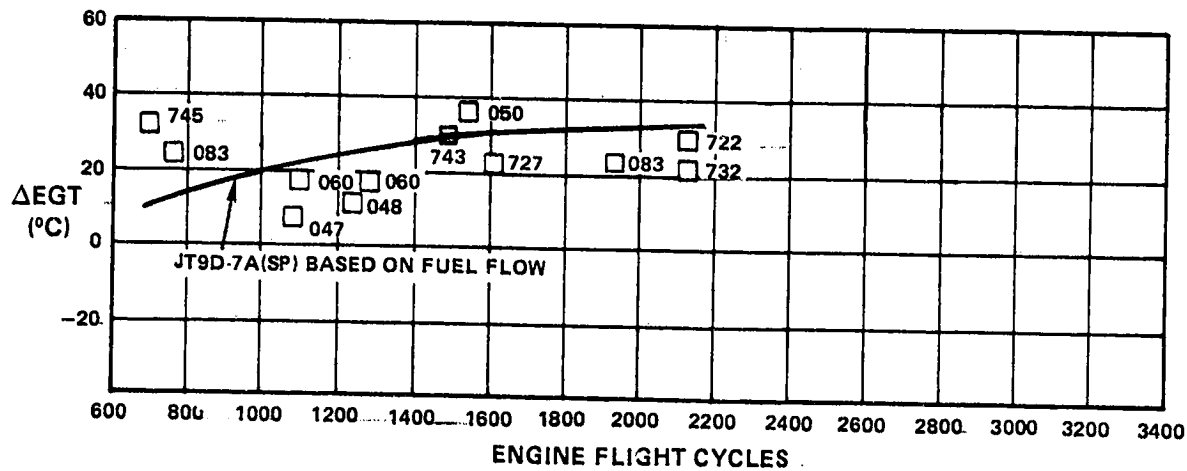
Figure 27   Long-Term Prerepair EGT Deterioration, Measured at Take-Off EPR, as a Function of Flight Cycles - After temperature profile adjustments were made, the prerepair data agrees well with the average of the historical data.

in-service engine temperature profile shifts. Because of these profile shifts and the limited data sample, the least squares fit of the data is slightly different from the true average obtained from fuel flow.

The postrepair data are presented in Figures 28 and 29 where TSFC and EGT are shown as functions of engine flight cycles for 18 engines (22 tests). Solid symbols are used for those engines for which prerepair data were shown in Figure 26 and 27. The postrepair TSFC data relative to production engine level varies from about +0.5 percent at 700 flight cycles to about +2.8 percent at 2000 cycles. There is somewhat more data scatter in the postrepair TSFC data than in the prerepair data. Even if all repairs were the same at a given engine cyclic age and if production quality parts and build standards were used, a small amount of increased scatter (less than 0.6 percent) could be attributed to production tolerances. However, all repairs are not the same at a given cyclic age. Swapping of deteriorated modules with other used or partially refurbished modules was common practice to expedite repairs. In addition, part quality differs from production quality because only selected individual parts are replaced in a module repair/refurbishment, and some parts may be repaired rather than replaced. Finally, repair build clearance limits are generally broader than production clearances. All of these factors tend to cause increased data scatter in postrepair TSFC results and make it difficult to construct postrepair average trends.

LEGEND
O ENGINES WITHOUT PREREPAIR DATA
● ENGINES WITH PREREPAIR DATA
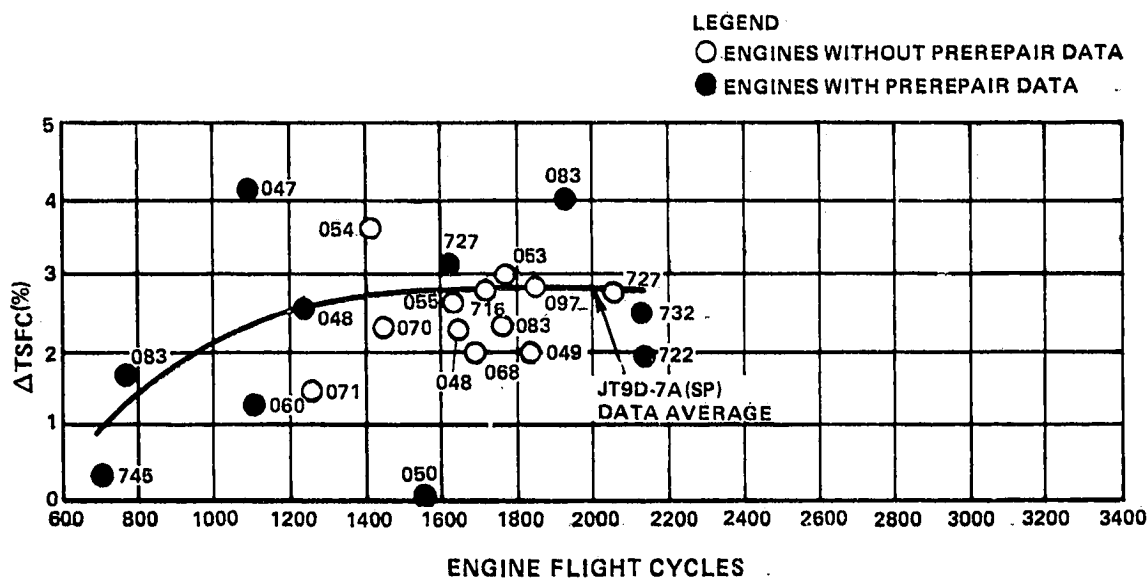
Figure 28   Long-Term Postrepair TSFC Deterioration, Measured at Constant Thrust, as a Function of Flight Cycles. - The postrepair data scatter shows results of a wide-range of repairs and broader repair build clearances.

53
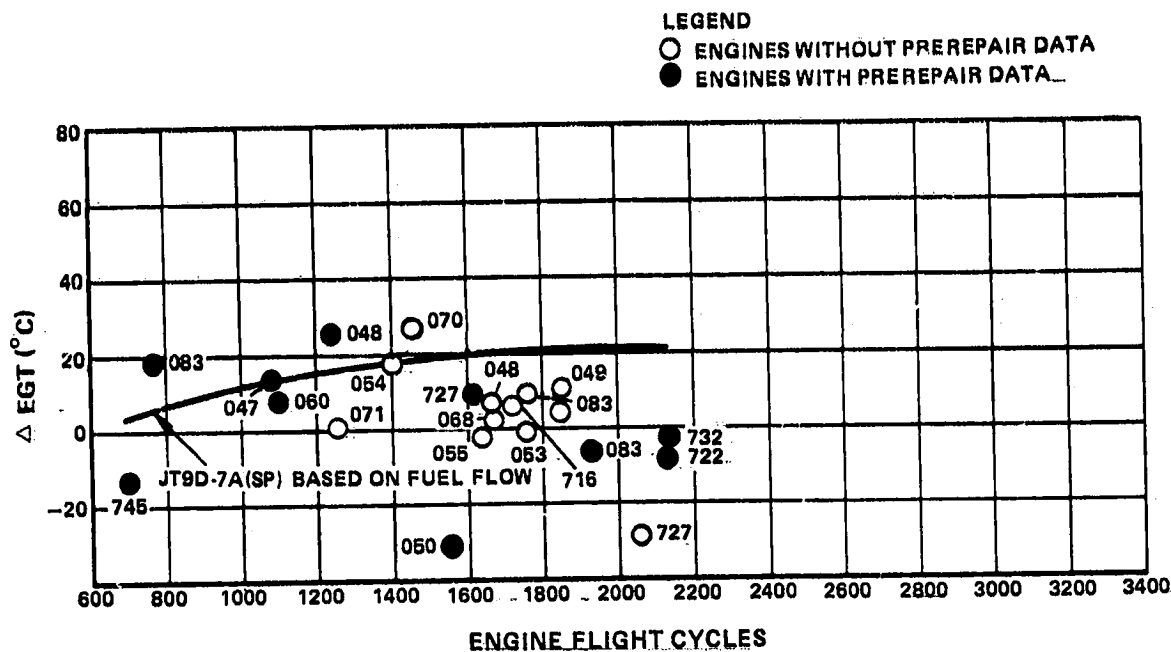
Figure 29   Long-Term Postrepair EGT Deterioration, Measured at Take-Off EPR, as a Function of Flight Cycles - The postrepair data agrees well, except for a degree of data scatter, with the average of the historical data.

The results of the prerepair/postrepair data are believed to have more credibility than the analysis results of the postrepair-only data. The greater credibility occurs because instrumentation, test stand correction, and data sampling uncertainties tend to be reduced through the process of iterating the analyses of prerepair/postrepair data until the results closely correspond to knowledge of actual part condition and repairs performed on the individual engines. This procedure is discussed in more detail in Section 3.4, Analysis Techniques.

The postrepair average exhaust gas temperature data (Figure 29) relative to the individual production engine level varies from +4°C at 700 flight cycles to about 21°C at 2000 cycles. Here again, considerable data scatter due to temperature profile shifts is evident. The profile changes are related to repairs performed; in particular, all engines had combustor liners replaced, in almost all cases by liners of a different type (Mod. 5 changed to Mod. 2). There is an average reduction in measured exhaust gas temperature of about 13°C associated with this burner liner change, based on Pratt & Whitney

Aircraft production data. The faired curve is the true average exhaust gas temperature determined from fuel flow and is about 13°C higher than a least squares fit of the measured data.

The curves presented in Figures 30 and 31 use the faired curves shown on the previous four figures to compare the prerepair and postrepair results. Figures 30 and 31 show changes in TSFC and EGT as functions of engine flight cycles. On average, repairs result in about a 1 percent reduction in TSFC and a 10°C reduction in EGT. As previously noted for an individual engine, considerable variation in this 10°C reduction can occur because of data scatter and the effect of temperature profile shift resulting from the repair.
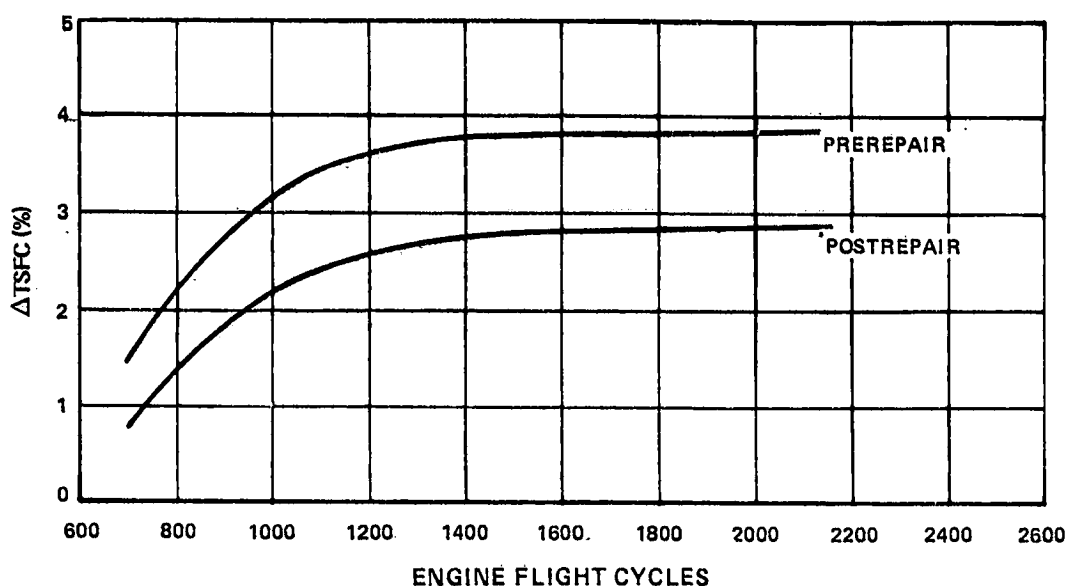
Figure 30   Long-Term TSFC Deterioration, Measured at Constant Thrust, as a Function of Flight Cycles; Comparison of Average Prerepair to Average Postrepair Performance - The repair process did not attempt to maximize performance restoration.

4.1.4   Plug-In Console (PIC) Data

PIC Data were obtained on four engines on two 747(SP) airplanes, engine P-695743 and P-695745 on airplane N536PA and engines P-695760 and P-695763 on airplane N537PA. The method of and schedule for data acquisition are discussed in detail in Section 3.0. In addition to the

standard PIC data acquisition, engine P-695743 was given special
treatment. After 1081 flight hours (141 cycles), the engine was
returned to Pratt & Whitney Aircraft's production test facility where
it was tested "as-received" in the original production test stand.
After water and detergent washing to remove surface contamination from
engine parts, and engine vane control trim, the engine was retested.
Next, the production engine cases were replaced with fully instrumented
engine cases and a performance test was run. An analytical teardown of
the engine followed during which the condition of all seals and other
parts which might affect performance was documented. The engine was
then reassembled and returned to service during which PIC data
collection was continued.
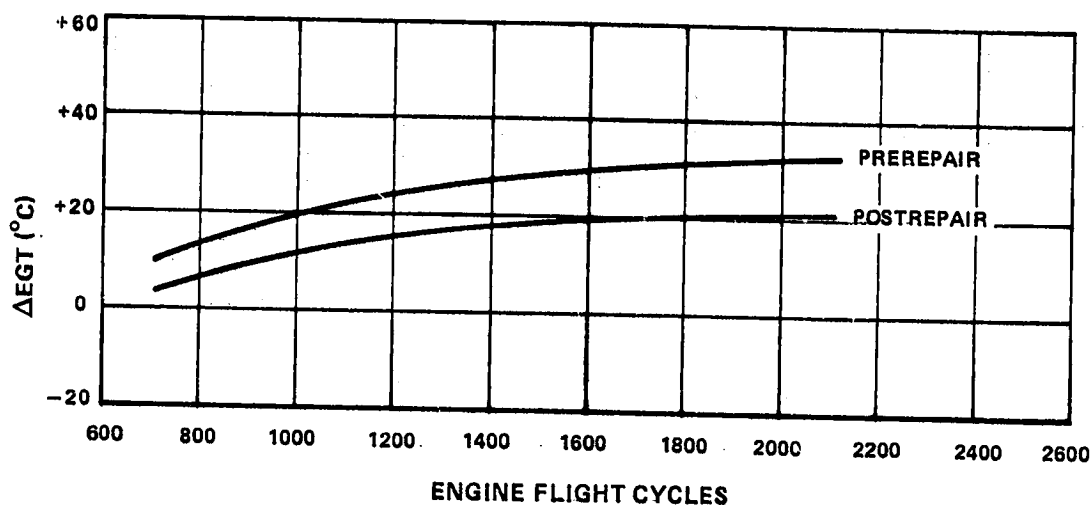
Figure 31   Long-Term EGT Deterioration, Measured at Take-Off EPR, as
             a Function of Flight Cycles; Comparison of Average
             Prerepair to Average Postrepair Performance -- An average
             of about 10°C in EGT is recovered as a result of repair.

In terms of overall engine performance deterioration, the "as-received"
engine had a TSFC increase (loss) of 1.5 percent. Water and detergent
wash plus vane control trim regained 0.3 percent of this loss. Because
thrust is not measured while acquiring PIC data and EGT is subject to
measurement problems associated with temperature profile shifts,
overall engine performance deterioration based on PIC data is obtained
by using the gas generator measurements to determine individual module
losses. An example of gas generator data is shown in Figures 32 through
37. These module losses in conjunction with module influence
coefficients can then be used to calculate TSFC and EGT. The results of
this approach is shown in Figures 38 and 39 where TSFC and EGT are

56

plotted as functions of engine flight cycles. TSFC increases rapidly at a rate of about one percent in the first 25 to 50 cycles and then more gradually to 2.2 percent at 1000 cycles. In a similar fashion, EGT increases 5 to 7°C after 25 to 50 cycles and then to about 10°C at 1000 cycles.

4.2 OVERALL ENGINE PERFORMANCE DETERIORATION COMPARISON

Now that the results of the various sources of performance deterioration data have been presented, a comparison of these results with the previously acquired historical deterioration data is given in the subsequent figures. Figure 40 shows a comparison of the ECM, in-flight calibration, and the PIC data. Changes in fuel flow, exhaust gas temperature, and low- and high-pressure rotor speeds are shown as functions of engine flight cycles. All data have been normalized at 100 flight cycles. The PIC data which were taken on the ground have been analytically corrected to altitude conditions. Agreement between the various data sources is reasonably good.

Prerepair performance deterioration data are shown in Figures 41 and 42 where the changes in TSFC in percent and EGT in °C are shown as functions of engine flight cycles. On these figures, the data sources included: PIC data, shown covering a range of flight cycles from 1 to 1000 cycles; historical data, obtained from a limited number of tests of engines returned to the manufacturer after 5 to 300 cycles; the one special prerepair data point at 141 cycles, obtained on engine P-695743 and discussed in Section 4.1.4; the prerepair data from the JT9D-7A(SP) fleet, covering a range from 700 to 2100 cycles; and the historical airline data, reported in Reference 1, over a range of engine flight cycles from 1200 to 3500 cycles. Data from the various data sources agrees quite well. The results show a rapid deterioration over the first 100 cycles where the change in TSFC increases over 1 percent and EGT rises to 7°C. The performance continues to deteriorate so that at 1000 cycles TSFC and EGT have increased 3 percent and 21°C, respectively, and at 2500 cycles these parameters are up 4.2 percent and 36°C, respectively. The sources and causes of this performance deterioration are discussed in detail in the next paragraphs where engine module performance deterioration is discussed.

The postrepair performance deterioration data are presented in Figures 43 and 44 where the changes in TSFC in percent and EGT in °C are shown as functions of engine flight cycles. The data sources are JT9D-7A(SP) fleet postrepair data and historical airline data from Reference 1.
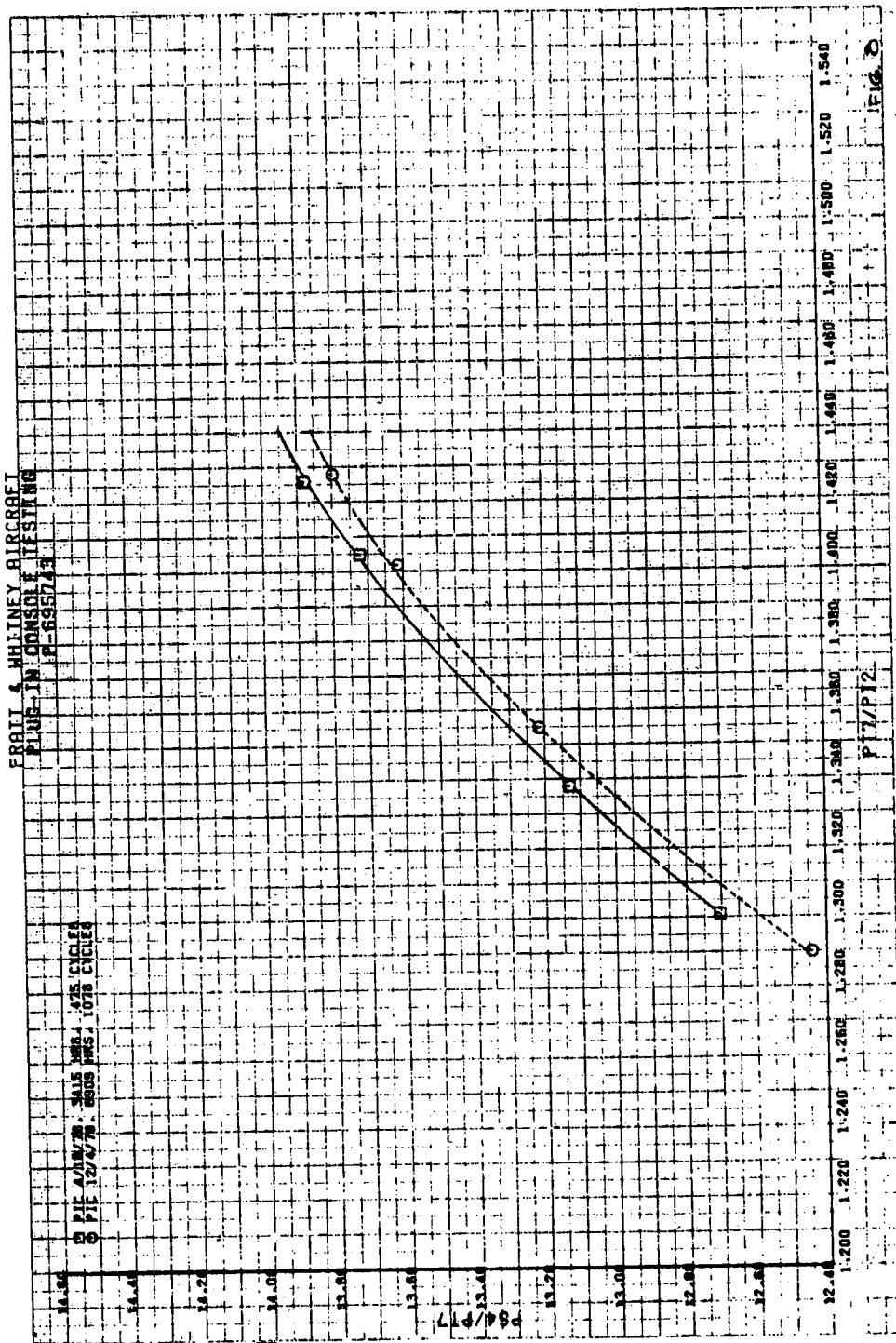
Figure 32 Typical Gas Generator Plot - Expansion ratio is plotted
as a function of EPR for two PIC calibrations of engine
P-695743 and used in the data analysis.

58
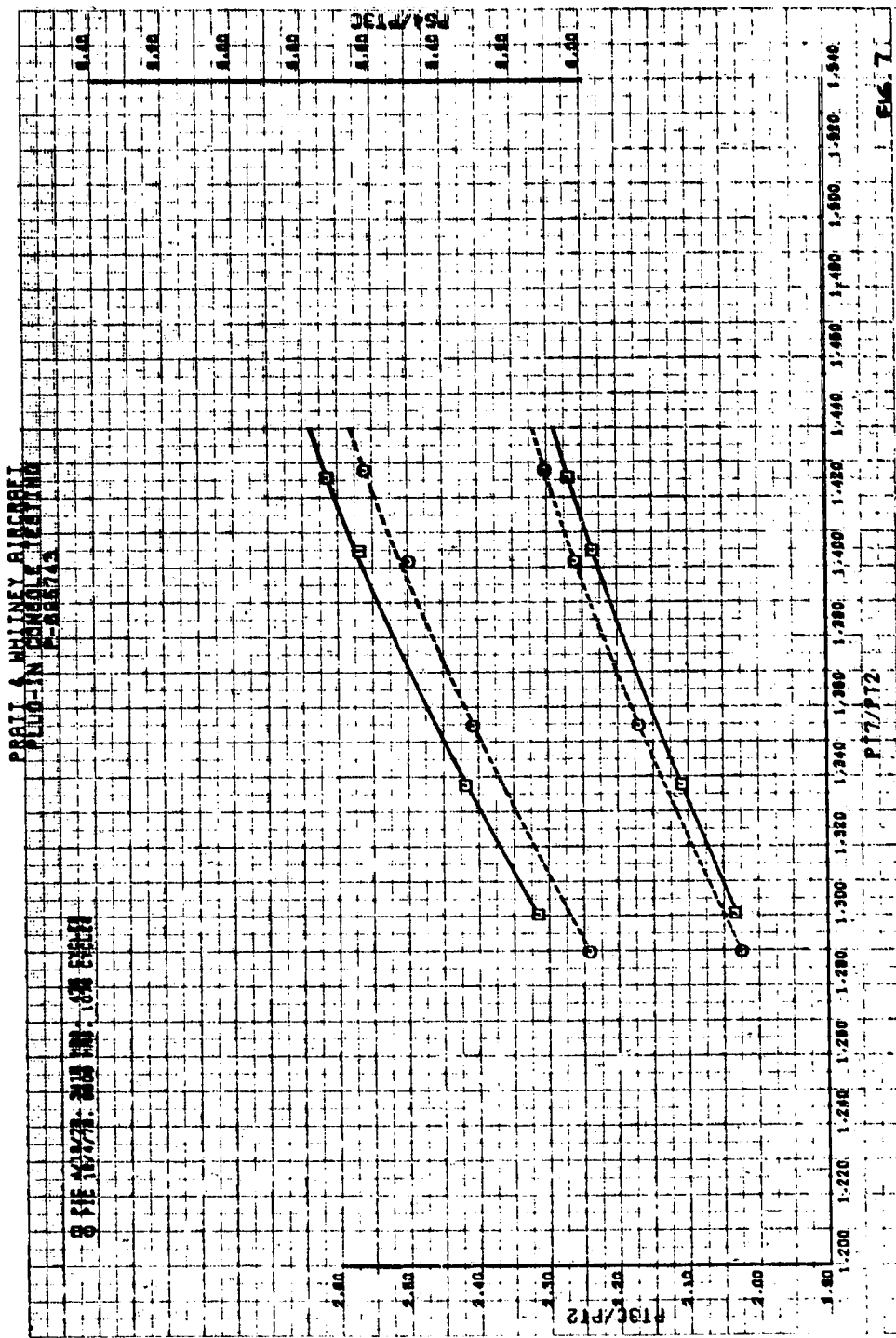
Figure 33 Typical Gas Generator Plot – Corrected low-pressure and high-pressure compressor compression ratios are plotted as functions of EPR for two PIC calibrations of engine P-695743 and used in the data analysis.

59
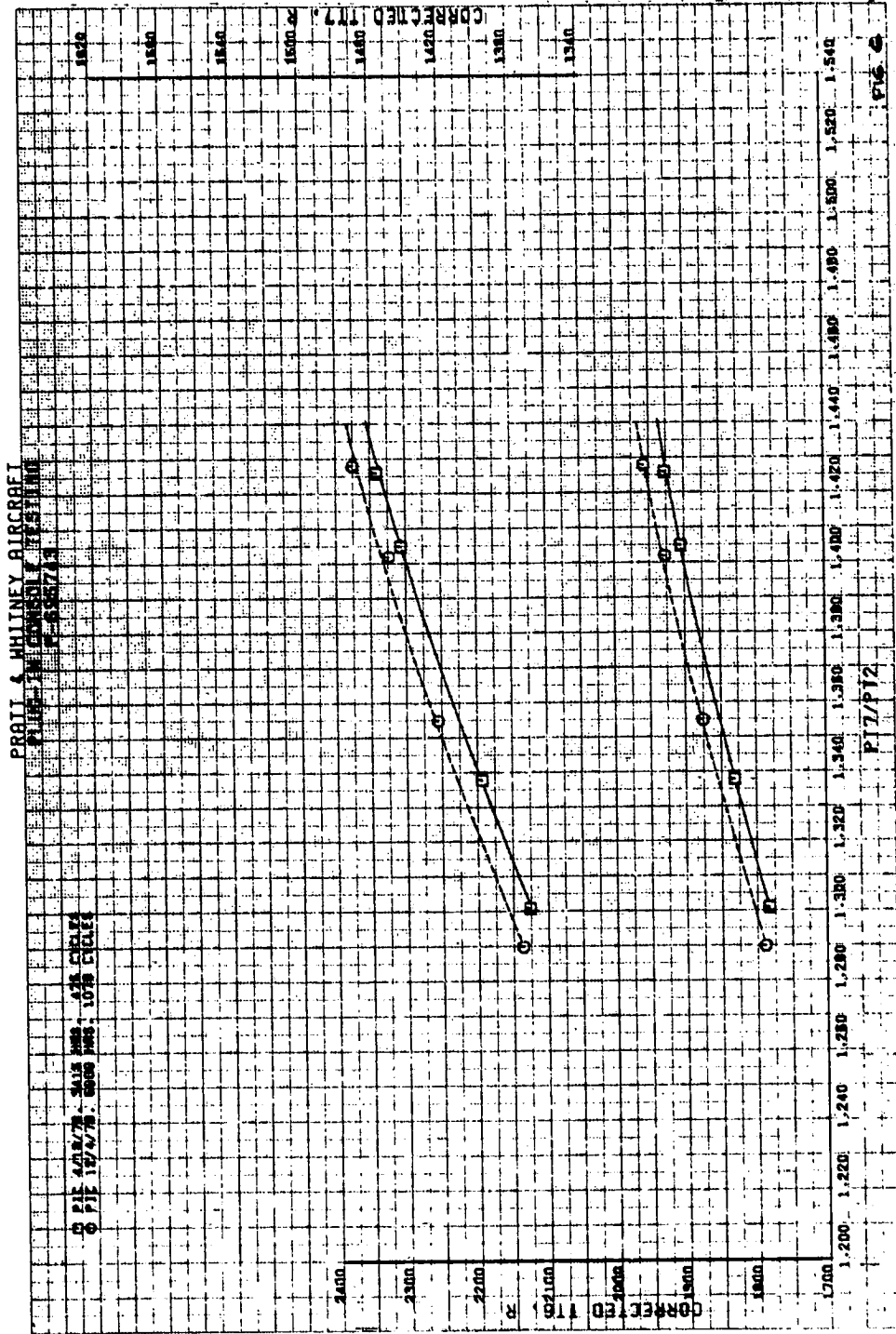
Figure 34 Typical Gas Generator Plot – Corrected high-pressure and low-pressure turbine discharge total temperatures are plotted as functions of EPR for two PIC calibrations of engine P-695743 and used in the data analysis.
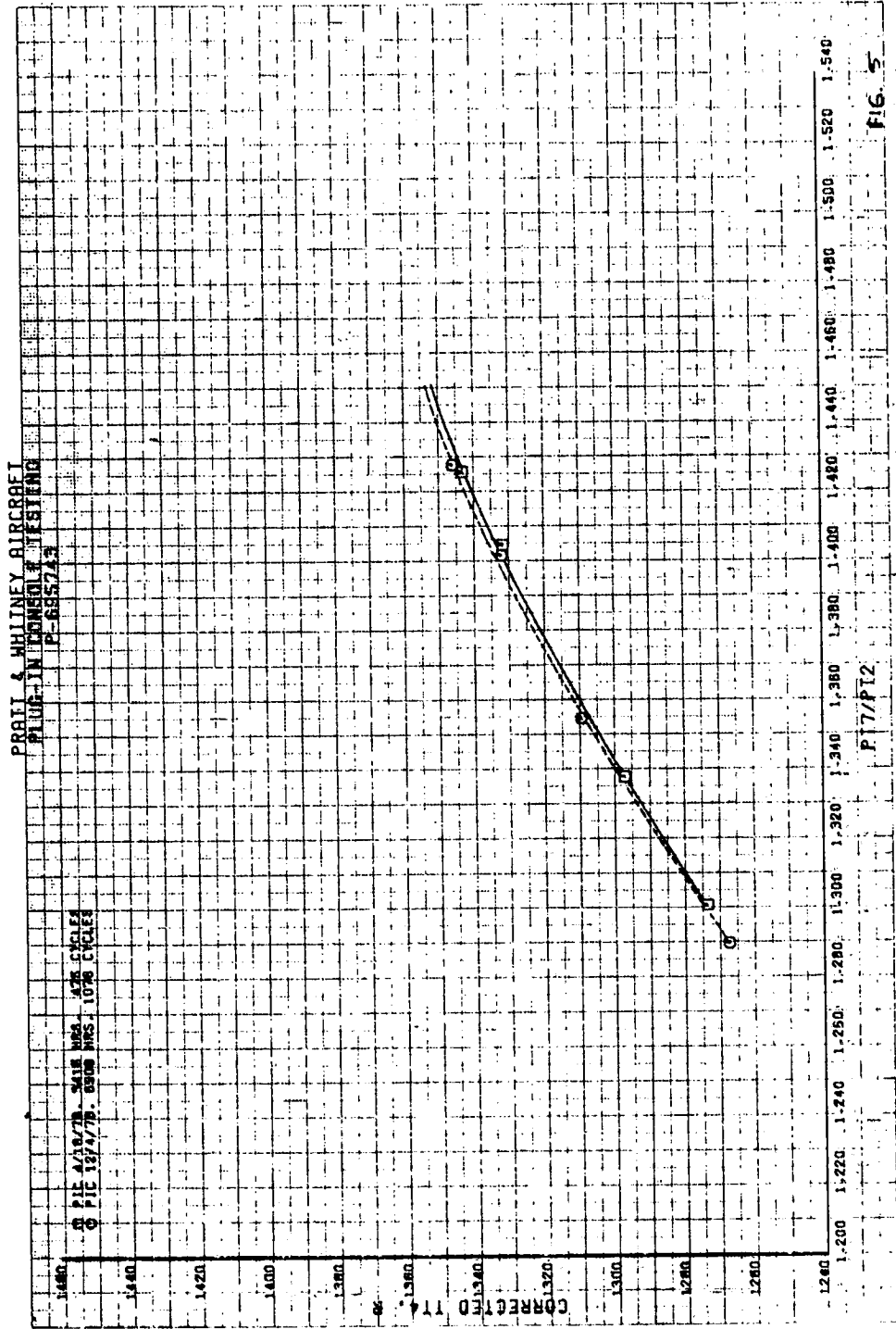
Figure 35 Typical Gas Generator Plot - Corrected high-pressure compressor discharge total temperature is plotted as a function of EPR for two PIC calibrations of engine P-695743 and used in the data analysis.
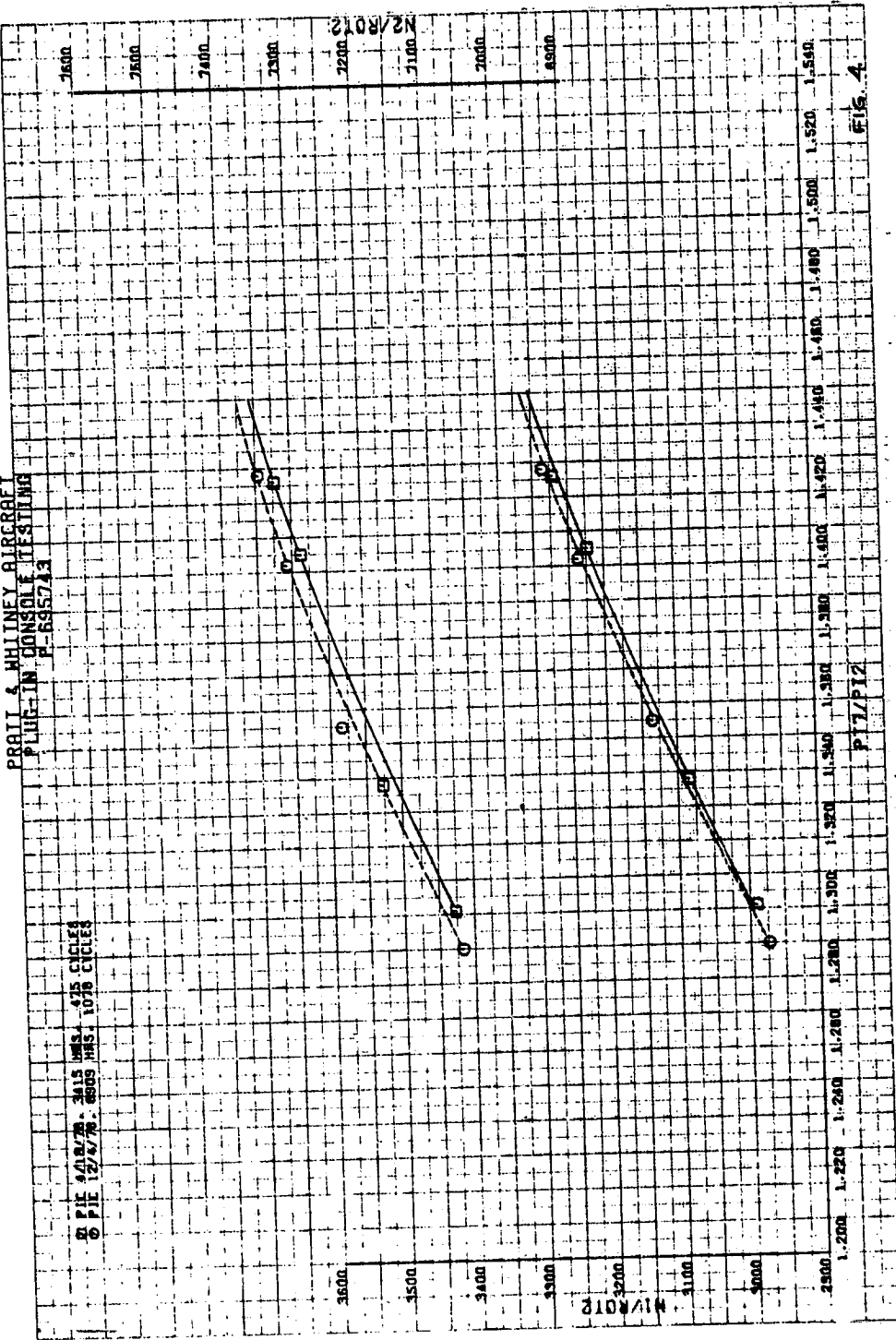
Figure 36 Typical Gas Generator Plot - Low-pressure and high-pressure rotor speeds are plotted as functions of EPR for two PIC calibrations of engine P-695743 and used in the data analysis.
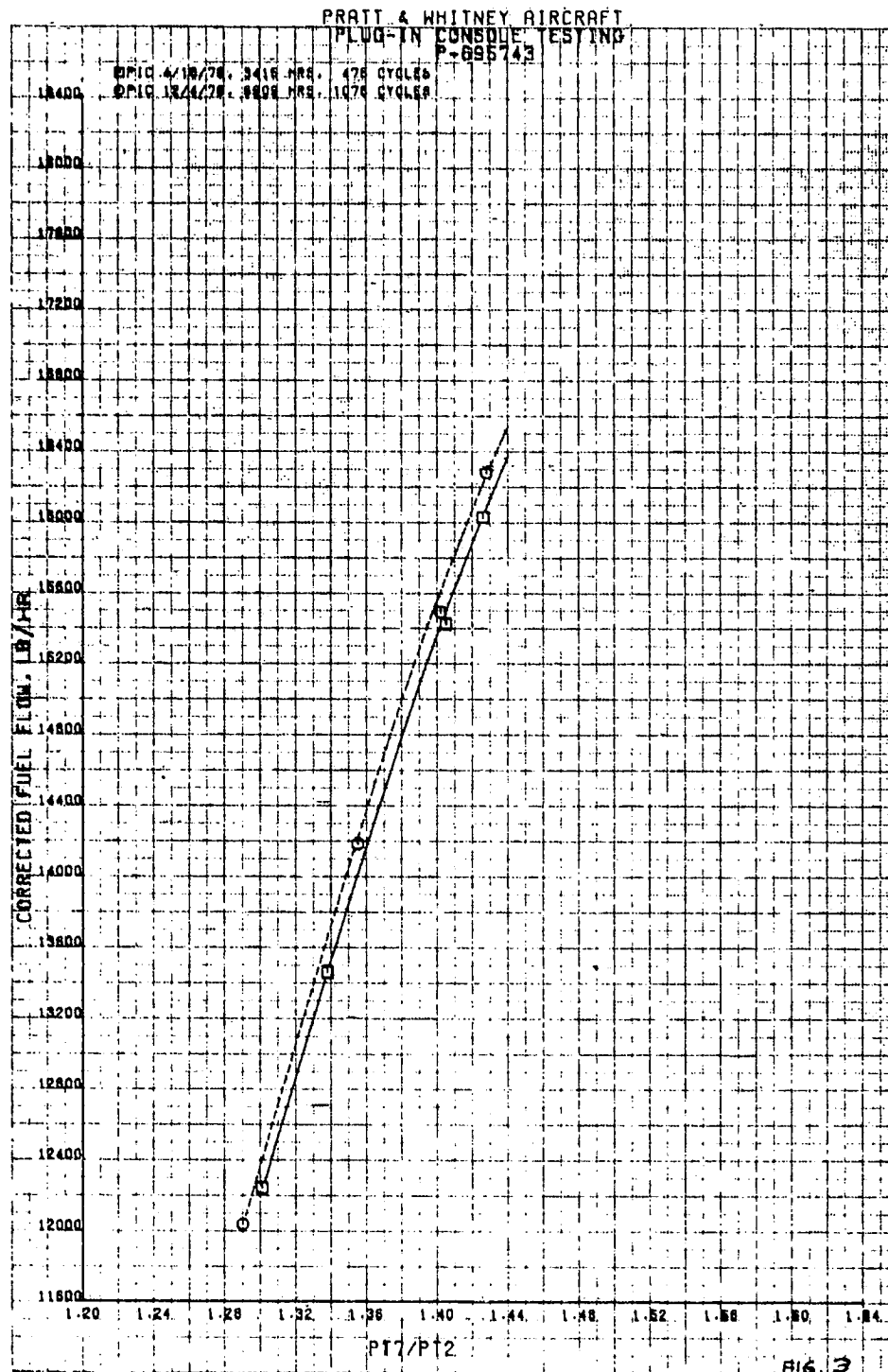
Figure 37 Typical Gas Generator Plot - Corrected fuel flow is plotted as a function of EPR for two PIC calibrations of engine P-695743 and used in the data analysis.
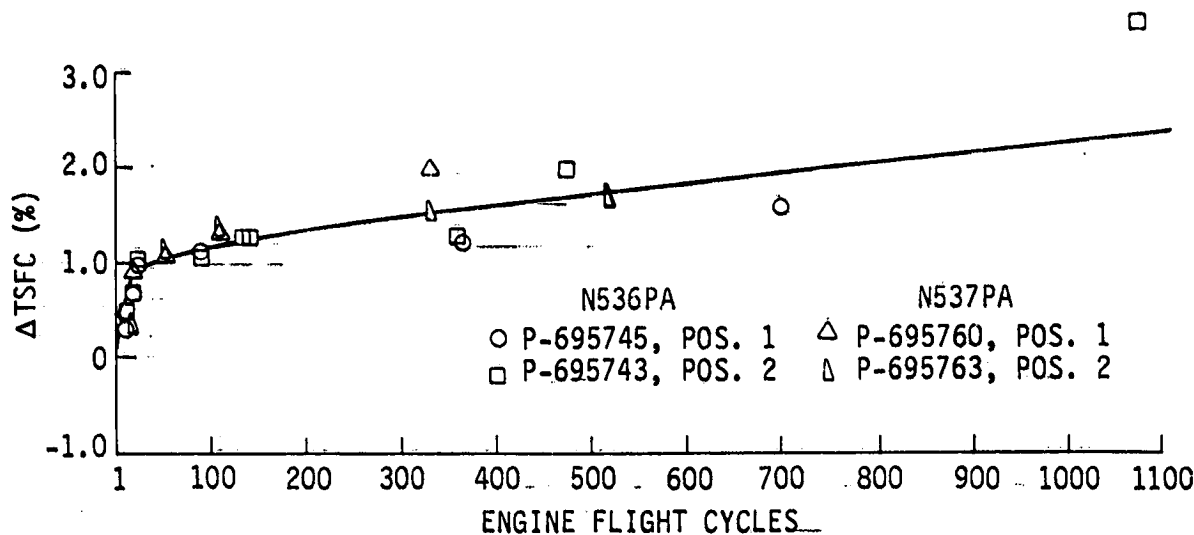
Figure 38 Estimated Sea Level Static TSFC Deterioration - Overall TSFC.
Prerepair deterioration, based on module deterioration and
influence coefficients, shows a rapid deterioration of 1
percent in the first 50 cycles followed by long-term
deterioration at a much slower rate to 2.2 percent at 1000
cycles.
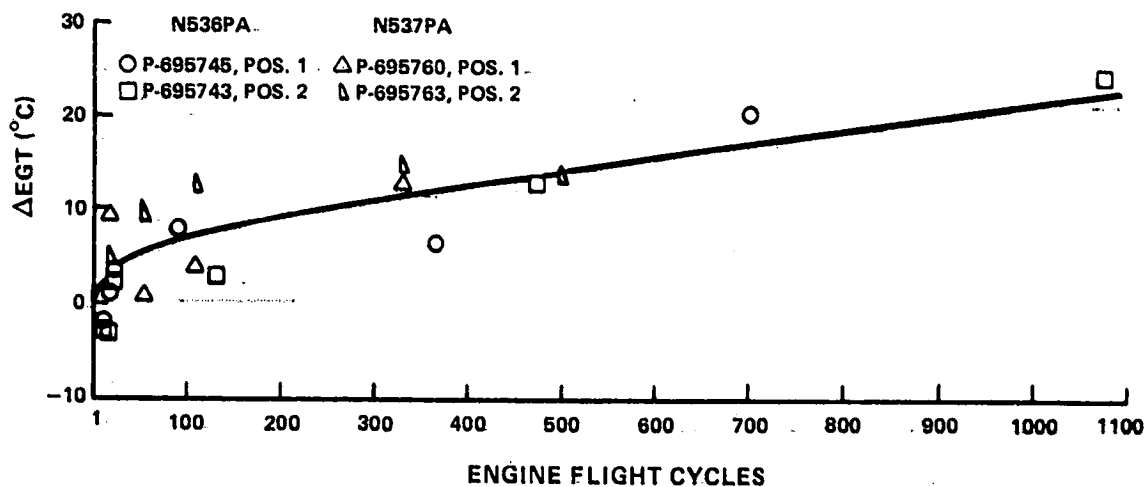
Figure 39 Estimated Sea Level Static Prerepair EGT Deterioration -
Overall EGT deterioration, based on module deterioration and
influence coefficients, shows a rapid deterioration of 6°C
in the first 50 cycles followed by a long-term deterioration
at a slower rate to 22°C at 1000 cycles.

64
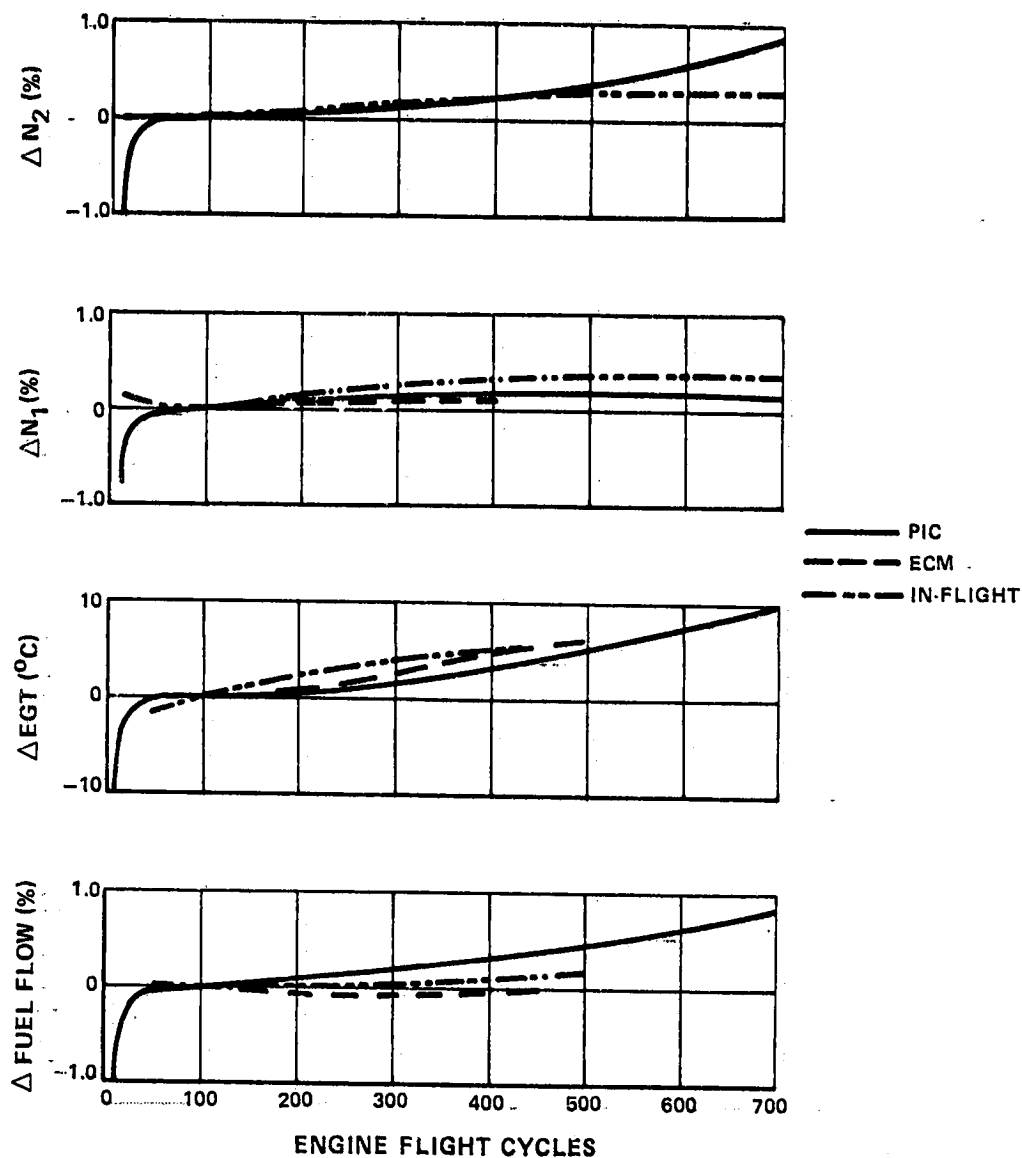
Figure 40 Comparison of Prerepair Gas Generator Parameters as Functions of Cycles as Determined by PIC Data Corrected For Altitude, In-Flight Calibration Data, and ECM Data. Agreement among the three trends is fairly good although wide variations in fuel flow occurred in in-flight calibration data and ECM data for engine P-695745 and thus influenced the average values.
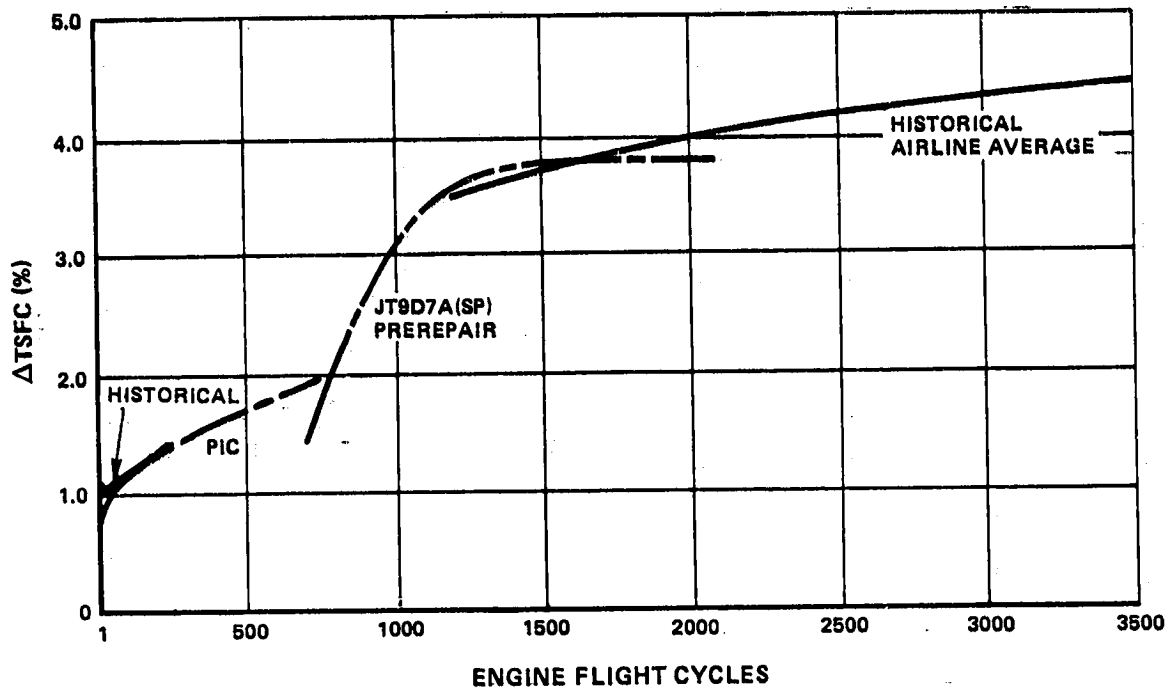
Figure 41 Prerepair Sea Level Static TSFC Performance of JT9D Engines at Constant Thrust - JT9D-7A(SP) test stand data correlates well with historical airline data; PIC data shows a somewhat more rapid TSFC loss.
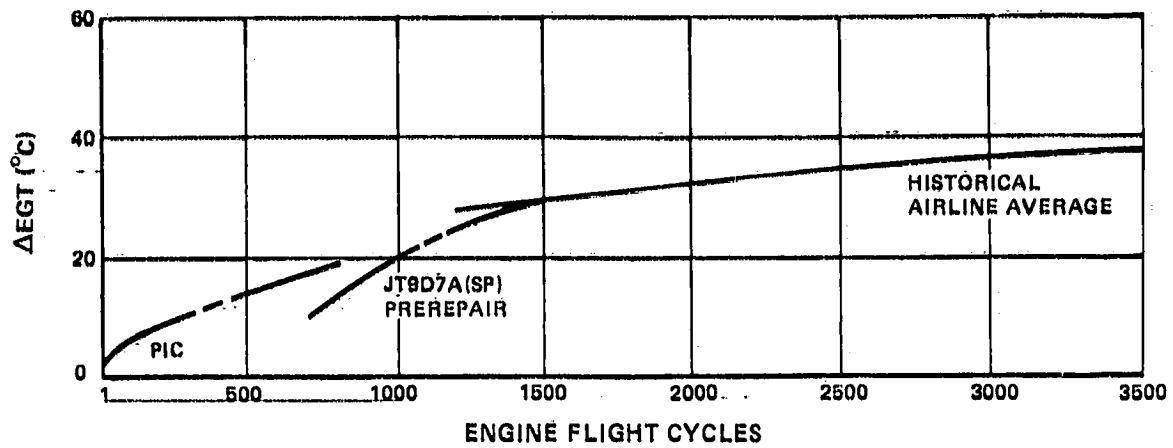
Figure 42 Prerepair Sea Level Static EGT Performance of JT9D Engines at Constant EPR - JT9D-7A(SP) test stand data correlates well with historical airline data; PIC data shows a somewhat steeper EGT increase in the low flight cycle range.
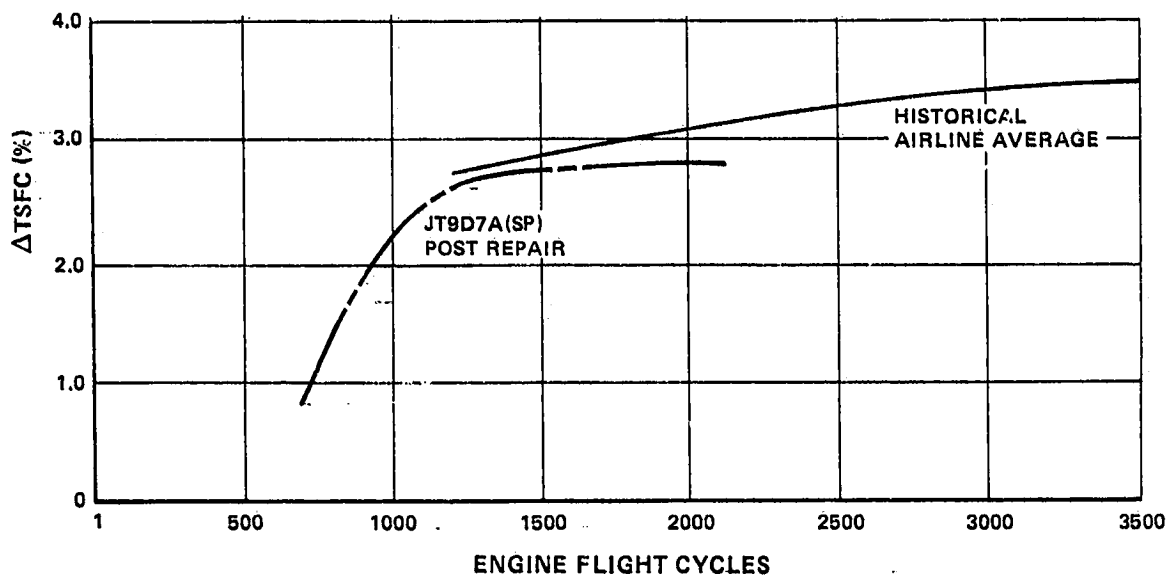
Figure 43 Postrepair Sea Level Static TSFC Performance of JT9D Engines at Constant Thrust - JT9D-7A(SP) test stand data and historical airline data show similar trends with the historical data slightly higher in level.

67
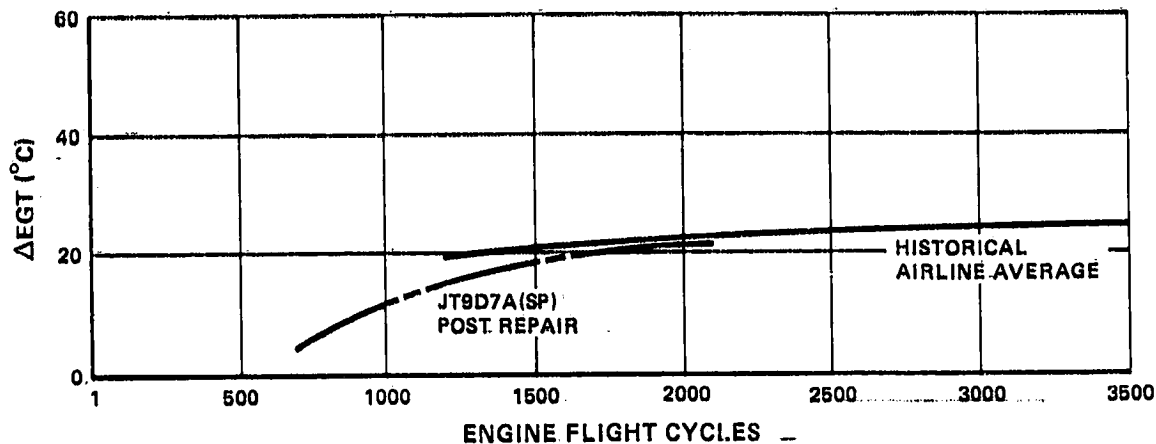
Figure 44   Postrepair Sea Level Static EGT Performance for JT9D Engines at Constant EPR - JT9D-7A(SP) test stand data and historical airline data are very similar in both trend and level.

4.3 MODULE PERFORMANCE DETERIORATION

As previously stated, module performance deterioration was determined only when prerepair, postrepair, and PIC data were obtained. These were the only sources of data which were associated with instrumentation suitable for module performance evaluation. A typical example of the PIC data being used to obtain module deterioration is illustrated in Table XVII. The change in measured gas generator parameters listed in the upper left column were obtained at an engine pressure ratio (EPR) of 1.43 from Figures 32 through 37, presented earlier. The change in gas generator parameters in the Analytical Results column represents the result of engine cycle calculations using the module performance changes analyzed to have occurred. The only significance differences between the measured and analyzed gas generator parameter changes were in turbine temperature, where temperature profile variations make measurements unrepresentative of the average temperature in many instances. The values of module performance changes in efficiency and flow capacity analyzed to have occured are therefore reasonable.

The analyses of the prerepair and postrepair data were similar but used the JT9D engine simulation rather than influence coefficients in the analysis procedue. Module efficiency and flow capacity were "coupled" in an attempt to more accurately reflect the effect of one component or module on another. "Coupling" refers to using a known relationship between the efficiency and flow capacity of a given component. Another feature of prerepair and postrepair analyses is the relating of the

known module repairs with the test data obtained before and after repair. The details of these procedures are discussed in Section 3.0

TABLE XVII

TYPICAL GAS GENERATOR ANALYSIS BASED ON PIC CALIBRATIONS OF ENGINE P-695743 ON 12-4-78 RELATIVE TO 4-18-78

Engine Parameters	Change in Measured Parameter	Analytical Results
Low-Pressure Rotor Speed (%)	+0.21	+0.23
High-Pressure Rotor Speed (%)	+0.29	+0.29
HPC Discharge Total Temperature (^{O}R)	+1.0	+2.0
HPT Discharge Total Temperature (^{O}R)	+28.	+21.
LPT Discharge Total Temperature (^{O}R)	+11.	+17.
Pt3/Pt2 (%)	+1.41	+1.44
Ps4/Pt7 (%)	-0.65	-0.67
Engine Air Flow (%)	-0.41	-0.63
Fuel Flow (%)	+1.07	+0.99

Analyzed Module Parameters

Fan Efficiency (points)	-0.80
Fan Flow Capacity (%)	-0.50
Low-Pressure Compressor Efficiency (points)	-0.65
Low-Pressure Compressor Flow Capacity (%)	-0.40
High-Pressure Compressor Efficiency (points)	-0.60
High-Pressure Compressor Flow Capacity; (%)	-0.45
High-Pressure Turbine Efficiency (points)	-0.40
High-Pressure Turbine Flow Capacity (%)	+0.40
Low-Pressure Turbine Efficiency (points)	0.
Low-Pressure Turbine Flow Capacity (%)	0.

Some typical tabular results using the approaches mentioned above are given in Table XVIII which shows the modular breakdown from an analysis of historical data from Reference 1. This analysis was done

at 149 engine flight cycles and, as such, represents short-term deterioration. It should be noted that the estimated contribution of the individual components/modules to the overall performance loses may be somewhat inaccurate because of the lack of detailed instrumentation for a more complete analysis. However, the breakdown between the high- and low-pressure spool performance losses is reasonably accurate. As shown in the table, this analysis indicates that the low-pressure spool contributes 55 percent to the overall engine deterioration while the high-pressure spool contributes 45 percent.

TABLE XVIII

MODULE CONTRIBUTION TO SHORT-TERM DETERIORATION
BASED ON ANALYSIS (AT 149 CYCLES) OF HISTORICAL DATA

	Efficiency Change (%)	Flow Capacity Change (%)	TSFC Change (%)
Fan	-0.25	-0.25	+0.15
Low-Pressure Compressor	-0.5	-0.5	+0.15
High-Pressure Compressor	-0.5	-1.25	+0.30
High-Pressure Turbine	-0.5	+0.25	+0.35
Low-Pressure Turbine	-0.5	0.0	+0.50

Total	+1.45
Measured	+1.45
Low-Pressure Spool	+0.80
High-Pressure Spool	+0.65

Table XIX shows the short-term performance deterioration of engine P-695743 which was one of the four engines subjected to PIC Tests. These results are based on the test stand data after the engine had been washed and the engine vane control (EVC) trimmed. These procedures improved the overall engine TSFC loss from 1.5 to 1.2 percent. After these tests, the engine was subjected to a complete analytical teardown where the condition of all the seals and other parts which affect performance were documented. Based on this information, the performance of each module was estimated. These estimates correlated well with the performance data shown in the table and other historical short-term deteriortion data (Reference 1). The details of this specific test effort are described in detail in Reference 2.

As discussed in Section 4.1.4 (Plug-In Console Data), the gas generator data and component influence coefficients were used to derive the TSFC deterioration shown in Figure 38. A detailed breakdown of each module's

70

contribution to the TSFC loss is given in Table XX for 50, 150, and 500 engine flight cycles. At 50 cycles, the TSFC loss is dominated by the high-pressure turbine deterioration with lesser impacts by the fan and low-pressure compressor. At 500 cycles, the high-pressure turbine and low-pressure compressor are equal in their contribution to the total loss; the impact of the low-pressure turbine is practically negligible. Over the short term, the TSFC losses are nearly equally split between the hot section and cold section as well as between the high-pressure spool and the low-pressure spool. At 500 cycles, the cold section dominates the TSFC losses; the low-pressure spool exhibits more deterioration than does the high-pressure spool.

TABLE XIX.

MODULE CONTRIBUTION TO SHORT-TERM DETERIORATION BASED ON MEASURED PERFORMANCE OF ENGINE P-695743 AFTER CLEANING, RETRIMMING (AT 141 CYCLES), AND PARTS INSPECTION

Module	Change in TSFC — Since New (%)
Fan	+0.15
Low-Pressure Compressor	+0.35
High-Pressure Compresor	+0.12
High-Pressure Turbine	+0.47
Low-Pressure Turbine	+0.10
Total	+1.19

A comparison of the three sources of short-term data is presented on Table XXI in terms of module contribution to TSFC loss at approximately 150 cycles. In general, all three sources are in agreement. The low-pressure turbine loss based on historical data is considerably higher than that for the other analyses, but this result could be due to the lack of suitable instrumentation to accurately assess the distribution of low-pressure spool losses. That is, part of this loss could easily be assigned to the fan or low-pressure compressor with no significant effect on the analysis.

The short-term losses are due largely to high-pressure turbine and low-pressure compressor deterioration with the low-pressure turbine

71

contributing very little to the total loss. The losses are evenly split between the high-pressure and low-pressure spool modules. Cold section deterioration seems to be slightly greater than that for the hot section.

TABLE XX

AVERAGE MODULE CONTRIBUTION TSFC DETERIORATION
USING PIC DATA

	Change in TSFC (%)		
	50 Cycles	150 Cycles	500 Cycles
Fan	0.20	0.25	0.30
Low-Pressure Compressor	0.25	0.40	0.60
High-Pressure Compresor	0.10	0.20	0.30
High-Pressure Turbine	0.40	0.50	0.60
Low-Pressure Turbine	0.	0.05	0.15
Total	0.95	1.40	1.95
High-Pressure Spool	0.50	0.70	0.90
Low-Pressure Spool	0.45	0.70	1.05
Cold Section	0.55	0.85	1.20
Hot Section	0.40	0.55	0.75

Figures 36 thru 50 show the performance losses for each major component which directly affects the loss in TSFC (that is, fan, low- and high-pressure compressors, and high- and low-pressure turbines). These data are based on PIC tests, prerepair and postrepair tests, and previously acquired historical data. The PIC data show no discernable effect of engine location on the airplane (that is, inboard versus outboard) for any of the engine modules.

4.3.1   Fan

The efficiency and flow capacity losses due to deterioration of the fan are shown in Figure 45 for the PIC tests. The fan performance for all engines deteriorates rapidly at first. The engines of airplane N536A show a higher initial fan module loss.

The same fan performance loss parameters are shown in Figure 46 using prerepair and postrepair data. The data covers a range of flight cycles from 700 to 2100 and represents the deterioration for the

72

unrepaired modules. Losses in fan efficiency and flow capacity due to deterioration are predicted by "top down" analyses of the JT9D-7A(SP) engine prerepair data. This figure also shows module losses predicted from analyses of postrepair data in those cases when no changes or refurbishment were accomplished on that particular module during the repair. The prerepair-based loss estimates are believed to have better credibility than the postrepair-based estimates for reasons previously discussed in Section 3.4, Analysis Techniques. Module cyclic age is identical with engine name-plate cyclic age if no repairs have been performed on that particular module previously, which is generally the case for these prerepair data. Where there has been prior module repair, module age is engine flight cycles since the module was last repaired.

TABLE XXI

COMPARISON OF MODULE CONTRIBUTION TO
SHORT-TERM TSFC DETERIORATION

| | Data Source | | |
	Historical Data Analysis (149 Cycles)	P-695743 P&WA Testing (As Received with 141 Cycles)	Analysis of PIC Data (150 Cycles)
		Change in TSFC (%)	
Fan	+0.15	+0.05	+0.25
Low-Pressure Compressor	+0.15	+0.40	+0.40
High-Pressure Compressor	+0.30	+0.35	+0.20
High-Pressure Turbine	+0.35	+0.60	+0.40
Low-Pressure Turbine	+0.50	+0.10	+0.05
Total	+1.45	+1.50	+1.30
Low-Pressure Spool	+0.80	+0.55	+0.70
High-Pressure Spool	+0.65	+0.95	+0.60
Cold Section	+0.60	+0.80	+0.85
Hot Section	+0.85	+0.70	+0.45

Figure 47 is presented to show fan deterioration using data from all available sources, that is, PIC tests, prerepair and postrepair tests, and the previously acquired historical data. There is very good agreement between the prerepair and postrepair data and the historical data. The PIC data show a more rapid short-term deterioration (that is,

the first 100 cycles). The slope of the PIC data curve at about 100 cycles would seem to indicate similar deterioration levels for all three data sources by the time 2000 to 3000 cycles are obtained.

Figure 45   Fan Module Performance Deterioration - PIC calibrations from four engines, on two airplanes, show very rapid initial deterioration followed by long-term deterioration at a much slower rate.

Analyses of the short-term fan flow capacity losses have received special attention because their effect on engine performance is appreciable and because the effects are considerably different between take-off and cruise conditions. The results of this analysis shows that for a 2 percent fan flow capacity loss, which is typical for high-time fan blades, the take-off TSFC improves about 0.5 percent, but there is a 0.6 percent TSFC penalty at maximum cruise power at altitude. When the flow capacity loss is 4 percent (extreme deterioration), the take-off TSFC is about 0.8 percent better than when new, but there is a 2.2 percent penalty at maximum cruise.
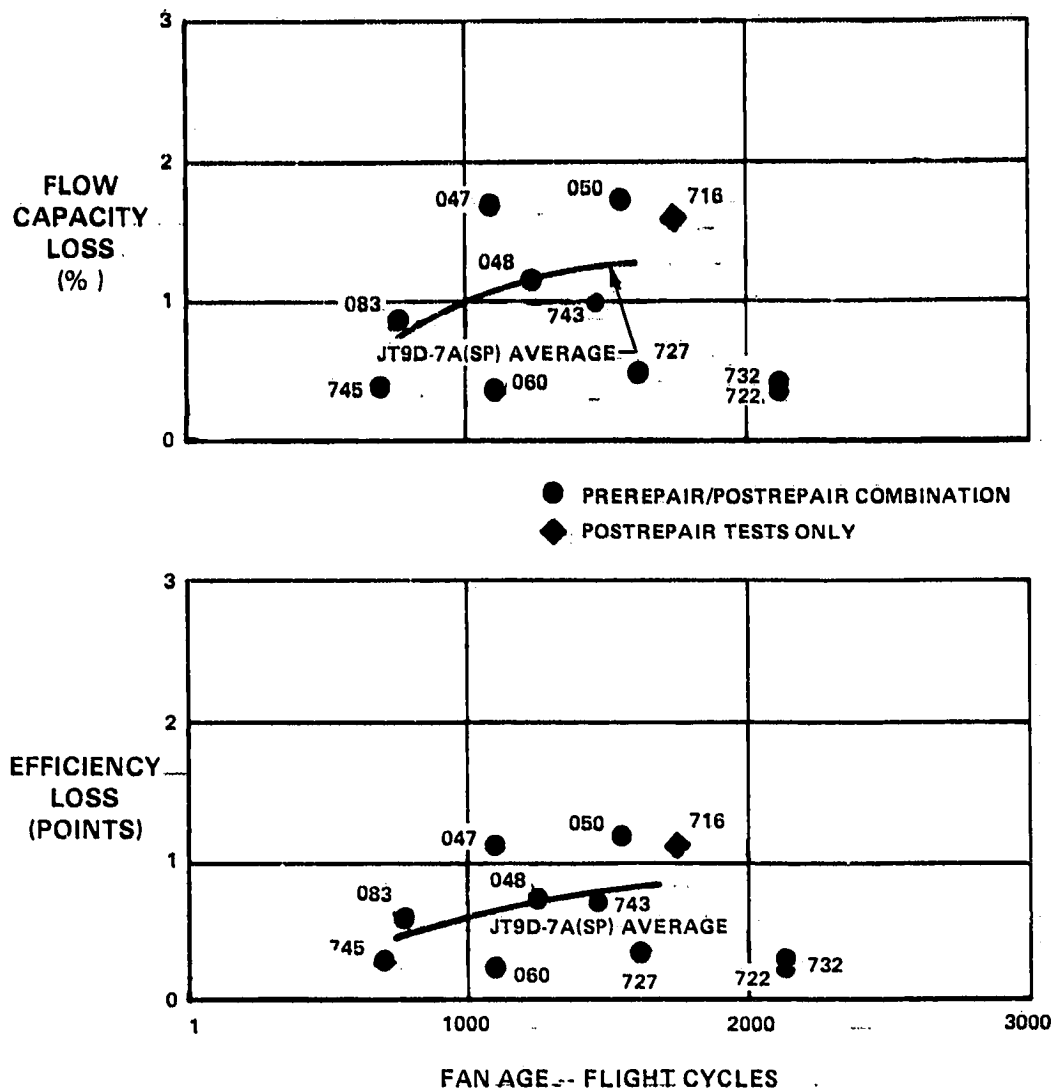
Figure 46   Estimated Fan Module Deterioration with Usage - The average
estimated losses in fan efficiency and flow capacity are
shown.

4.3.2   Low-Pressure Compressor

The efficiency and flow capacity losses due to deterioration of the
low-pressure compressor for the PIC tests are shown in Figure 48. The
low-pressure compressor exhibits a deterioration characteristic similar
to the fan.
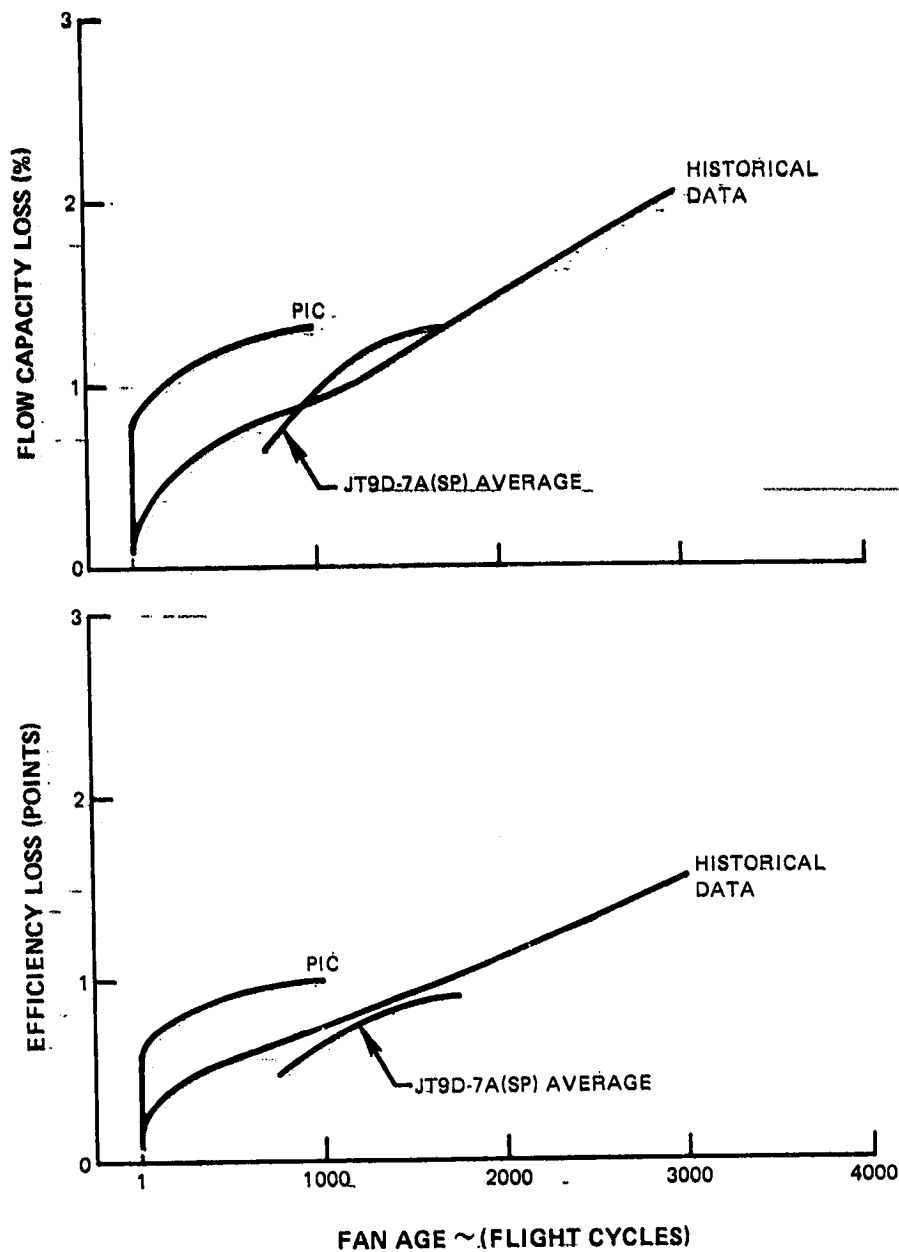
Figure 47 Comparison of PIC, JT9D-7A(SP) Prerepair, and Historical Fan Performance Deterioration Data - The prerepair test stand data shows good agreement while the PIC data shows a higher level of loss.

LPC AGE ~ FLIGHT CYCLES

Figure 48 Low-Pressure Compressor Module Performance Deterioration --
PIC calibrations from four engines, on two airplanes, show
rapid initial deterioration (less than that for the fan)
followed by long-term deterioration at a much slower rate.

The prerepair and postrepair data for the low-pressure compressor
module are presented in Figure 49. Only prerepair results are shown,
since there were no available postrepair data for engines with
unrepaired low-pressure compressor modules. It will be observed that
most of the engines showing high low-pressure compressor losses also
exhibit high fan module losses and vice versa. This observation leads
to the conclusion that, while fan/low-pressure compressor losses are
variable (possibly because of the differing flight experience of
individual engines), the losses are interrelated. Fan deflections and

resulting rubs from flight maneuvers and loads also tend to cause
low-pressure compressor deflections and rubs.
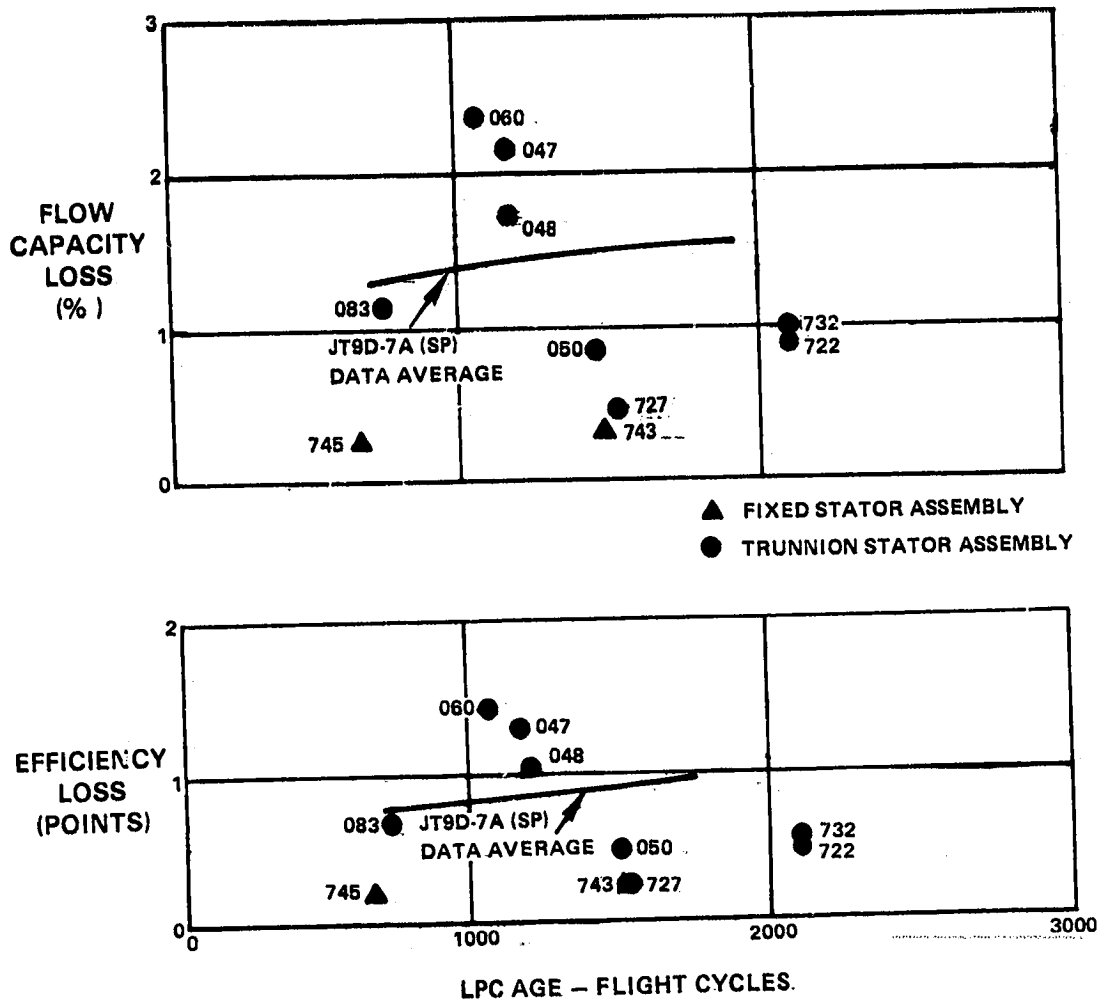
Figure 49 Estimated Low-Pressure Compressor Module Deterioration with
          Usage - The magnitude of low-pressure compressor
          deterioration appears related to the magnitude of fan
          deterioration for individual engines. It is belived that the
          data scatter is aggravated by the greater potential for
          leakage in the case of the trunnion stator.

Additionally, there are two different physical low-pressure compressor
configurations represented in the data: 1) first-stage compressor fixed
stator (engines P-695745 and P-695743), and 2) first-stage compressor
trunion stator. While there are insufficient fixed stator data to be

conclusive, it is believed that the physical differences contribute to lower losses for the fixed stator low-pressure compressor because the trunnion stator low-pressure compressor is known to present greater potential for leakage as a result of relative movement between the case and trunion bearings during service use.

Figure 50 compares the data from the three sources (that is, PIC, preprepair and postrepair, and historical). The loss in efficiency is reasonably comparable for all sources of data. The flow capacity trends are similar but the levels of loss are highest for the historical data and lowest for the PIC data.

As with the fan, the low-pressure compressor was analyzed to determine how flow capacity losses affect performance. A detailed description of this study is presented in Appendix B.

The analysis showed that a 2 precent loss in flow capacity (that is, a typical low-pressure compressor with 2000 flight cycles) results in a 10°C increase in EGT at take-off and a 0.6 percent increase in TSFC at maximum cruise power at altitude. A 4 percent loss in flow capacity (extreme deterioration) increases the take-off EGT by 25°C and the maximum cruise TSFC by 1.5 percent.

4.3.3 High-Pressure Compressor

The efficiency losses due to deterioration of the high-pressure compressor for the PIC tests are shown in Figure 51. On airplane N537A, the deterioration losses show the characteristic short-term losses. However, on airplane N536A the high-pressure compressor short-term losses are relatively small. No explanation is known for this latter trend.

The prerepair and postrepair data for the high-pressure compressor module are shown in Figure 52. Estimated loss in flow capacity for the high-pressure compressor is not shown. While the "top down" analysis method predicts high-pressure compressor flow capacity changes in order to match the test data, the results are biased by variable stator indexing resulting from field trim. Thus, the results include vane trim effects in addition to flow capacity loss due to deterioration. Additionally, engine performance is not strongly influenced by changes in high-pressure compressor flow capacity changes resulting from either deterioration or vane trim. For these reasons, the analytical flow capacity changes are not presented.

The losses in efficiency due to deterioration range from about 0.5 point at 700 cycles to 1 point at 2000 cycles.

Figure 50 Comparison of PIC, JT9D-7A(SP) Prerepair and Postrepair, and Historical Low-Pressure Compressor Performance Deterioration Data - The loss in efficiency is comparable for all data sources.
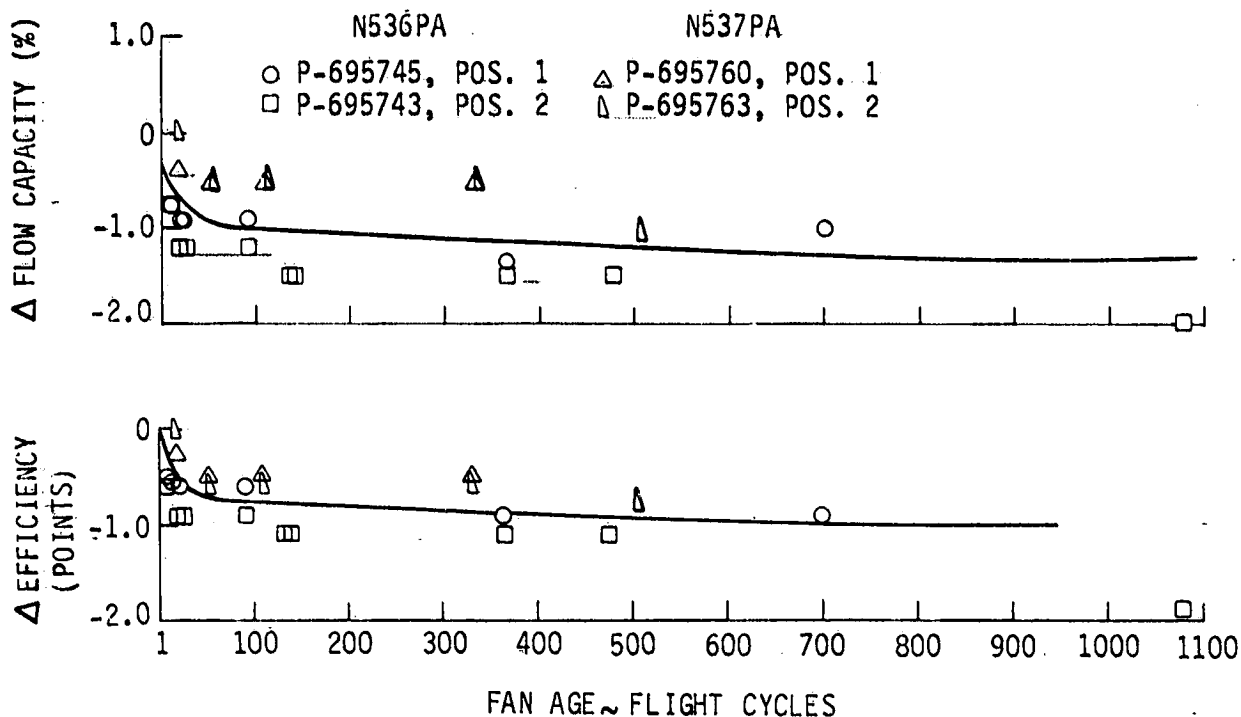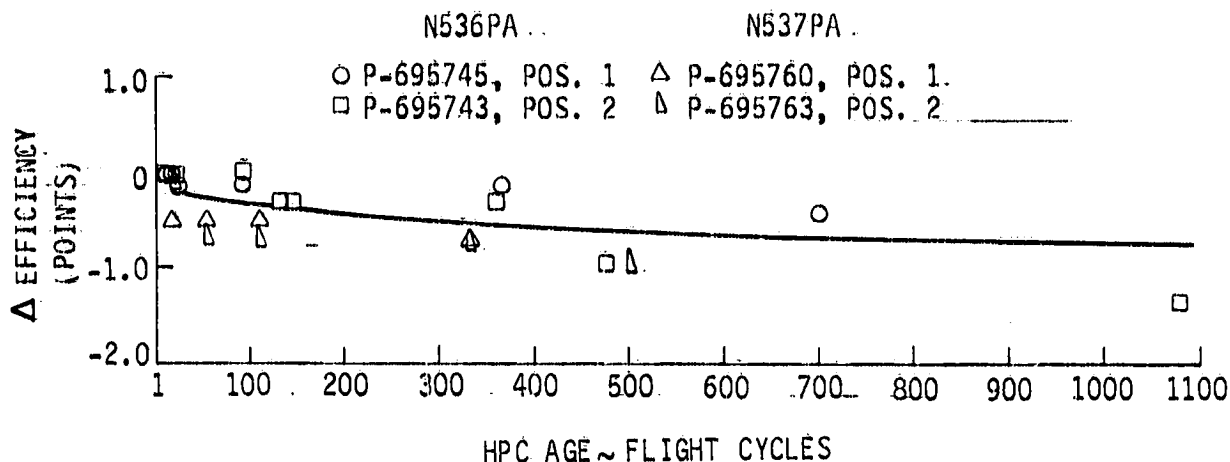
Figure 51   High-Pressure Compressor Module Performance Deterioration - ——
PIC calibrations from four engines, on two airplanes, show
characteristic initial deterioration for engines on one of
the airplanes but a reduced initial deterioration for
engines on the other airplane, followed by _long-term
deterioration at a much slower rate.
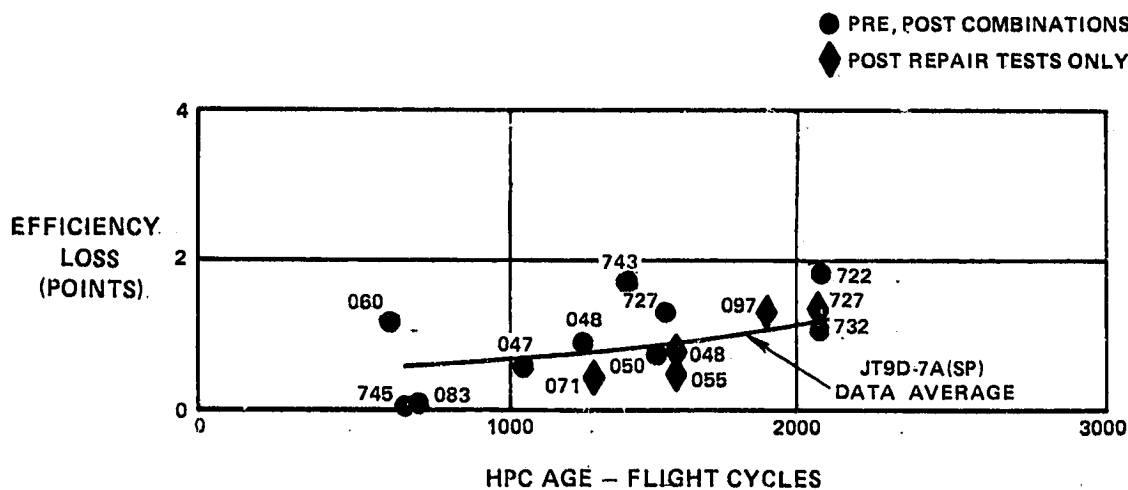
Figure 52   Estimated High-Pressure Compressor Module Deterioration with
Usage - Results are shown for only efficiency loss since
analytical flow capacity loss results include the effect of
variable vane trim in addition to deterioration

81

Figure 53 compares the data from the three data sources. The historical data showns a deterioration level about twice as great on the PIC and prerepair and postrepair data at 1000 flight cycles. Possible reasons for this difference are: 1) the relatively few and possibly cleaner airports served by the Pan American 747(SP) aircraft, which may have biased the data in some fashion (is less erosion), and 2) more careful control in the 747(SP) of thrust reverse usage resulting in less dirt ingestion.

4.3.4 High-Pressure Turbine

The efficiency losses and flow capacity increases due to deterioration of the high-pressure turbine based om the PIC tests are shown in Figure 54. Most of the losses in the high-pressure turbine occur in the first 50 to 100 flight cycles.

The prerepair and postrepair data for the high-pressure turbine are shown in Figure 55. Only prerepair data results are shown, since there were no available postrepair data for engines with unrepaired high-pressure turbine modules. Predicted efficiency loss has relatively little data scatter, while considerably more scatter is seen for flow capacity increase. The reason for this variation in scatter is attributed primarily to the fact that predicted flow capacity is strongly dependent on the measured value of Ps4/Pt7, which, in turn, is influenced by the condition of the high-pressure compressor module and the resulting exit temperature profile effect on measured Ps4. Also, burner pressure loss variations associated with burner liner configuration will affect predicted flow capacity since burner pressure loss changes are not separately accounted for, as discussed in Section 3.4.

Figure 56 compares the data from the three data sources. The losses in efficiency are greater for the historical data than those from the other sources. The differences are related to design improvements that were incorporated in the JT9D-7A(SP) engines evaluated during this program.

4.3.5 Low-Pressure Turbine

The efficiency losses and flow capacity losses due to deterioration of the low-pressure turbine based on the PIC tests are presented in Figure 57. The deterioration losses of this module are negligble.

The prerepair and postrepair data for the low-pressure turbine are shown in Figure 58. The average low-pressure turbine efficiency loss and flow capacity increase is greater than that shown by the PIC data on the previous figure. A point of interest is that the rate of

82
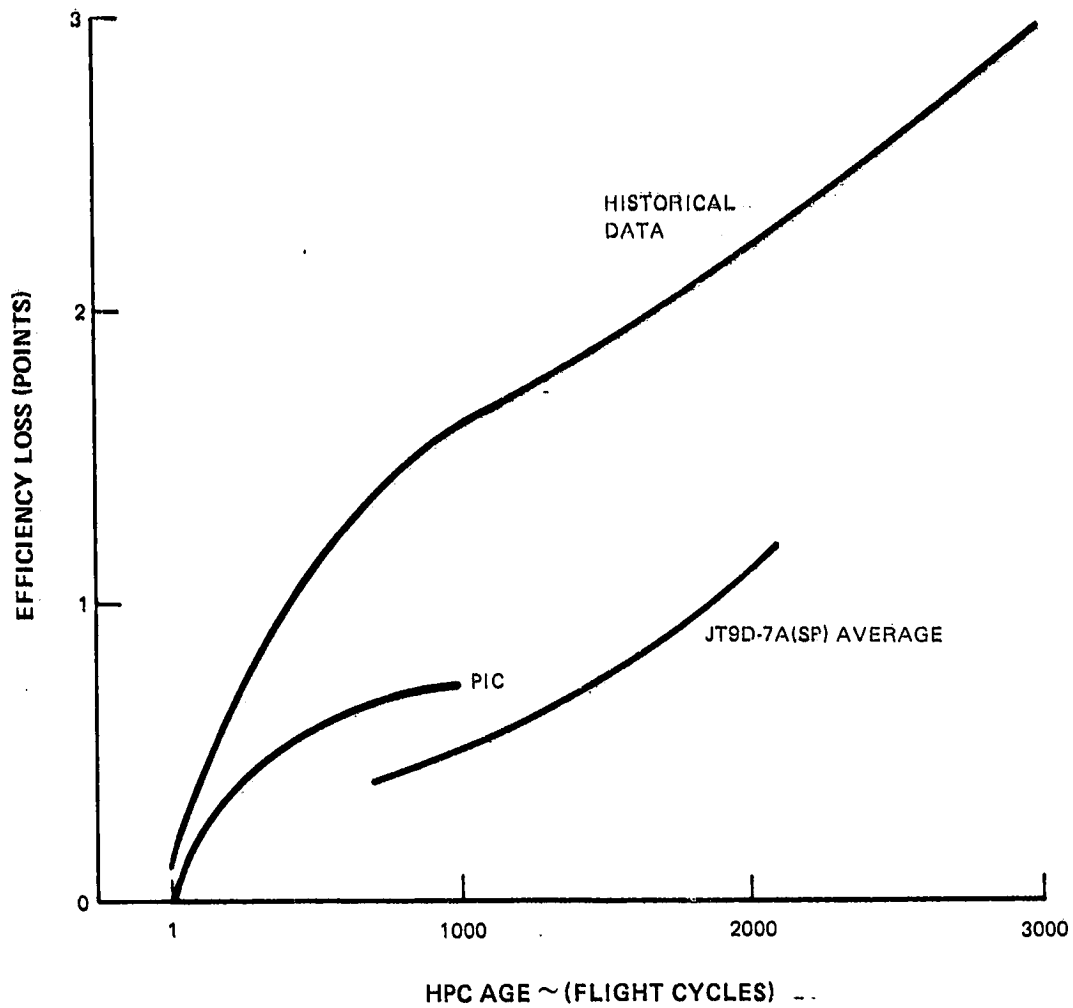
Figure 53 Comparison of PIC, JT9D-7A(SP) Prerepair and Postrepair, and Historical High-Pressure Compressor Performance Deterioration Data - The PIC and test stand data indicate less high-pressure compressor loss than does the historical data.
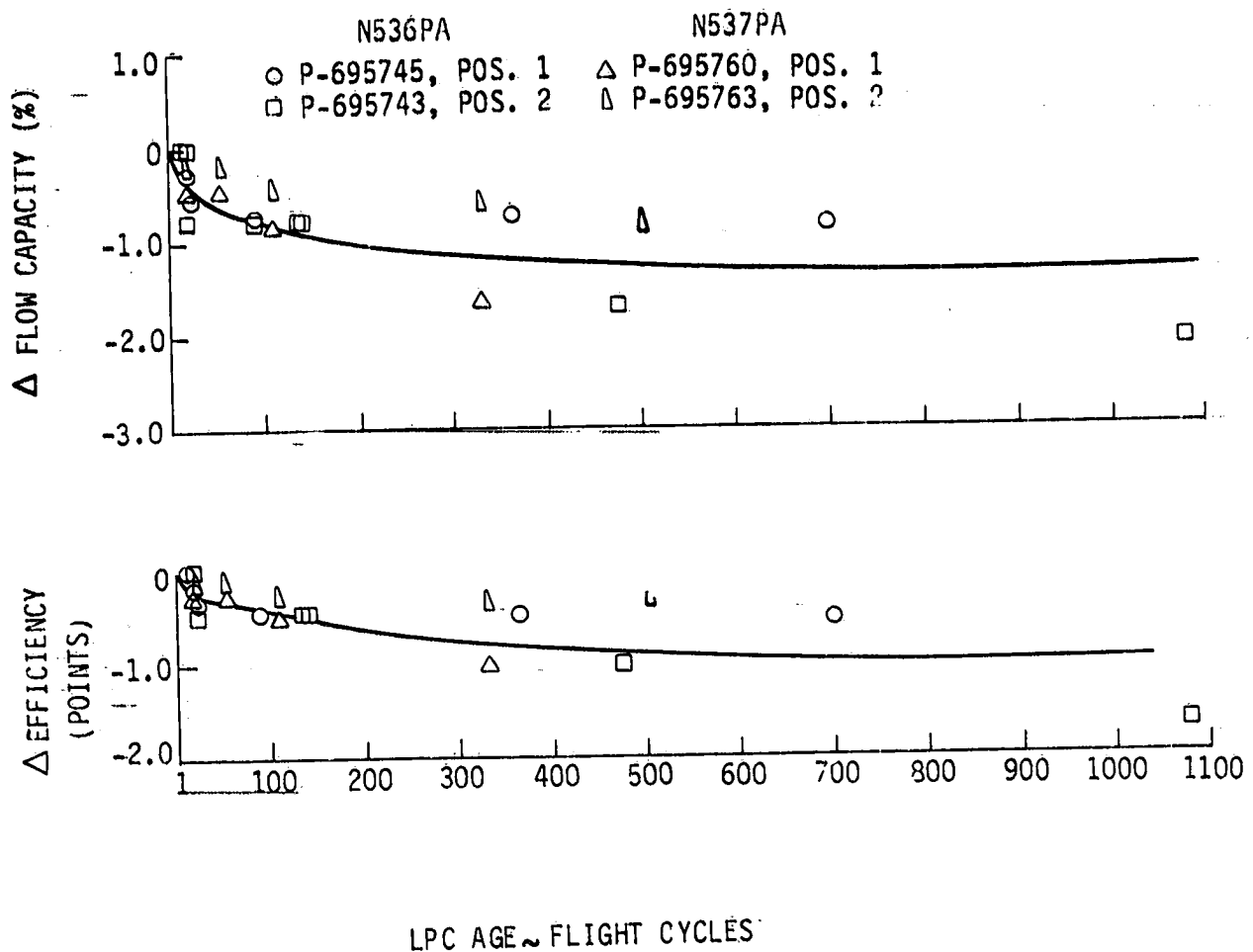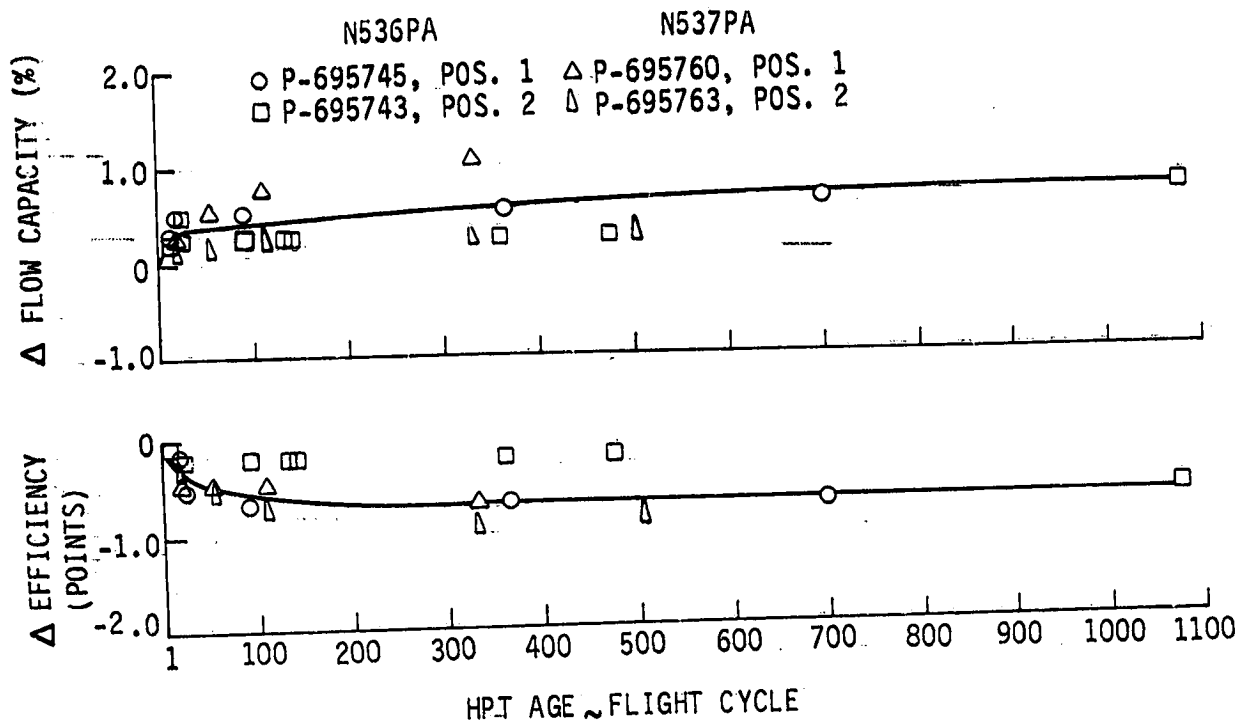
Figure 54 High-Pressure Turbine Module Performance Deterioration - PIC calibrations from four engines, on two airplanes show characteristic initial deterioration followed by long-term deterioration at a much slower rate.

C-2
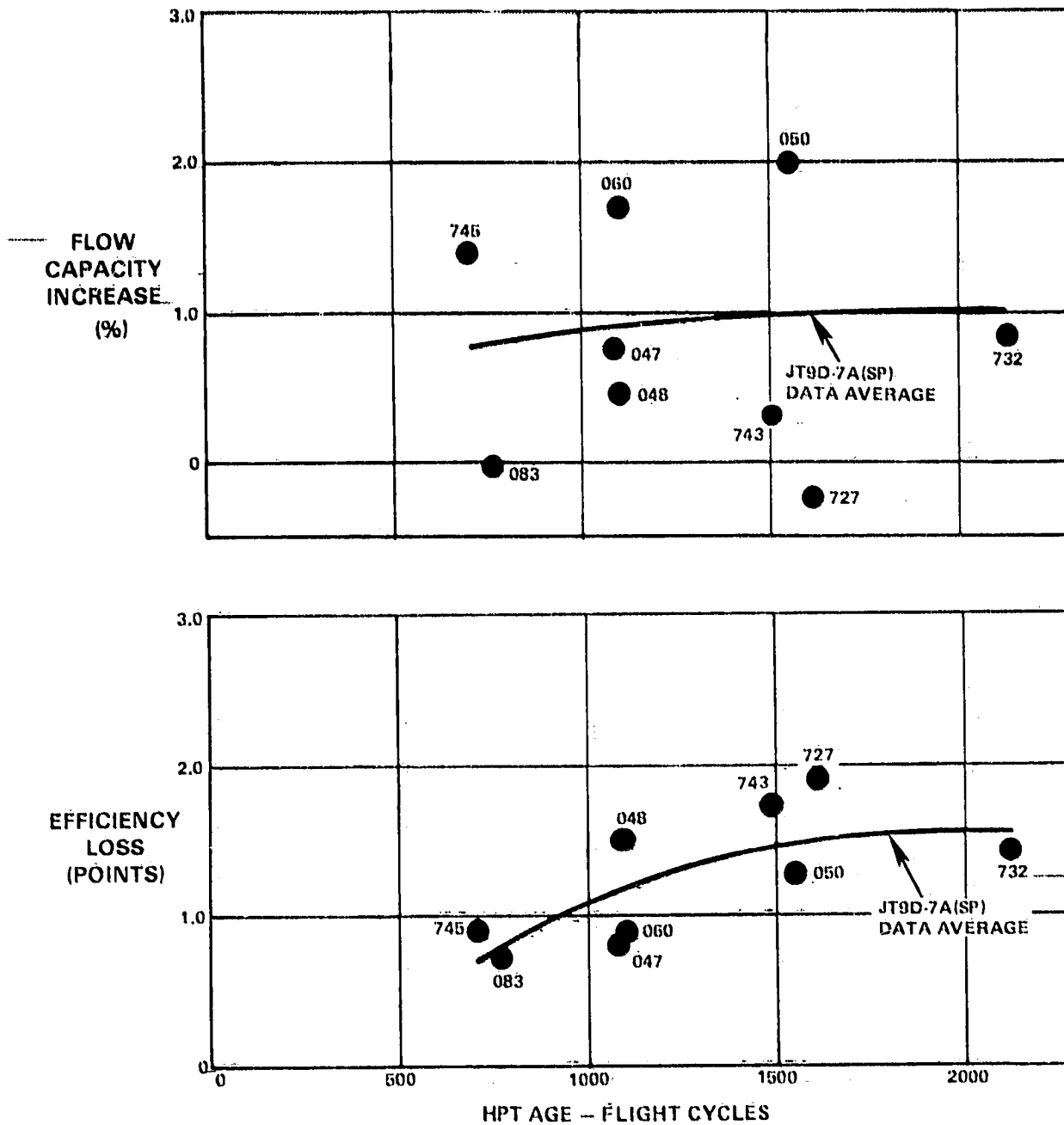
Figure 55   Estimated High-Pressure Turbine Module Deterioration with Usage -- The greater data scatter in the case of flow capacity increase is attributed to the strong dependency of predicted flow capacity on measured Ps4/Pt7 and the associated influence of compressor condition on exit profile and measured Ps4.
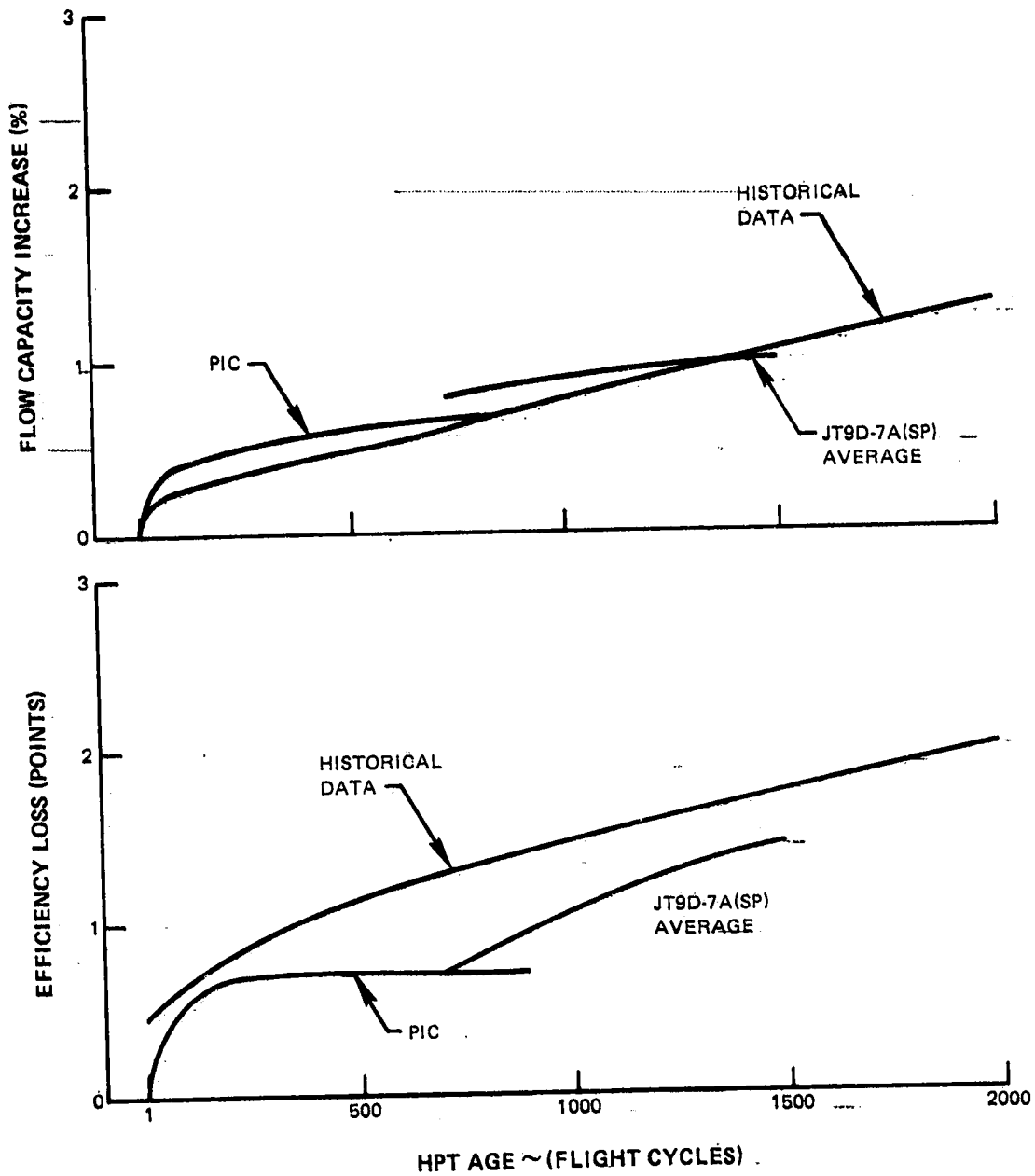
Figure 56 Comparison of PIC, JT9D-7A(SP) Prerepair and Postrepair, and Historical High-Pressure Turbine Performance Deterioration Data - The PIC and test stand data indicate lower high-pressure turbine losses than does the historical data.
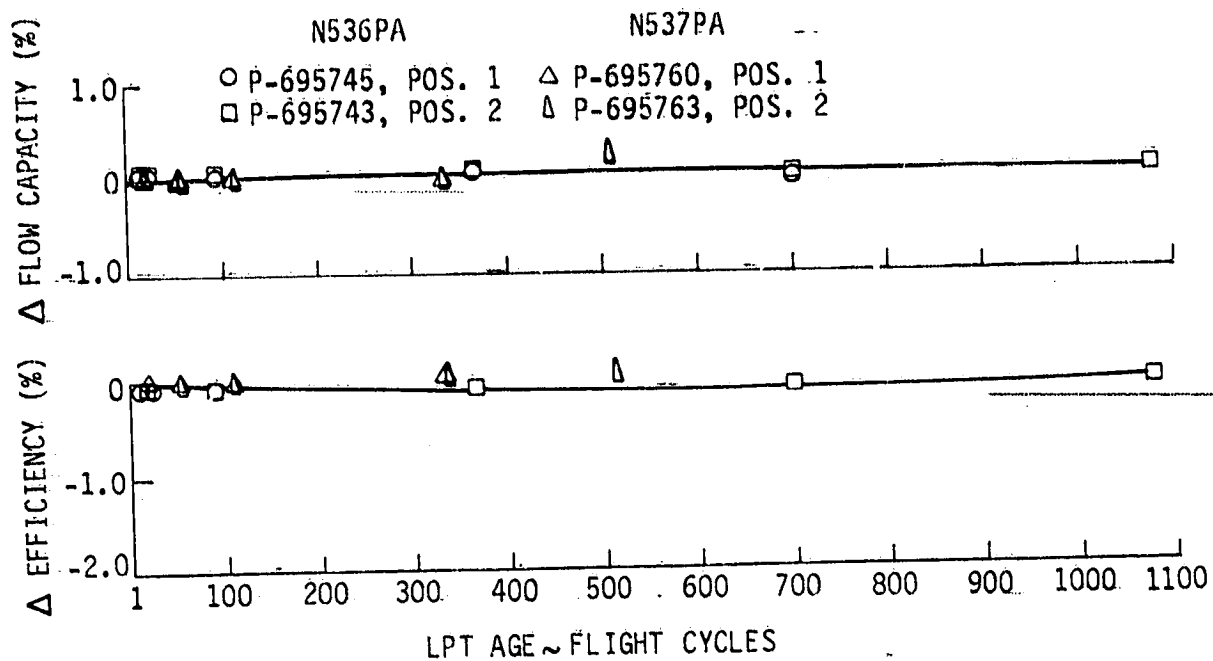
Figure 57   Low-Pressure Turbine Module Performance Deterioration - PIC calibrations from four engines, on two airplanes, show that both initial and long-term deterioration is practically negligible.

low-pressure turbine deterioration appears to be related to the rate of fan/low-pressure compressor deterioration. Engines with high fan/low-pressure compressor losses tend to be high in low-pressure turbine losses and vice versa.

Figure 59 compares the data from the three data sources. The efficiency losses and flow capacity increases are lowest for the PIC and historical data and greater for the prerepair and postrepair data.
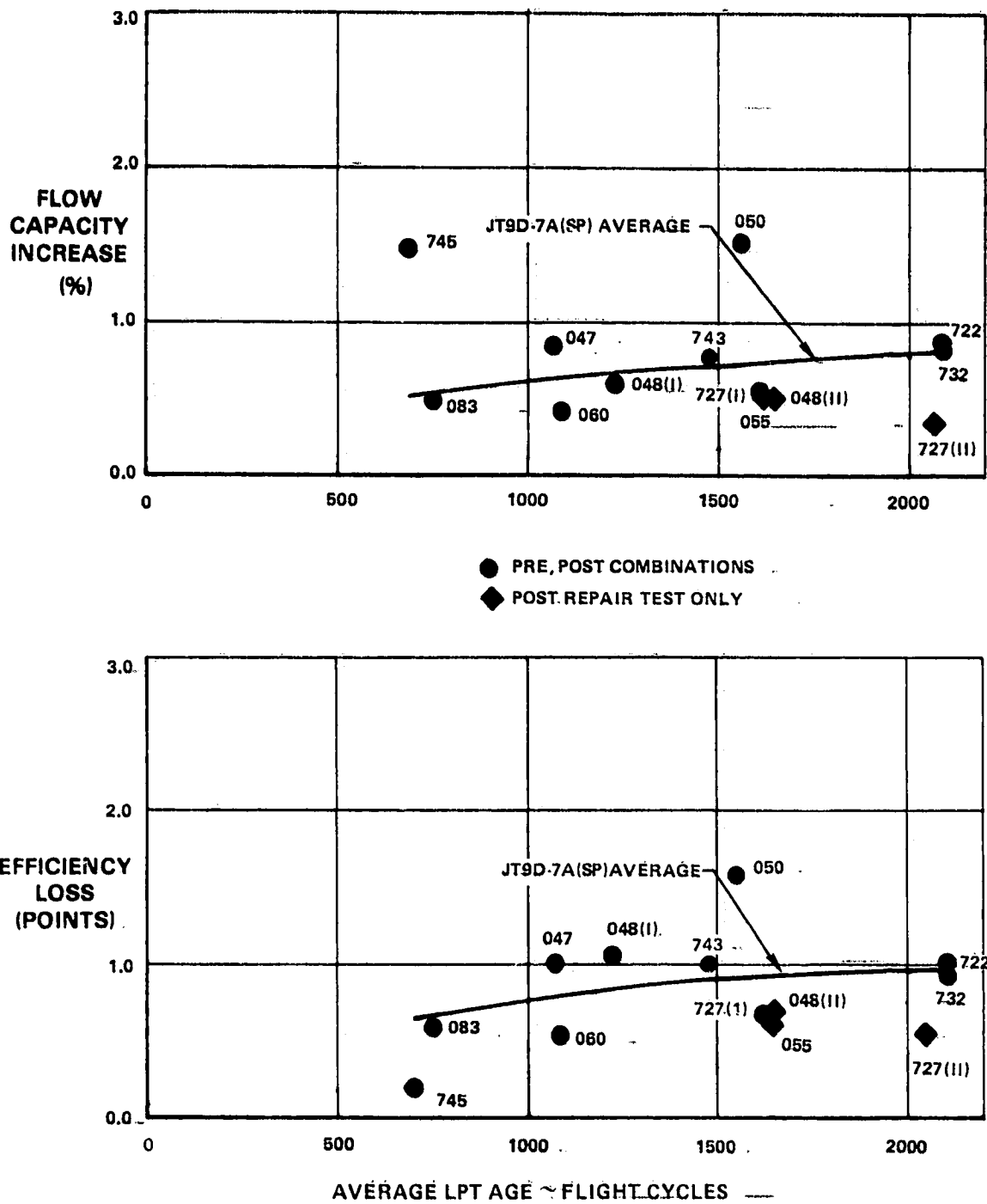
Figure 58   Low-Pressure Turbine Module Deterioration with Usage - The
rate of low-pressure turbine deterioration appears to be
related to the rate of fan/low-pressure compressor
deterioration; engines that are high in fan and
low-pressure compressor losses also tend to be high in
low-pressure turbine loss and vice versa.

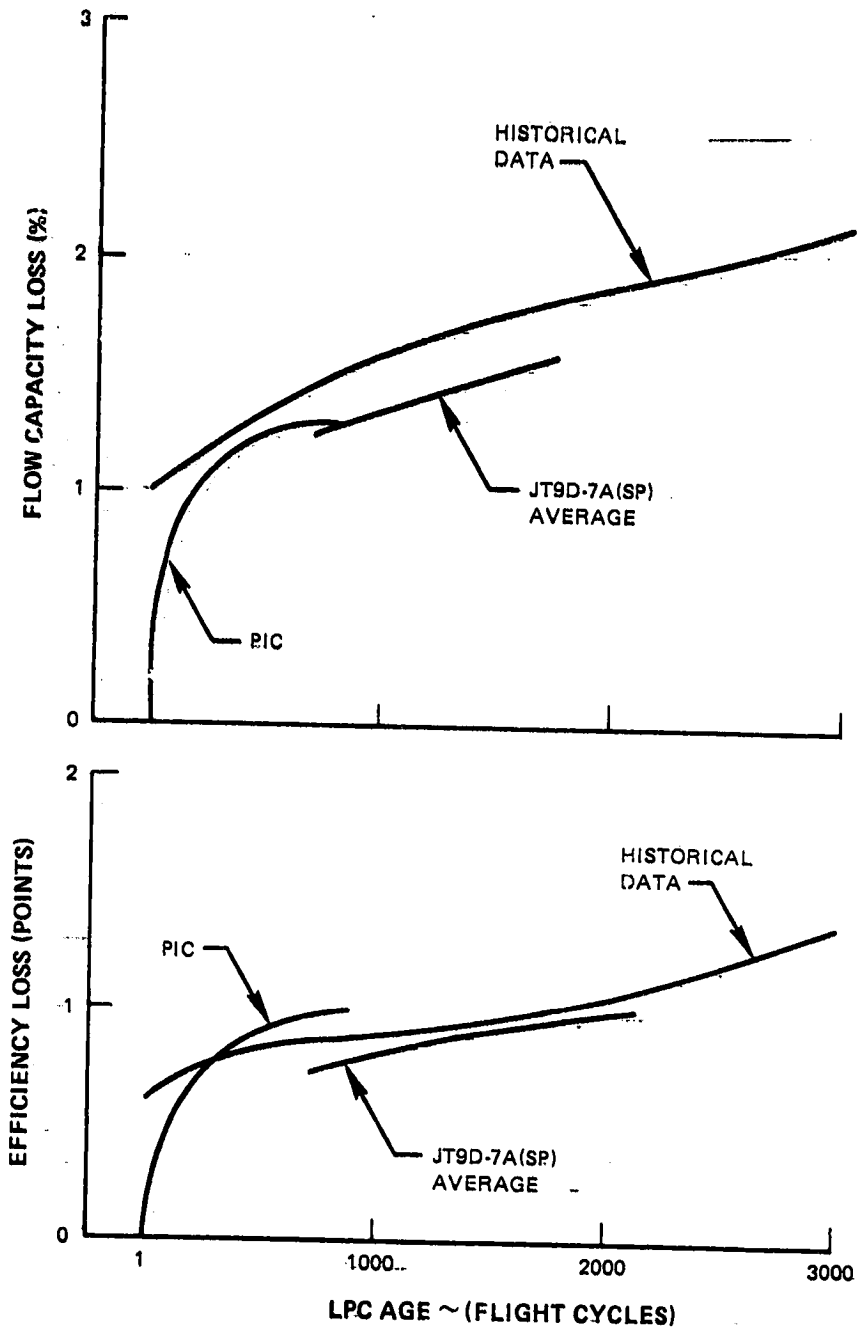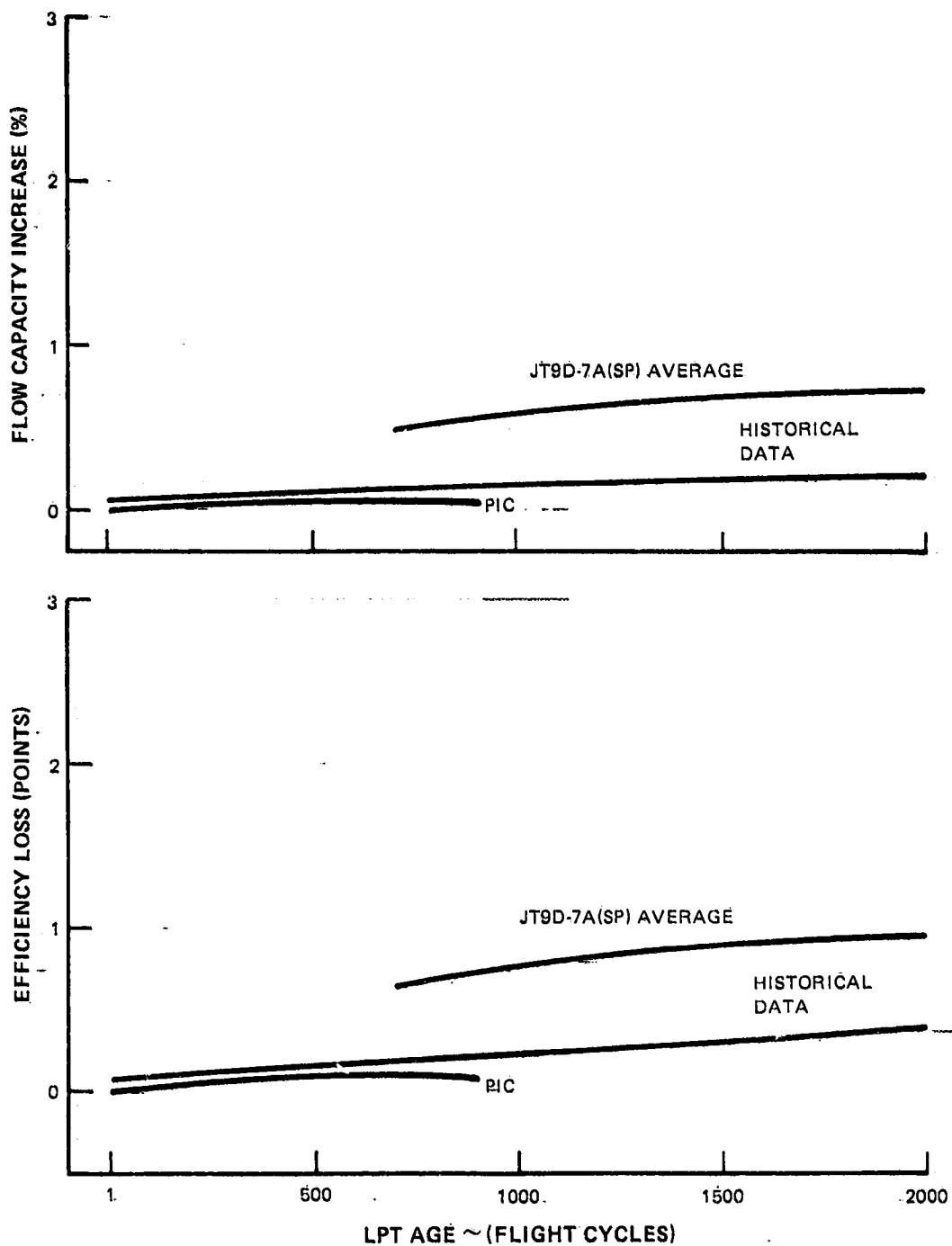Figure 59   Comparison of PIC,   JT9D-7A(SP) Prerepair and Postrepair,
           and   Historical   Low-Pressure   Turbine —   Performance
           Deterioration Data - The test stand data shows greater
           low-pressure turbine losses than does either the PIC or
           historical data.

SECTION 5.0

REFINED MODELS OF JT9D
ENGINE PERFORMANCE DETERIORATION

5.1 REFINEMENT OF PERFORMANCE DETERIORATION MODELS

One of the end results of the initial phase of the JT9D Engine Diagnostics Program was the establishment of preliminary performance deterioration models for the JT9D engine and its modules (fan, low- and high-pressure compressors, and high- and low-pressure turbines). These preliminary models were based on the analysis of Pratt & Whitney Aircraft and airline historical and used parts data. This section of the report discusses the refinement of these models as influenced by the in-service data gathered from the Pan American 747 JT9D-7A(SP) fleet. This latter data included PIC tests data and prerepair and post-repair test stand data.

5.1.1 Fan

Figure 60 shows the refined fan efficiency and flow capacity loss model. The refined performance deterioration model is an average curve fit through the three curves (which were not weighted equally). Prerepair test stand data analysis results have been favored over PIC analysis results. During PIC tests, the presence of the inlet cowl caused inlet flow field instabilities which led to low rotor speed variations. The prediction of the fan flow capacity and efficiency from the PIC data alone is, therefore, considered less reliable than predictions based on test stand data. Prerepair test stand data and historical data (preliminary model) are in fairly good agreement with each other. The refined model represents an average fit through these two sources.

Figure 61 presents the refined fan model curves with the scatter bands. These bands represent the approximate scatter in the JT9D-7A(SP) data and thus represents the possible engine-to-engine variations for each model.

5.1.2 Low-Pressure Compressor

Figure 62 shows the Low-Pressure Compressor refined models. The three data sources are in fairly good agreement with each other except that the historical data shows somewhat greater flow capcity loss. The JT9D-7A(SP) prerepair and PIC data has been favored over the historical data because the expanded instrumentation (include Tt3) used in the JT9D-7A(SP) engine testing permitted more accurate analysis of low-pressure compressor deterioration.
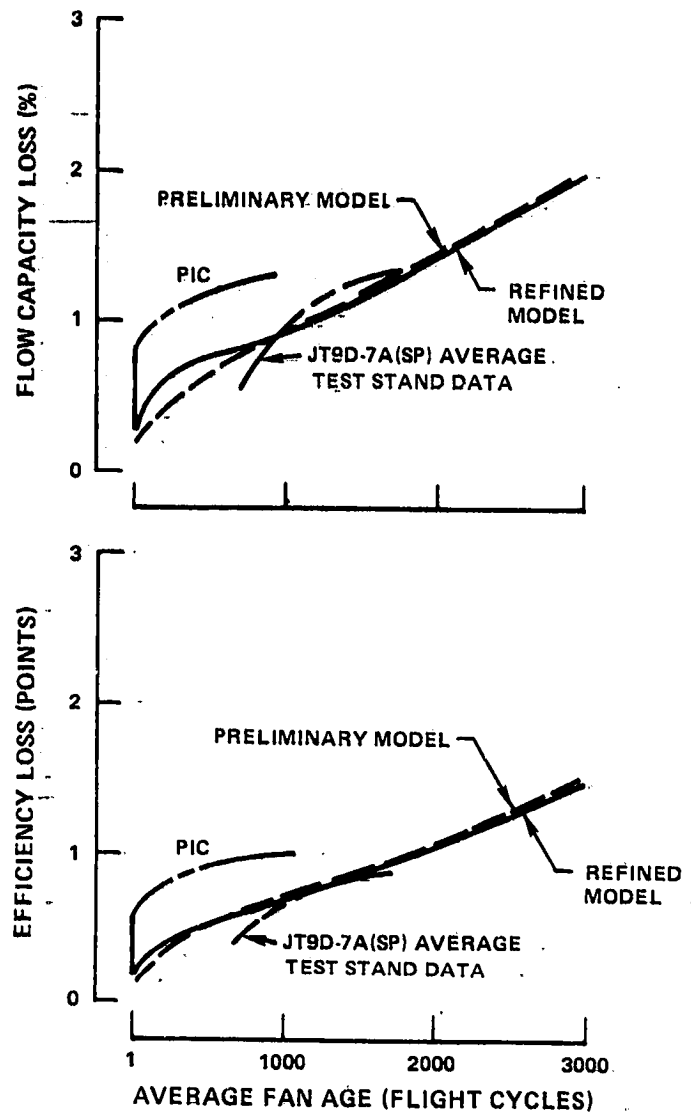
Figure 60   Development of Fan Performance Deterioration Refined Model
           - The refined model is based predominately on the
           JT9D-7A(S) test stand data and the preliminary model.

Figure 63 presents the refined low-pressure-compressor models with the
scatter bands of possible variations among individual engines.
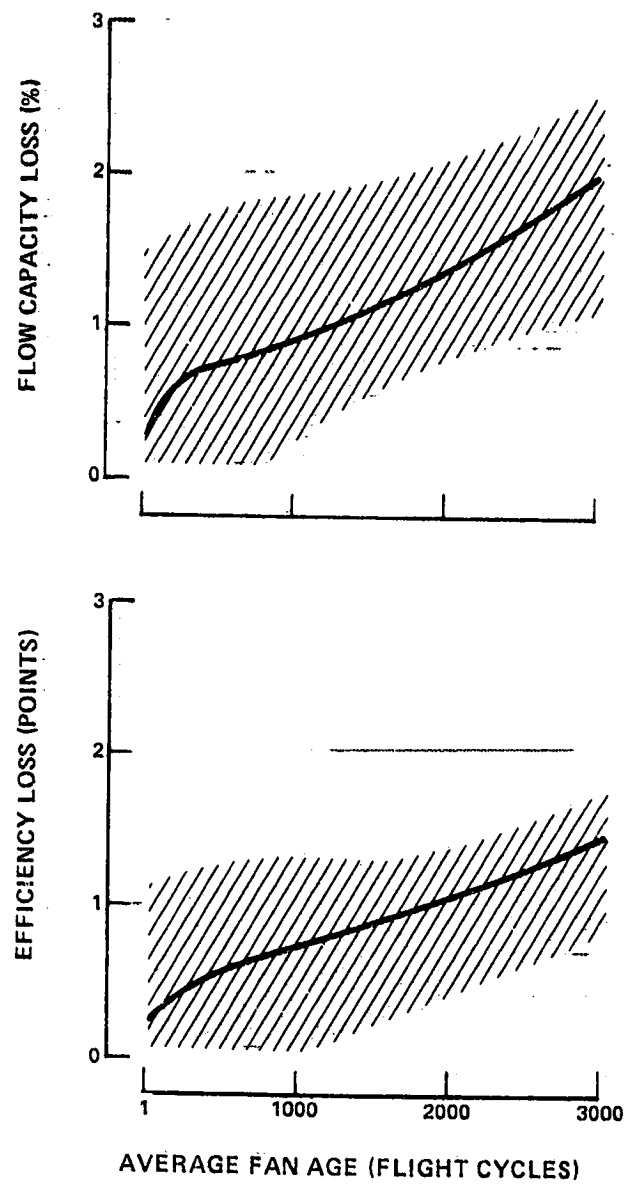
Figure 61   Fan Performance Deterioration Refined Model and Variation
            Band - The variation band represents data scatter among
            individual JT9D-7A(SP) engines.
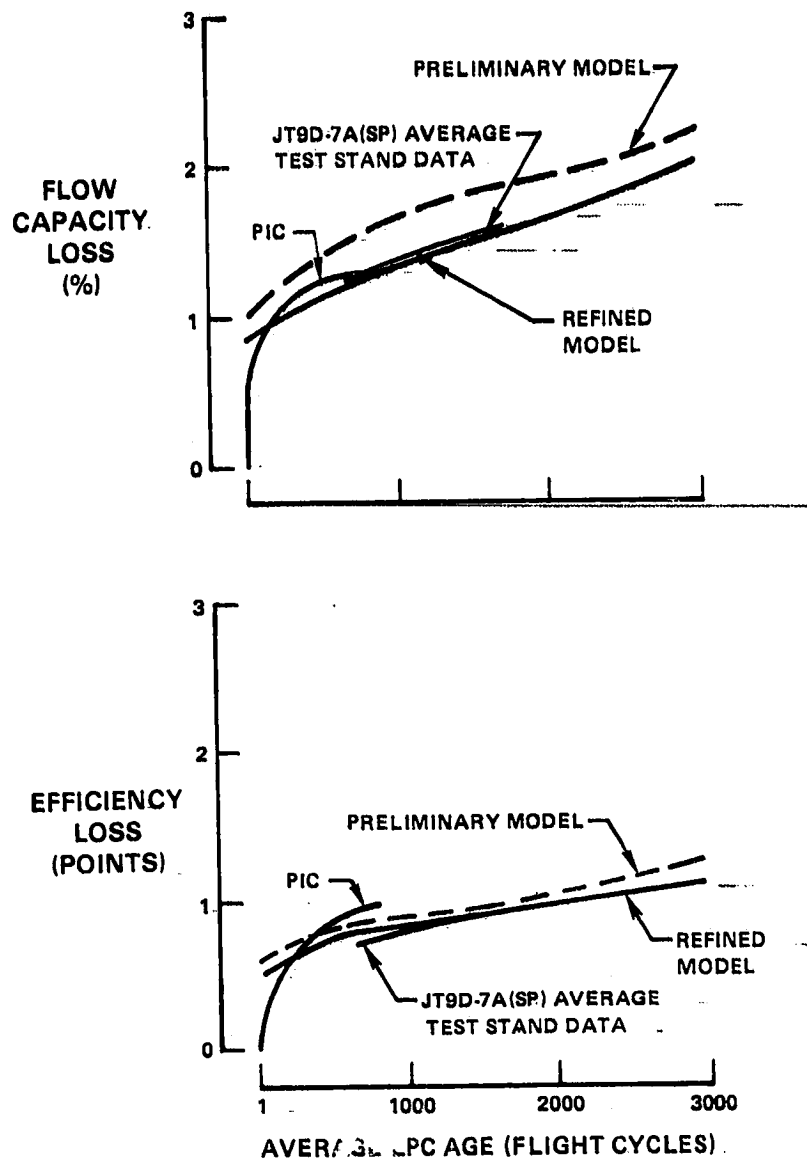
Figure 62   Development   of   Low-Pressure   Compressor   Performance
Deterioration Refined Model - The refined model shows less
flow capacity loss than the preliminary model.

5.1.3 High-Pressure Compressor

The refined high-pressure model is shown on Figure 64. It is weighted
toward the JT9D-7A(SP) engine data and is somewhat lower than the
preliminary model. The JT9D-7A(SP) PIC and test stand data trends have
been favored over the historical results because there is relatively
little Tt4 instrumentation data in the historical test results, leading
to uncertainty as to high-pressure compressor efficiency losses. The

refined model lies above the JT9D-7A(SP) data based on engineering judgment. The 747 JT9D-7A(SP) serves relatively few city pairs and the exposure to dirt ingestion is estimated to be less than would be experienced on the average airline operator aircraft or engine to which the model is addressed. No flow capacity deterioration model is shown for reasons previously discussed in Section 4.0

AVERAGE LPC AGE (FLIGHT CYCLES)
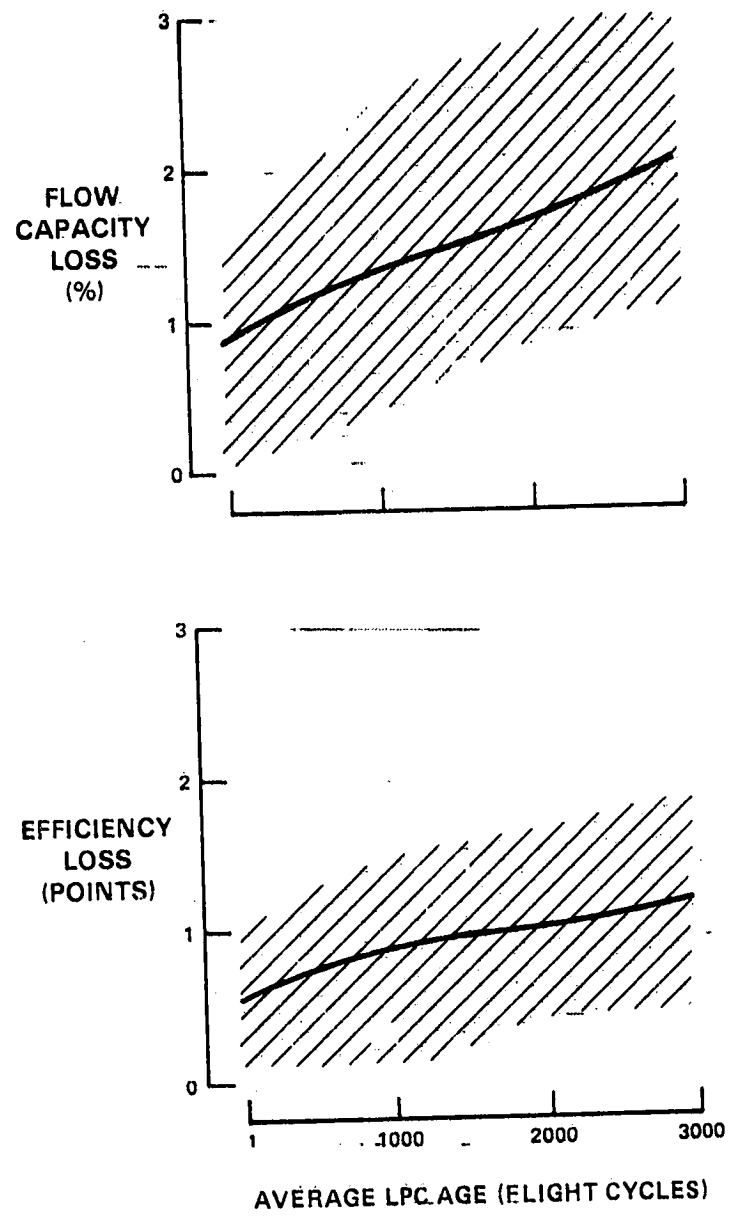
Figure 63   Low-Pressure Compressor Performance Deterioration Refined Model and Variation Band - The variation band represents scatter among individual JT9D-7A(SP) engines.
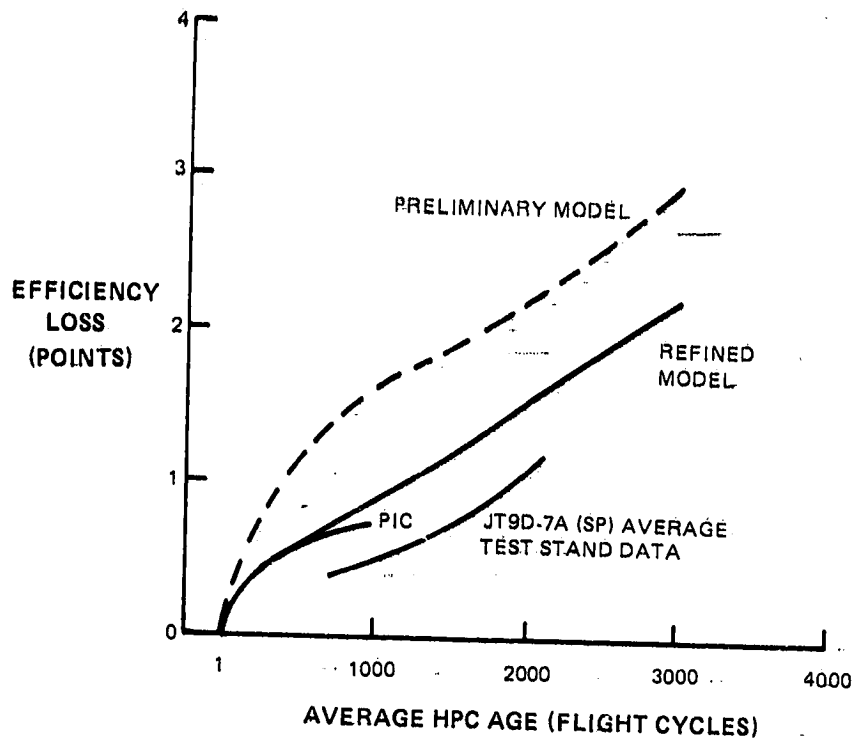
Figure 64   Development of High-Pressure Compressor Performance Deterioration Refined Model - The refined model lies between the historical data and JT9D-7A(SP) data which indicate lower deterioration with respect to usage.

The refined model with the performance scatter band is shown on Figure 65.

5.1.4 High-Pressure Turbine

The refined High-Pressure Turbine models are shown on Figure 66. The efficiency loss for the refined model is somewhat less severe than for the preliminary model. The flow capacity increase is slightly greater. The refined model represents an average fit of PIC, prerepair, and historical data, although PIC and prerepair data are favored because of the higher quality of the JT9D-7A(SP) data as discussed in Section 4.0.

3

2

EFFICIENCY
LOSS
(POINTS)

1

0

1   1000   2000   3000

AVERAGE HPC AGE (FLIGHT CYCLES)
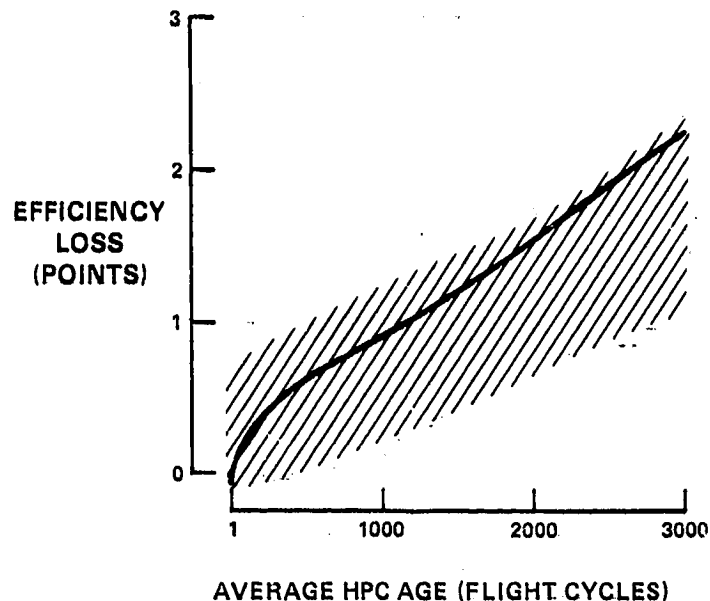
Figure 65   High-Pressure Compressor Performance Deterioration Refined
Model and Variation Band - The variation band represents
data scatter among individual JT9D-7A(SP) engines.

The flow capacity increase for both the preliminary and refined models
may be partly due to high-pressure compressor discharge pressure
profile changes resulting from tip clearance losses in the low- and
high-pressure compressors. Measured $P_{s}4$ strongly influences analysis of
high-pressure turbine flow capacity as discussed in Section 4.0. The
refined models with their possible scatter bands are shown on Figure 67.

5.1.5 Low-Pressure Turbine

The refined low-pressure turbine models are shown on Figure 68. Both
efficiency losses and flow capacity increases are greater than the
preliminary models. Again, the JT9D-7A(SP) test stand data analysis
results were favored over the historical data because the JT9D-7A(SP)
data are believed to be more credible. The refined model trend was
weighted toward the test stand (700 to 2000 cycle) analysis results.
The PIC analysis of low-pressure spool loss split between the fan and
low-pressure compressor is considered less reliable because of inlet
instabilities as previously discussed in the fan section (5.1.1).

97
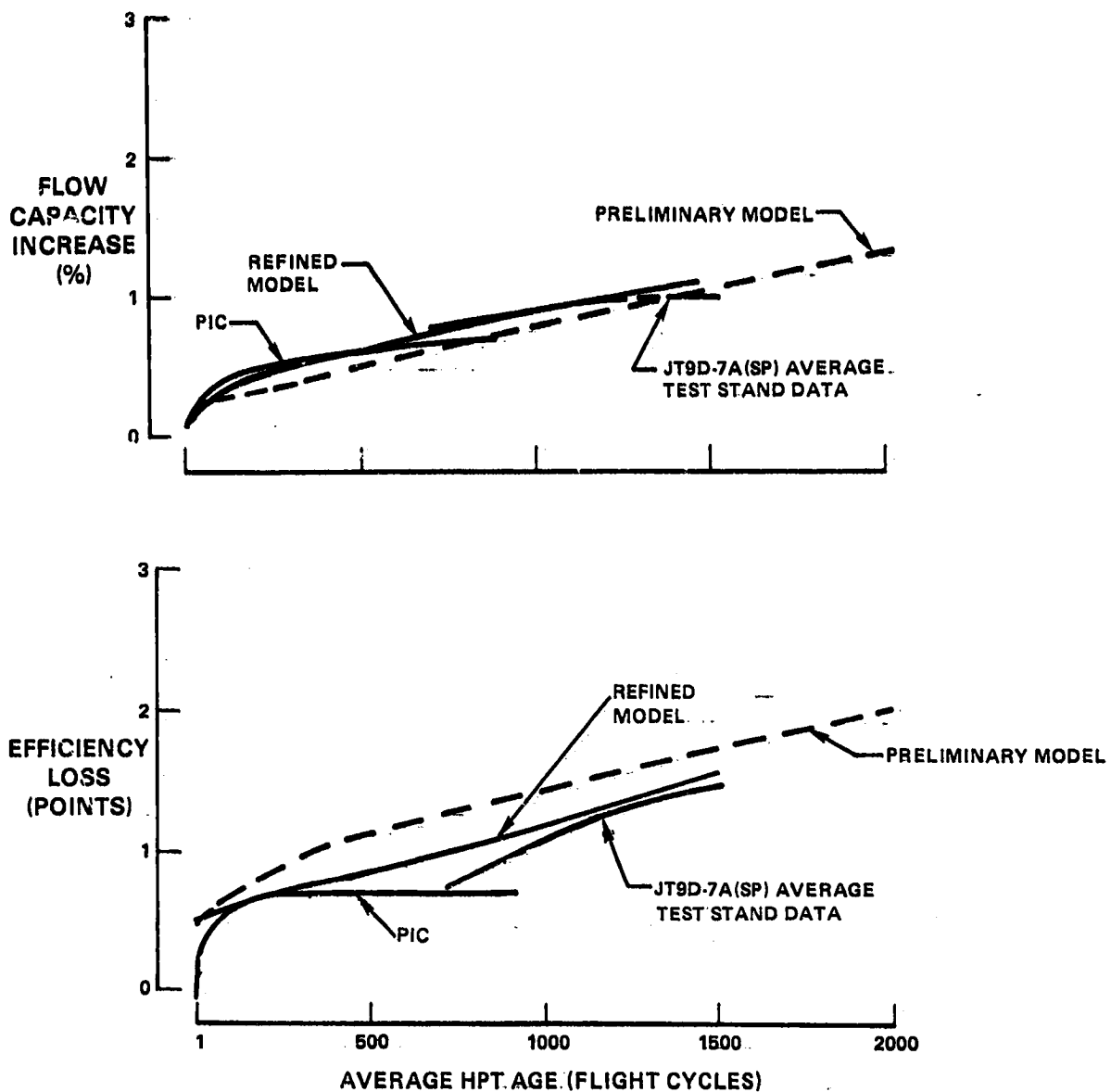
Figure 66   Development   of   High-Pressure   Turbine   Performance
Deterioration Refined Model - JT9D-7A(SP) engine data
showed lower efficiency deterioration and slightly higher
flow capacity increase than that for the historical data.
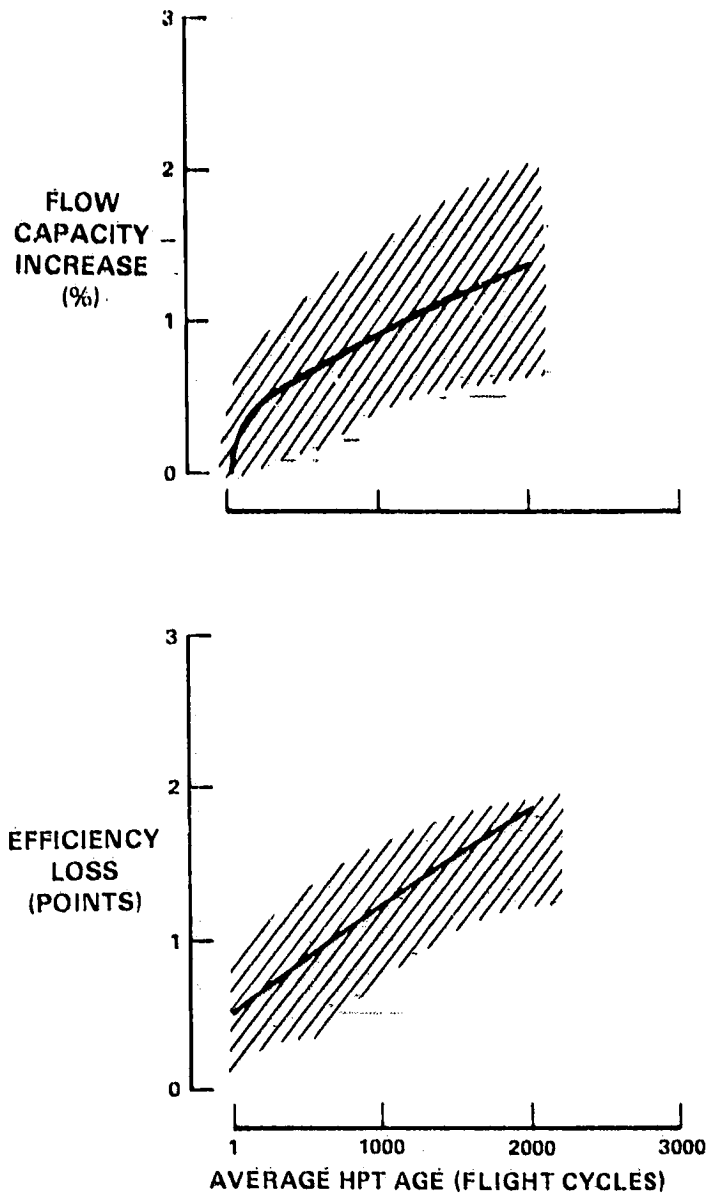
Figure 67   High-Pressure Turbine Performance Deterioration Refined
             Model and Variation Band - The variation band represents
             data scatter among individual JT9D-7A(SP) engines.

The refined models with the possible scatter bands are shown on Figure 69.
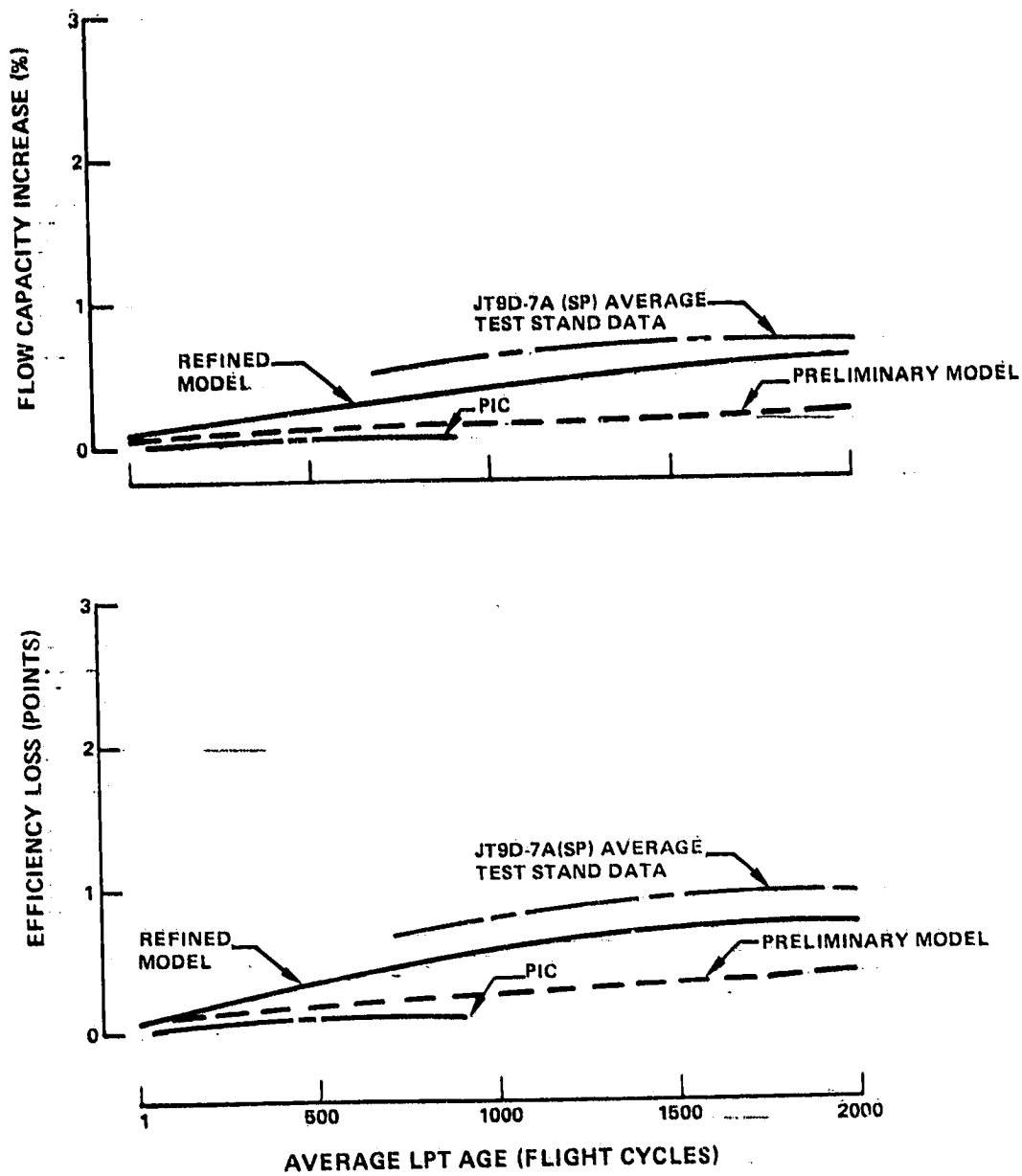
Figure 68 Development of Low-Pressure Turbine Performance Deterioration Refined Model - JT9D-7A(SP) engine data shows increased deterioration relative to historical data trends.
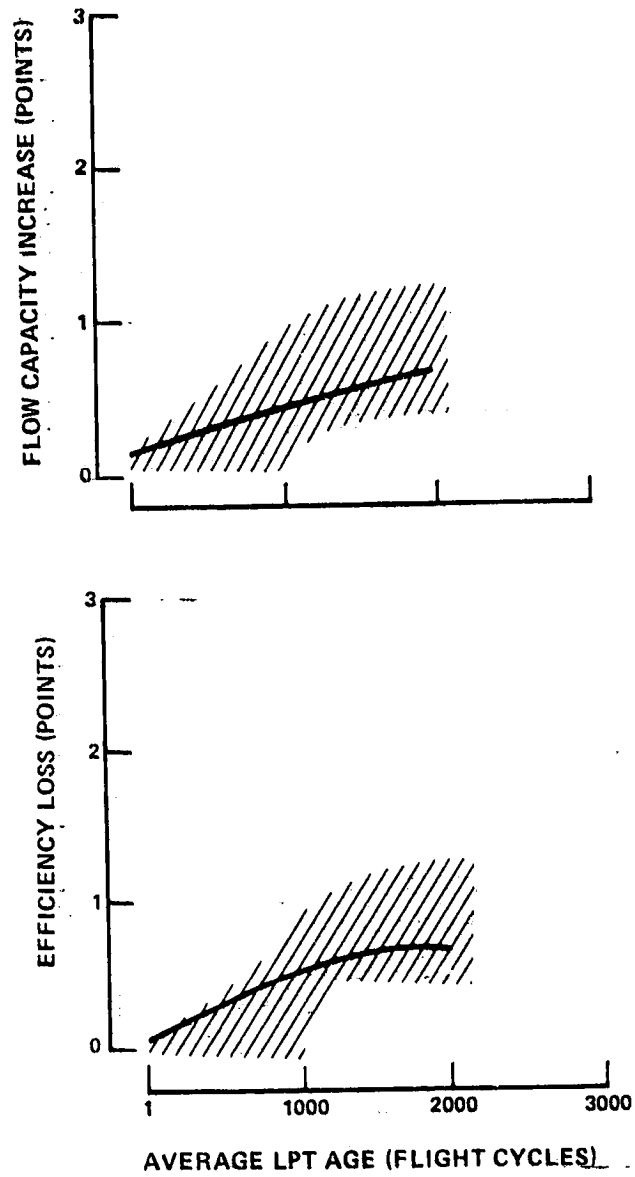
Figure 69   Low-Pressure Turbine Performance Deterioration Refined Model - The variation band includes all data collected to date.

5.2 ENGINE PERFORMANCE TRENDS—MODEL VERSUS DATA

The refined models of component deterioration have been combined to predict overall engine sea level take-off TSFC deterioration (at constant thrust) and EGT increase (at constant EPR). Stabilized high-pressure turbine performance beyond 1000 cycles and low-pressure turbine performance beyond 2000 cycles are assumed. The results are shown in Figures 70 and 71.
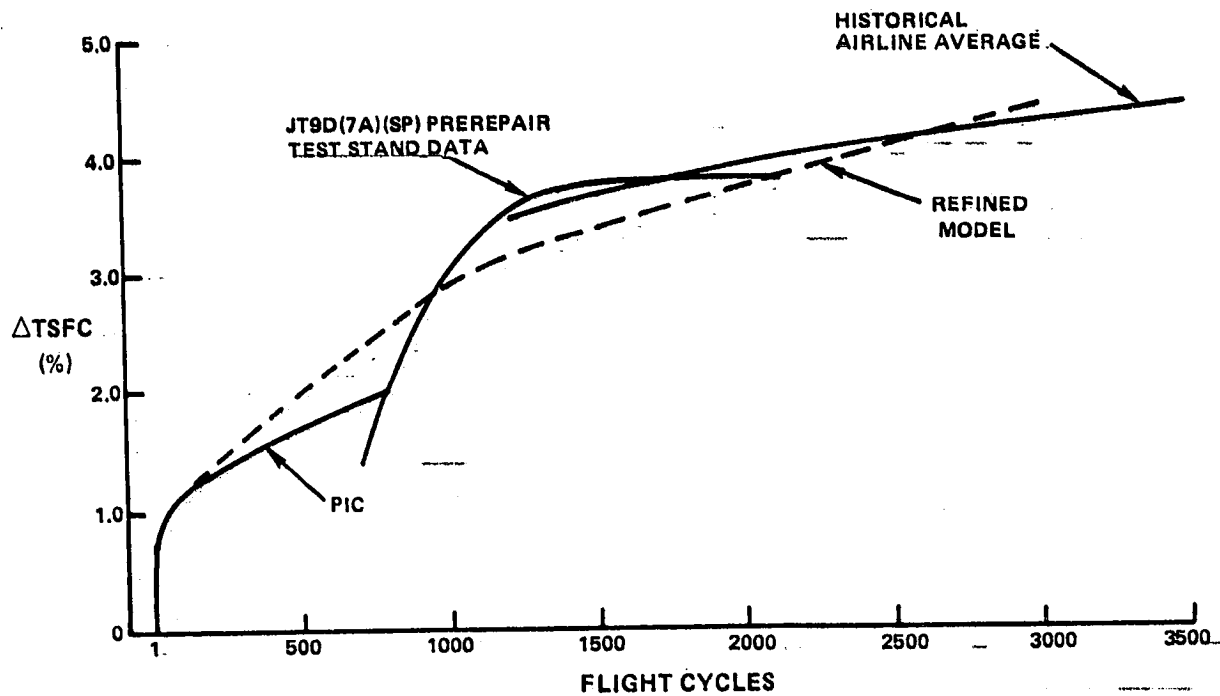
Figure 70   Prerepair TSFC Performance Data, Measured at Constant Thrust, as a Function of Usage — The refined model of engine performance loss shows good agreement with historical data and 747 SP engine test stand and PIC data.

Figure 70 shows engine TSFC deterioration at three usage intervals obtained by curve fits through JT9D-7A(SP) engine test stand data, PIC data, and the historical data. The refined model shows good correlation with the various data sources. Prerepair TSFC deterioration for unrepaired engines, as predicted by the model, ranges from nearly 1 percent in 50 cycles to about 3.7 percent in 2000 cycles. The historical data (engines generally having had some prior repair) and

102

the model (with stabilized turbine damage) show TSFC deterioration increasing to about 4.4 percent in 3000 cycles.

FLIGHT.CYCLES
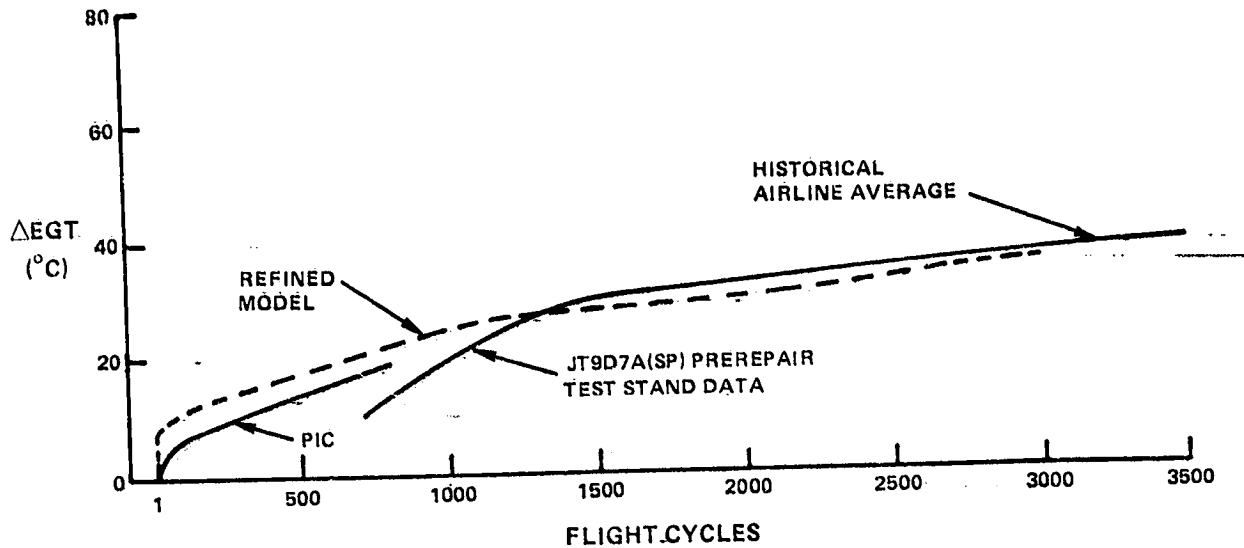
Figure 71   Prerepair EGT Performance Data, Measured at Constant EPR, as a Function of Usage -- The refined model of engine performance loss shows good agreement with historical data and 747 SP engine test stand and PIC data.

Figure 71 presents prerepair EGT increase for unrepaired engines, relative to production EGT level, as predicted by the models. This deterioration trend is compared to the trends from JT9D-7A(SP) engine test stand data (based on fuel flow) and from PIC data, as well as to the historical test stand data. The model, with stabilized high-pressure turbine damage assumed, shows good correlation with the various data sources. Prerepair (unrepaired) EGT increase is about 30°C at 2000 flight cycles.

There are no module loss models for postrepair data because of the variability of repair levels and repair standards. However, Figure 72 compares postrepair TSFC deterioration trends from JT9D-7A(SP) engine test stand data with the trends of the historical data. An average fit of the data is shown. Average postrepair TSFC deterioration relative to the production level ranges from about 2 percent at 1000 flight cycles to about 3.5 percent at 3000 cycles.

103
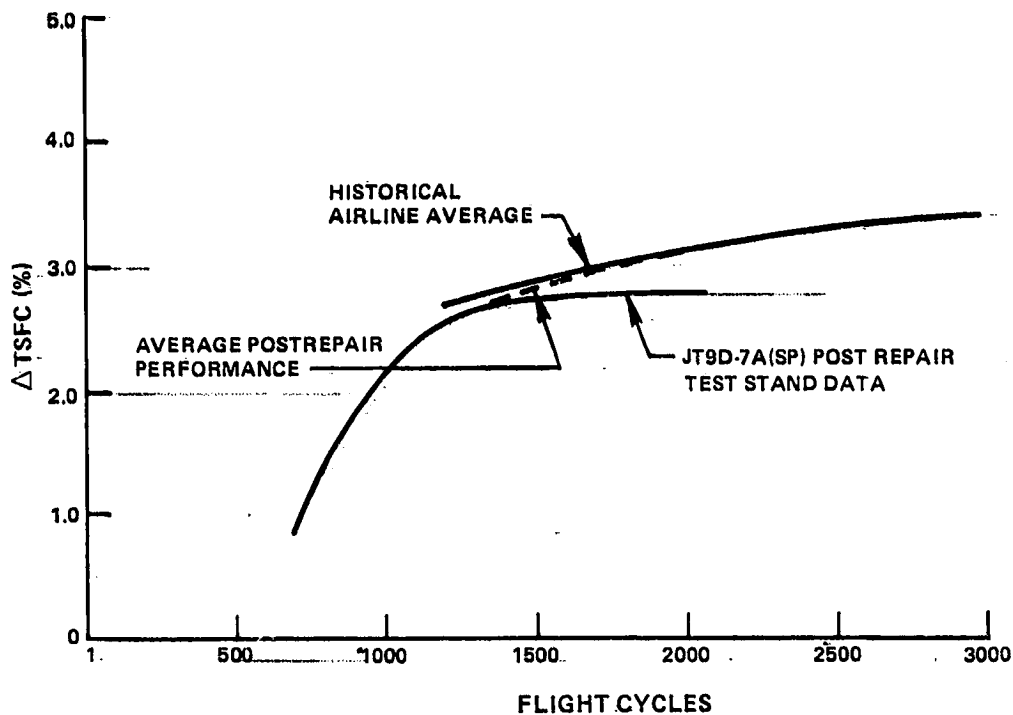
Figure 72   Postrepair TSFC Performance Data, Measured at Constant Thrust, as a Function of Usage - The-average postrepair performance shows good correlation with the 747SP engine test stand data and the historical data.

Similarly, Figure 73 shows postrepair EGT trends, relative to the production level, for the various data sources. An average fit of the data is shown. Average postrepair EGT deterioration is about 20°C at 2000 cycles.

5.3 MODEL PREDICTIONS

The individual module loss models have been used in the engine simulation to estimate losses at given flight cycle periods, by module and by damage mechanism. These TSFC predictions are at sea level static constant take-off thrust.

The bar chart shown in Figure 74 compares the individual module losses estimated using the models at 50, 500, 1000, 2000, and 3000 flight cycles. No cold section repair was assumed for the preparation of the comparison in Figure 74. However, high-pressure turbine damage was assumed to be stabilized at 1000 cycles and low-pressure turbine damage at 2000 cycles to reflect typical prerepair engines.

104
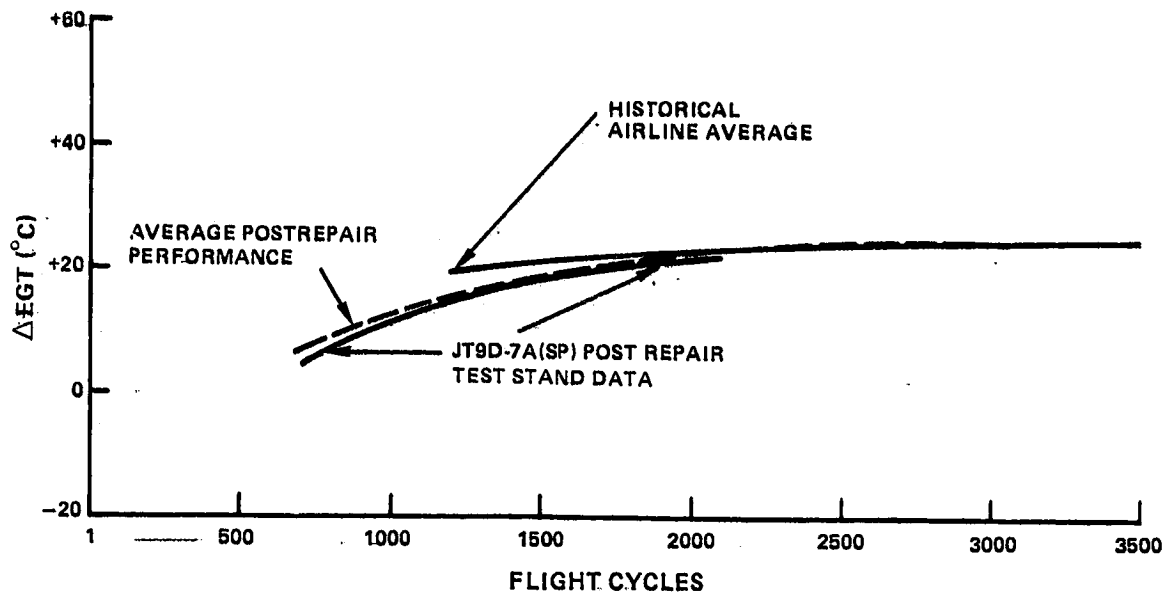
Figure 73. Postrepair EGT Performance Data, Measured at Constant EPR, as a Function of Usage - The average postrepair performance shows good correlation with the 747SP engine test stand data and the historical data.
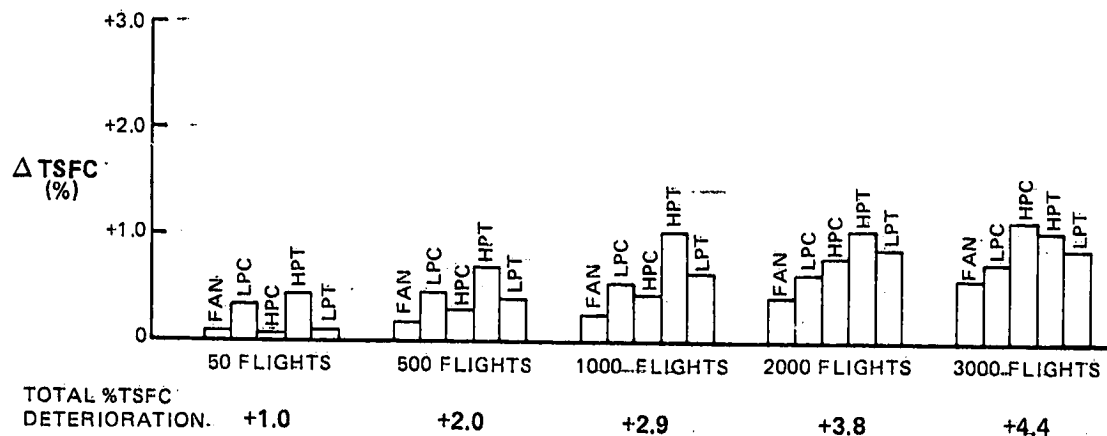
Figure 74 Module Performance Deterioration, at Constant Undeteriorated Sea Level Static Take-Off Thrust, Based on the Refined Engine Deterioration Model - Early performance losses are most significant for the low-pressure compressor and the high-pressure turbine; as flight cycles increase, high-pressure compressor and low pressure turbine become increasingly important.

105

Figure 75. presents a module-by-module comparison between the refined model and the preliminary model which resulted from the historical data study. The refined model total TSFC loss at a given cyclic age is somewhat less than that predicted by the preliminary model through 1000 cycles, and similar to that predicted by the preliminary model at 2000 and 3000 cycles. However, the distribution of losses by module is different. The refined model shows less high-pressure compressor loss at a given cyclic age, and more low-pressure turbine loss. Fan, low-pressure compressor and high-pressure turbine losses are similar. These differences are attributed primarily to increased data quality in this study relative to the data from the historical study, permitting more rigorous analysis (earlier data had greater test stand correction uncertainty).

Figure 76 presents the refined model showing the revised estimates of the contribution of the three major causes of performance deterioration to module performance losses.

Early performance losses are due primarily to tip clearance increases and are most significant for the low-pressure compressor and the high pressure turbine. As flight cycles increase, cold section erosion and thermal distortion becomes increasingly important.

Figure 77 presents the refined model showing the estimated relative contribution of the three major causes to engine performance deterioration versus flight cycles. Comparison with the preliminary model would show minor changes in the overall level and distribution by cause in the 500 to 1500 flight cycle period resulting from the improved quality of the JT9D-7A(SP) data.
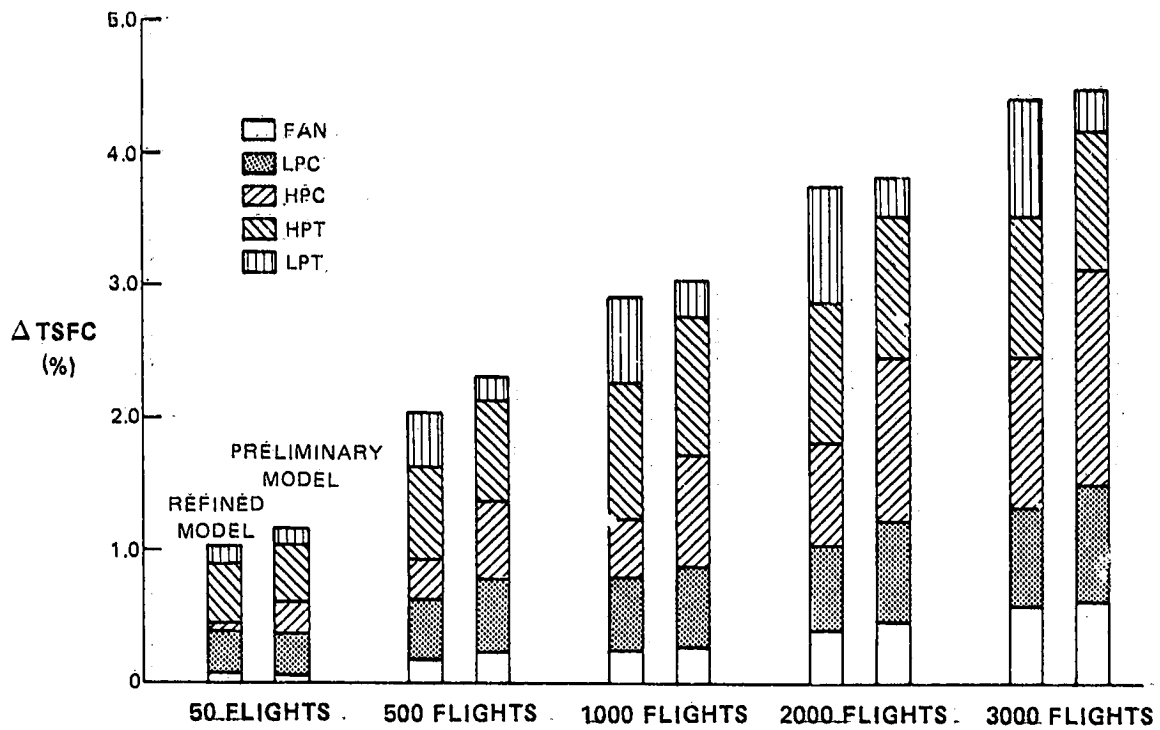
Figure 75   Module Performance Deterioration, at Constant Undeterior-
             ated Sea Level Static Take-Off Thrust; Refined Model
             Results Compared to Preliminary Model Results - The refined
             model shows slightly less short term loss; as flight cycles
             increase, the refined model loss is similar to the prelim-
             inary model, but the distribution of losses by module is
             somewhat different.
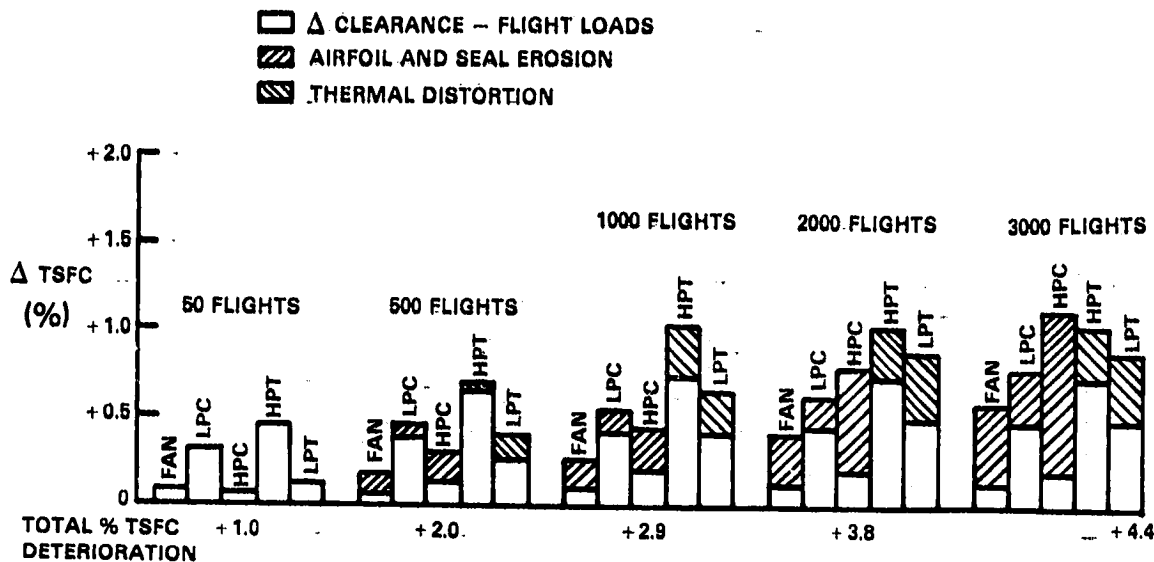
Figure 76   Major Causes for Module Performance Deterioration - The estimated contribution of flight loads, erosion, and thermal distortion to module performance losses are shown.
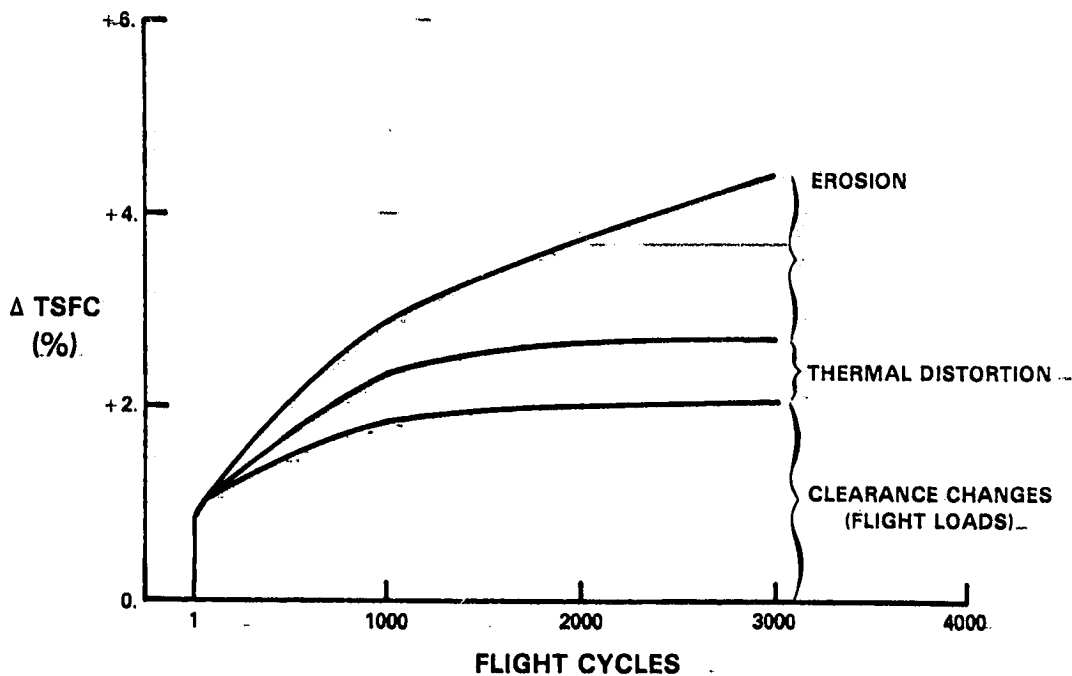
Figure 77   Contribution of Major Causes to Overall Engine Performance Deterioration - The refined model shows negligable difference to the preliminary model with respect to the proportion of overall engine performance loss due to each cause.

SECTION 6.0

RECOMMENDATIONS

Based on the analysis of the data collected during the current efforts of the NASA JT9D Engine Diagnostic Program, and considering the preliminary recommendations presented in NASA CR-135488 (Ref. 1) a number of refined recommendations can be made.

- o Action that the airlines could take now to improve fleet average performance,

- o Areas where design and development of improvements are required, and

- o Areas where additional diagnostics efforts are required.

Recommended engine operating procedures, discussed in Section 6.2, lists operating do's and don'ts for the airlines to minimize deterioration during transient engine operation.

A simple and accurate system of performance monitoring and maintenance documentation would permit each airline to optimize maintenance procedures and minimize fuel consumption and operating costs. Section 6.2 discusses what the airlines can do now and what additional tools are required.

Section 6.3 recommends maintenance actions and frequencies by module to minimize performance deterioration and to achieve the maximum practical performance restoration. The recommendations, based on the historical data and the Pan American 747SP engine prerepair and postrepair data and analyses, may be put into practice now.

Section 6.4 discusses the four generic performance deterioration mechanisms and the design and development criteria that should be investigated to reduce the influence of these mechanisms.

Finally, Section 6.5 discusses experimental and analytical efforts needed to better understand the complex causes of specific deterioration phenomenon and permit identification of potential solutions to engine performance deterioration.

6.1 ENGINE OPERATING PROCEDURES

Production acceptance testing of new engines at Pratt & Whitney Aircraft has shown very little deterioration (0.2 percent TSFC change

maximum) from the initial data point to the final calibration. This running includes all of the various types of operation (including snap acceleration and deceleration transients) that are required in customer test stands or during ground test operation in the aircraft. The following guidelines have been developed to minimize deterioration during this type of post-repair engine operation:

1. Operate at idle power for a minimum of 5 minutes after start before accelerating above idle.

2. The initial acceleration from idle on a restored engine should consist of gradual incremental power increases.

3. Unnecessary hot, fast accelerations or decelerations should be avoided:

    a. Whenever possible, accelerations or declerations should be slow, that is, at a rate equivalent to a minimum of 60 seconds for a full power-lever excursion between idle and take-off power.

    b. Following more than one minute of operation at or above bleeds closed power, the engine should be operated at idle for:

        (1) 7 minutes prior to a slow acceleration (that is, 60 seconds minimum, idle to take-off);

        (2) 15 minutes prior to a snap acceleration, which is defined as a power lever movement of one second or less for a full excursion.

    c. When snap decelerations are required, they should be performed as soon as possible after reaching high power (0 to 10 seconds preferred, 30 seconds maximum).

    d. Engine calibrations should be performed in a decreasing power direction so that the engine will be "cool" at the end of the calibration prior to shutdown or other operation.

    e. Run at idle for a minimum of 5 minutes before shutting down.

Adherence to these procedures will minimize blade to rub-strip contact by allowing the contact to occur gradually rather than abruptly. Abrupt contact in high-pressure turbine stages can cause localized metal

110

transfer and build-up on the rub strip which would result in excessive blade tip wear.

Sufficient "cool down" time at idle after being at high power and prior to an acceleration to high power (as prescribed in 3.b. above) is required to prevent excessive blade to rub-strip contact resulting from a hot rotor accelerating in a relatively cool case. Similarly, if snap decelerations are to be made, they should be performed as soon as possible after reaching high power (3.c above) to minimize the amount of thermal growth of the rotor disk which can potentially rub the "cool" case after the deceleration is made. Figure 78 graphically presents the interaction of a typical hot rotor and rub strip (that is, tip clearance) during an acceleration/deceleration cycle. Revised test stand procedures that are consistent with the above recommendations are soon to be released for revision of the JT9D engine manual.

An unfortunate incident during the postrepair testing of JT9D-7A(SP) engine P-695745 showed the effects of inadvertently not following the above operating guidelines. Following the April 1978 repair and postrepair test of this JT9D engine by Pratt & Whitney Aircraft, it was returned to Pan American for their testing. On June 19th, the engine was run in the test stand for the purpose of correlating their stand with the Pratt & Whitney Aircraft Middletown engine test stand. During the second calibration run, after stabilizing for 3 to 5 minutes at take-off power level, the engine was accidentally shutdown. The engine was restarted within 2 minutes, and the test was continued. There was no indication of rotor seizure; however, subsequent analysis of the test data indicated that there was a performance deterioration of 1.2 percent in Wf and a 12°C increase in EGT relative to the prior calibration run.

The effect of this shutdown and restart was similar to the transient shown in steps 3, 4, 5, and 6 on Figure 78. The accidental shutdown removed the centrifugal forces on the disk, allowing the disk to shrink, and opening the clearances (point 3 → 4). The turbine case and outer rub strip then started cooling and shrinking at a more rapid rate than the disk, causing the blade tip/rub-strip clearance in the slowing down engine, to close (point 4 → 5). The engine was restarted before the high-pressure turbine disks had cooled and the clearances had sufficiently reopened. The resulting centrifugal force on the hot disks caused them to expand, closing the gaps between the blades and the relatively cool rub strips (point 5 → 6). The rub which ensued was not sufficiently severe to cause a seizure but did open blade tip/rub strip clearances enough to cause the measured performance loss.

Thus, the failure to observe the recommended operating procedures during test stand or installed engine operation can result in

111

significant loss of performance. If the resulting rub occurs during a postrepair test, the restored performance from a careful refurbishment can be lost before the engine is returned to service, and the benefit of the refurbishment will be obscured to airline maintenance and operating personnel.

HOT SNAP DECEL

SNAP ACCEL

N_2

SNAP ACCEL

HOT SNAP DECEL

SNAP ACCEL

GAP

① RUBSTRIP EXPANDS FIRST ④ RUBSTRIP COOLS DOWN FASTER THAN DISK DISK COOLS 15 MINUTES OK FOR SNAP ACCEL

ROTOR DISK GROWS

DISK STILL HOT

② ③ ⑤

0.

RE-ACCEL HOT ACCEL RUB

S.S. IDLE S.S. SLTO ⑥ S.S. IDLE

TIME

ACCEL DECEL

① → ② SNAP ACCEL — INITIAL CLEARANCE DECREASE DUE TO CENTRIFUGAL GROWTH AND BLADE THERMALS

③ → ④ HOT SNAP DECEL — INITIAL CLEARANCE INCREASE DUE TO CENTRIFUGAL RELAXATION AND REDUCED BLADE TEMPERATURE

⑤ → ⑥ IF SNAP ACCEL PERFORMED BEFORE DISK COOLS, CENTRIFUGAL GROWTH AND BLADE THERMALS ON HOT ROTOR WILL CAUSE ABRUPT BLADE/RUBSTRIP CONTACT

Figure 78   Hot Rotor/Rub-Strip Interaction - Because the thermal expansion and contraction rate of the case (and the rub strip) is faster than that of the rotor disk, an abrupt blade/rub-strip contact will occur if a snap acceleration is performed before the disk cools.

6.2. PERFORMANCE MONITORING

6.2.1 Performance Trending and Management

Efforts during the historical and current in-service data collection activities highlighted the need for improved management information concerning individual engine and fleet deterioration if improvements in

112

fuel burned and operating costs are to be achieved. It has been clearly identified that large variations exist between operator practices that have an impact on average engine performance level. An operator's fleet fuel consumption is dependent on two factors: performance retention while on the wing, and performance recovery while in the shop. To effectively manage these factors, complete records of individual engine performance histories and repairs are required. These data should include:

o——Initial engine performance data;

o   Periodic installed engine performance data to define trends, including fuel costs and range/payload limitations;

o   Representative airplane operating cycle data;

o   Accurate performance restoration and engine modification data, including cost and shop turn-around data; and

o   Expanded instrumentation testing before and after major refurbishment actions.

A computerized management tool could then be used by each airline to optimize engine owning and operating costs for its fleet and route structure. This tool could provide each airline's management with a means to evaluate effectiveness of shop visits and could assist in controlling those factors that increase fuel consumed. To develop such a management tool, several steps are necessary, including:

o   Performance data collection and processing should be revised to provide more accurate tracking of individual engine performance.

o   Accurate repair rebuild and operational histories should be maintained for engines, modules, and performance sensitive components.

o   A reliable and simple system for measuring and analyzing engine performance before and after repair is necessary.

o   A rigorous instrument calibration system is required to ensure test measurement accuracy.

Each of these requirements is discussed in the following paragraphs.

6.2.2 Engine Condition Monitoring

The existing flight performance Engine Condition Monitoring (ECM) system does not provide data of sufficient accuracy for precise performance monitoring of individual engines. It is desirable to develop a standardized, simple, and sufficiently accurate system for determination of engine flight performance deterioration trends. The AID'S system, which is available, may be the answer to this problem. AID'S is an automated data system which monitors in-flight performance more directly than the current ECM approach.

6.2.3 Operating History and Repair Data Collection

This basic information exists in various forms at all operators. It would be desirable to develop a uniform program with the capability of comparison of operator characteristics. Such a common program would permit identification and comparison of relative deterioration rates for operators in adverse operating environments, such as mid-East deserts, with operators in clean climates. A program of this nature would provide the tool each operator needs to assess their own performance retention and restoration.

6.2.4 Analysis of Performance and Repair Data

The NASA JT9D Jet Engine Diagnostics Program has produced a preliminary analytical tool for isolating performance deterioration by module as a function of test stand testing and Plug-In Console (PIC) testing data. Further refinements will be necessary before such a diagnostic tool would be available to each airline to determine what repairs should be made on an engine and to measure the performance improvement, by module, of a repair action. See Section 5.4.

6.2.5 Test Stand Instrumentation and Calibration

Based on the observations made during visits to the airlines' test facilities during the historical and JT9D-7A(SP) data collection activities, several areas were noted where improvements could be made in the instrument calibration procedures. The recommendations are not directed toward any one airline, but to the test facilities in general. The recommendations fall into five categories as shown below:

o   Calibration standards,

o   Written calibration procedures,

o   Data retention,

114

o   Calibration techniques, and

o   Calibration analysis.

The problems and recommended solutions are discussed in detail in Section 6.2.2 of the report on historical data studies, NASA CR-135448 (Ref. 1) and will, therefore, not be repeated in this document. The general problem is that the errors which can develop in the test stand instrumentation system are of the same magnitude as the performance changes which need to be measured. Thus, a rigorous program of instrument calibration is required to accurately assess the magnitude of a specific performance problem and to provide an indication of the most likely cause of the problem.

6.3   MAINTENANCE PRACTICES

This section presents recommendations for the retention of engine performance which are based on the results of the earlier study effort with refinements resulting from the later data analysis. A principal result of these analyses is the knowledge that the relative influence of low-pressure spool module deterioration is greater on flight cruise performance than on sea level performance. Thus, greater emphasis should be placed on low-pressure spool module performance restoration than ground testing would suggest.

6.3.1   Fan

Fan performance deterioration is caused by the increased tip clearances which result from flight loads and which appear to stabilize after 1000 flights. Surface roughness increases with usage and then also appears to stabilize. Fan blade leading edge bluntness, however, continues to increase and the performance penalty grows.

Based on these damage mechanisms, periodic hand cleaning of the fan blades and stator vanes when the engine is in the shop and restoration of leading edges are the two recommended maintenance actions. As long as the fan rub strip is mechanically sound and the tip clearances are within Overhaul Manual limits, no restoration of fan blade clearance is recommended due to the short-term rub-out from the effect of flight loads. The recommended refurbishment period is between 2000 and 3000 cycles with strong preference given to the shorter interval because of rapidly increasing fuel prices.

6.3.2   Low-Pressure Compressor

The mechanisms that reduce performance in the low-pressure compressor are tip clearance, roughness, and airfoil leading edge shape. Surface

roughness increases —and then appears to stabilize. Tip clearances, however, continue to increase from the effects of erosion on the rubber outer airseals. Airfoil leading edge shape or bluntness is not judged to be significant up to the current level of usage (4000 to 5000 cycles).

The low-pressure compressor should be chemically cleaned at every exposure and the rub strips replaced between 2000 and 3000 cycles when the engine is in the shop. The first-stage trunnion stator vane should be replaced with a fixed first-stage stator vane to reduce flow loss. The effect of airflow losses, particularly on EGT, as well as TSFC, suggest that more attention should be placed on this module. The airfoils inspected showed signs of thinning from the samples inspected with 5000 cycles usage. Consideration should be given to replacing these airfoils between 5500 and 6500 cycles, depending on their condition at that time. The rapidly increasing cost of fuel will increasingly favor refurbishing at the louver end of the recommended interval.

6.3.3 High-Pressure Compressor

High pressure compressor performance losses caused by erosion are initially due to blade length reduction, loss of outer airseal material, and increased roughness. The effects of blade camber change, based on analysis, become important at usage levels beyond 3000 cycles in the blades.

The performance losses in the high-pressure compressor suggest that the compressor should be refurbished between 2500 and 3500 cycles with long blades and new/refurbished rub strips in all stages. The stators should also be chemically cleaned at this time. Based on stator thinning, the stators, as well as the blades, and outer airseals should be replaced at the next interval or 5000 to 7000 cycles.

The correlation of compressor blade-length to EGT improvement is strong. The measured EGT improvement due to reduced blade/OAS clearance appears greater than the expected average EGT improvement. Thus, it appears that reductions in compressor blade clearances improve combustor temperature profile and, hence, the EGT profiles and measured values.

6.3.4 Combustor System

Even after repair, the combustor should have 100 percent efficiency. While the direct effect of combustor deterioration on performance is insignificant, the indirect effects are major. Changes in radial and circumferential temperature patterns in the combustor exit gas affect

116

clearances, and a host of other mechanical shape changes in the turbine, as well as turbine durability.

When the combustor is repaired, the dimensions, and particularly the cone angle, should be restored. The fuel nozzles should also be removed and cleaned. The potential that cumulative damage even with repair will reduce the structural stability of the combustor front end suggest that the combustor not be used beyond the third installation. Turbine durability and performance losses can be traced to variations in combustor repair practices. More precise definition of which dimensions are the most critical must await further testing.

6.3.5 High-Pressure Turbine

The deterioration of the performance of the high-pressure turbine appears to be dominated by tip clearance changes and the second-stage vane inner shroud leakage.

Blade tip wear of first-stage turbine blades correlates with initial build clearances and build standards with respect to blade length. Control of first-stage blade length by hand selection or drum grinding to a constant diameter is recommended. The outer airseals should be offset ground to the requirement set forth in the Overhaul Manual. The tip clearance should be set to 0.073 +0.002 inch. The second-stage blade clearances should be set to the nominal dimension, and the second-stage vane inner foot dimensions should be set to the tight side of the tolerance band.

6.3.6 Low-Pressure Turbine

Blade tip clearances are a major cause of low-pressure turbine deterioration. Rebuild standards which allow larger tip clearances, cause an increase in postrepair performance deterioration. The ring seals of the low-pressure turbine are very responsive to temperature changes. Hot shutdowns will cause rubbing and performance loss due to the rapid contraction of these seals.

The performance penalties for increased tip clearance are larger in the third stage (first low-pressure turbine stage) than in the sixth stage. The tip clearances should be kept to nominal dimensions, particularly in the third and fourth stages during rebuild, and platform soldering should be eliminated by vane repair when the low-pressure turbine is opened for other reasons.

6.3.7 Rebuild Standards

Rebuilding an engine to the manufacturer's recommended standards is essential to achieving optimum performance recovery. The historical data study indicated that the TSFC recovery was less than that which was possible with recommended rebuild standards. Similarly with the Pan American engine repairs analyzed in the current study, there were numerous cases where shop production schedules required module "swapping" and did not allow time for modules and engines to be completely restored. This procedure is illustrated in Appendix C.

The Pratt & Whitney Aircraft JT9D Overhaul Manual and Repair Manual were originally developed with the objective of prolonging the useful life of parts to reduce maintenance costs on the basis of structural and safety criteria. The changing realities of higher fuel costs suggest the need to revise the manuals to provide information concerning the impact of various repair practices on fuel consumption such that each operator can determine the trade-offs between fuel consumption increases and maintenance cost increases.

Thus, it is recommended that the operators follow the current Pratt & Whitney Aircraft recommended repair practices until the results of this Diagnostics Program are used to revise and refine those practices.

6.4 DESIGN CRITERIA

6.4.1 Introduction

The results of the analysis of the historical data, in particular the parts inspection results, and the Pan American 747SP in-service engine data have provided detailed information from which recommendations can be made for specific design and development actions. These recommendations are presented in this section and are grouped below according to the three operation-related generic causes of deterioration. These causes are: the effect of flight loads on engine clearances, erosion and impact damage, and thermal distortion.

6.4.2 Flight-Load-Induced Losses

The increased diameter and tighter running clearances of current high bypass ratio turbofan engines have increased the sensitivity to the effects of flight maneuver loads. Historical and current engine studies have shown that there is a performance loss during the first few flights relative to production engine final acceptance test levels. The most likely cause of this performance loss is change in engine running clearances caused by either thermal or flight load conditions not experienced in the test stand environment. Analytical studies of the

118

effects of flight loads have indicated that the typical first-flight load conditions could cause a loss of 1 percent in TSFC. Projection of the increased level of flight loads that might be experienced as service time increases suggests that the initial level of loss could increase another 1 percent in TSFC by the time 3000 flights have been completed. The results of these analtyical studies are reported in NASA CR-135407 (Ref. 3). The initial 1 percent TSFC loss may occur in the airplane acceptance testing and delivery flight and, thus, may never be seen by the airlines. However, from a technical standpoint, this initial loss represents a real loss of engine performance that might be avoidable if the causitive factors were addressed during the original engine and installation designs and might be recoverable or avoidable in current engines by development of appropriate modifications.

The flight-load-induced deterioration occurs in all of the modules; however, the major impact is in the fan, low-pressure compressor, and high-pressure turbine. The increased gas-path clearances are caused by a combination of mechanical effects, namely, steady state and transient aerodynamic loads, gravity forces, gyroscopic effects, and engine transients, all of which tend to move the rotating blades and seals relative to the stationary case-mounted seals. The resulting rubs open the gas-path clearances. The losses for the most part are estimated to occur early in the engine life and shortly after engine rebuilds. Future engines and engine installations should address these flight load effects.

Further effort is in order to determine how engine thrust and externally induced forces can be more effectively transmitted through and around the engine. This achievement would permit retention of running clearances and lower rates of deterioration.

A Simulated Aerodynamic Load Test program has been initiated to measure and evaluate the effects of simulated aerodynamic loads on gas-path clearances. This program will significantly improve the understanding of the short-term deterioration problem and provide guidance for evaluation of potential solutions.

6.4.3. Performance Loss Due to Erosion

Erosion is the wearing away of airfoil and seal surfaces by the impingement of foreign matter in the gas path, and thus, occurs primarily during ground and near-ground operation. The extent of erosion damage is, therefore, a function of the number of take-offs to which the engine is subjected and the conditions at the airports served. Erosion reduces engine performance in two ways. It blunts and wears down airfoils, thereby reducing their efficiency, and it wears away blade ends and seal surfaces, resulting in increased gas-path leakages.

The documented effects of erosion on compressor airfoils and seals support the need to improve the erosion resistance of these parts. The rubber outer airseals should be replaced with a more erosion resistant material. Nickel graphite, nicrompolyester, or sintered metal materials are all candidates that should be assessed. Elimination of the squealer cut on the sixth-stage compressor blade should be examined to deterimine if it can be done without structural life loss. In the long term, either airfoil material changes or the development of erosion resistant coatings for application to both static and rotating airfoils are required. The development of suitable erosion resistant coatings is estimated to have the most likelihood of early success within reasonable levels of cost. Based on the damage rates and estimated performance losses, coatings for the high-pressure compressor airfoils are the most critical need, followed by application in the fan and low-pressure compressor.

The selection and screening of candidate coatings will take some period of time, and service evaluation testing is required prior to wide spread use of airfoil coatings for performance retention. Active programs currently exist in both areas on other Pratt & Whitney Aircraft engines (JT3D and JT8D) and have been initiatied on the JT9D. These coatings will not eliminate the need to periodically refurbish, replace, or recoat airfoils and seal materials. The potential improvement from coatings and new seal materials is at least a 50 percent increase in the performance life of these parts with an optimistically 100 percent increase.

The control of the quantity of erosive material that enters the compressor through the use of passage shaping is a possibility for foreign object damage control. The size of the particles that cause the bulk of the erosion damage are estimated to be such that passage shaping may have little effect. The use of boundary layer bleeds to remove the erosive material at positions where it tends to concentrate may have a somewhat higher probability of success. These areas will require extensive research and should be investigated until sufficient technical information is available to evaluate both feasibility and cost effectiveness of such concepts. For current in-service engines, the condition of compressor hardware should be monitored and airfoils should be replaced in accordance with a planned engine maintenance schedule.

6.4.4 Thermal Distortion Effects

Thermal distortion effects are primarily twisting, bowing, and soldiering of turbine vanes which results from the basic temperature and stress environment of the turbines and changes to that environment. These turbine environmental changes are caused by changes in the

120

compressor performance, combustor dimensional changes, and fuel nozzle coking with usage which produce changes in combustor exit temperature levels and profiles. The resulting increase in turbine airfoil losses and increased leakages reduce high- and low-pressure turbine efficiencies.

Based on turbine part mechanical conditions, compressor and combustor deterioration appear to cause radial and circumferential changes in temperature patterns into the turbine and cause elevated metal temperatures above the design levels, resulting in thermal distortion of turbine parts. Turbine vane bow results in flow area changes which control the operating lines of the compression systems. Platform curl and vane twist increase the secondary flow losses and reduce efficiency. Higher temperatures near the annulus walls increase running clearances due to the cases and seals running warmer than planned and increase clearances due to differential growth of rotors, seals, and cases.

Fundamental to corrective action is an understanding of the causal factors that produce combustor temperature profile shifts. The data collected and analyzed during the program show that such changes occur and are relatable to clearance changes in the high-pressure compressor, fuel nozzle clogging (coking), and combustor dimensional changes. Component and engine testing is required to quantify the relative importance of these variables prior to making definitive recommendations for design criteria changes. The impact of nozzle coking can be minimized by periodic on-wing fuel nozzle cleaning. This procedure is very effective for removing fuel nozzle coking when periodic cleaning is performed at periods less than 2000 hours.

6.5 RECOMMENDED PROGRAMS

6.5.1 Introduction

The completed efforts in the NASA JT9D Jet Engine Diagnostics Program have accomplished the following:

o Defined the four major causes of performance deterioration and estimated the magnitude of each cause as a function of engine usage,

o Identified the probable cause of engine short-term performance deterioration as flight-load-induced increases in gas-path clearances and established that the losses caused by flight loads most likely increase with usage.

121

o   Identified the relative importance of each deterioration mechanism in each module as a function of usage.

o   Developed analytical models for use in predicting and understanding the deterioration of the engine and engine modules as a function of usage.

o   Identified deficiencies in the current understanding of specific deterioration issues.

On the basis of these findings, several additional efforts or tasks are recommended. These recommended tasks are discussed in this section.

6.5.2 Flight Loads Test Program

The estimated flight-load-induced effects on gas-path clearances are a significant cause of increased fuel consumption with usage. The Simulated Aerodynamic Load Test program has been initiated to increase our knowledge of these effects by measuring the influences of simulated aerodynamic loads on the gas-path clearances. This program, however, cannot measure the influence of transient loads which would be caused by wind gusts, hard landings, and flight maneuvers. To thoroughly understand the effects of flight-induced loads on the engine/nacelle structure and on the various running clearances, a flight test program is needed and recommended. This program would require instrumentation of JT9D engines on a 747 airplane in inner and outer wing positions using instrumentation concepts investigated during the "Feasibility Study of Measuring In-Service Flight Loads" (see NASA CR-135395) (Ref. 4) and derived from the Simulated Aerodynamic Load Test program. This instrumentation would include:

o   Fan, fourth-stage low-pressure compressor, and first-stage high-pressure turbine tip clearance instrumentation;

o   Expanded PIC engine-performance instrumentation;

o   Velocimeters and accelerometers on engines, pylons, and airplane center of gravity (CG);

o   Pressure transducers in the engine inlet cowls.

Thus, forces, accelerations, clearance changes, and performance changes could be measured.

This program would supplement the Simulated Aerodynamic Load Test program and provide the necessary information to fully quantify cause and effect relationships.

6.5.3 Fan Engine Test at Altitude

A number of performance deterioration effects appear to be significant based on the analytical efforts to date but cannot be accurately quantified with the available data. These performance deterioration effects include:

o   The specific effects of erosion induced roughness and/or bluntness on fan airfoil efficiency and flow capacity.

o   The roughness effect on fan/low-pressure compressor flow choking in the low-pressure compressor inlet guide vanes.

o   The precise effect of fan and low-pressure compressor module deterioration at altitude.

o   The effect of specific deterioration mechanisms on off-design performance.

For these reasons, it is suggested that a fan-engine altitude test program be conducted. The program would include a series of tests in an altitude test stand at cruise conditions as well as at sea level. Modules with specific representative levels of deterioration would be tested to measure the effect on the performance of that module and its influence on the performance of the other engine modules. This test program would be very helpful in quantifying the effects of different damage mechanisms on component deterioration and engine performance at cruise altitude.

6.5.4 Engine Diagnostics Program for Use by Airlines

The earlier studies and this study program have shown that with their current performance monitoring, diagnostic, and repair practices, the airlines are not achieving optimum performance recovery. Use of the "JT9D Module Performance Analysis Program", available from Pratt & Whitney Aircraft, could improve the airlines' engine diagnostic capability. This computer program is currently being revised to incorporate data validity checks to reduce analysis uncertainties caused by test data scatter. Still further refinements in airline diagnostic capability can be achieved based on the knowledge gained and to be gained from this JT9D Jet Engine Diagnostics Program.

Further refinement of the engine and module deterioration models, as presented in Section 5.0, is planned following the completion of the current and proposed JT9D Engine Diagnostics Program tasks. These final models will aid in refining the "JT9D Module Performance Analysis Program" for use by airlines to plan engine maintenance based on performance calibrations and historical data on each engine.

123

SECTION 7.0

CONCLUSIONS

The in-service engine performance deteriortion investigation was the second phase of the NASA JT9D Engine Diagnostics Program to be completed. The performance data collected and analyzed included flight, special ground test using a Plug-In Console (PIC), and test stand prerepair and postrepair performance calibrations. The in-service fleet of 32 JT9D-7A (SP) engines in Pan American's fleet of 747 Special Performance aircraft were selected for this investigation. Analysis of these improved data resulted in a refinement of the preliminary performance deterioration models and conclusions. It would be improper, however, to conclude that a simple direct analysis of the data from any one of these three data systems would provide a sound basis for a comprehensive understanding of performance deterioration levels and trends in an engine. Therefore, further refinements of the models and recommendations are planned upon completion of other current and on-going program efforts.

There are a number of major points that could not be resolved from the available data. These points were:

First - The necessary data accuracy in individual engine flight performance deterioration levels was not and cannot be achieved with the installed airplane measurement system. There are several reasons for this limitation. The installed performance measuring system and instrumentation is not sufficiently precise to permit identification of individual engine performance changes. Nonuniform airplane-related effects on the four engines, and possible deterioration in airplane systems affecting the engine, appear to influence the flight performance data.

Second - The analyses of the historical and in-service JT9D-7A(SP) engine data suggest that the various deterioration mechanisms may influence performance differently at altitude than at sea level. Thus, the effect of changes in module condition on the cruise performance of a new or deteriorated engine may have a different influence than on the sea level performance of that engine. The central question that applies to deteriorated engines is the effect of efficiency and flow capacity changes in deteriorated fan and low-pressure compressor modules on cruise TSFC.

Third - Since reduction in fuel flow at cruise, where most fuel is burned, is the obvious goal, further efforts are required to develop an understanding of the cause and effect relationships in module deterioration and their relationship to engine cruise performance deterioration.

The in-service engine study was conducted concurrently with the normal flight operation and maintenance of the Pan American 747SP airplanes. In-flight data were collected with airplane-installed instrumentation and with various airplane systems influencing engine operation. PIC testing was conducted when and where the airplane was available between scheduled flights. Expanded instrumentation prerepair tests were conducted when a repair schedule permitted and when the engine was still in satisfactory condition prior to repair. Engine repairs involved extensive swapping of refurbished and partially refurbished modules to minimize the engine repair "turn-around" time. Thus, the program was conducted in a realistic operating environment. However, there were many factors that influenced the data obtained. In general, the flight data was useful in defining airplane average engine performance trends but was the least accurate data source in identifying individual engine deterioration trends and levels. The test-stand testing provided the most accurate measurement of engine and module performance and performance changes. However, the accurate measurement of small changes in engine and module performance with usage was inhibited by the accuracy of the test-stand instrumentation and calibration processes.

Thus, to obtain the desired understanding of engine performance deterioration required in-depth analyses of the three data systems, knowledge of their limitations, and, finally, a comparison of the results with the historical data study results, with the proper judgemental weighting of each.

From these analyses, it can be concluded that there is no single prime cause of performance deterioration in the JT9D engine. The results have shown the relative dominance of low-pressure compressor and high-pressure turbine deterioration in the short term. However, fan, high-pressure compressor, and low-pressure turbine deterioration increase at a steady rate with usage.

Furthermore, it would appear that flight testing of the airplane by the manufacturer prior to delivery to the operator does not have a significant influence on performance deterioration of the engines. The results indicate that if there was some engine deterioration due to production airplane testing, it was no more than a spare engine might incur in the first few revenue flight cycles.

7.1 OVERALL ENGINE PERFORMANCE DETERIORATION

Engine performance deterioration results from the degradation of the mechanical condition of engine parts. The causes for the degradation in mechanical condition may be categorized into four areas:

o   Flight loads, which cause distortion in the engine cases and produce changes in rotor motions with respect to the cases, the sum of which causes the rotating blades to rub against the seals. The resulting wear on both blades and seals opens gas-path clearances.

o   Erosion of airfoils and outer air seals, causing increased roughness and bluntness, loss of camber, and loss of blade length in airfoils plus the loss of seal material. These effects result in reduced airfoil efficiency and increased blade-to-seal clearances.

o   Thermal distortion of turbine airfoils and cases, caused by extended operation in a high temperature environment plus increases in average temperature and temperature profile with use. This distortion results in flow area changes, increased secondary flow leakage, and increased gas-path clearances.

o   Operator repair practices and rebuild standards, which influence the degree of performance restoration achieved during repair and the rate of subsequent performance deterioration.

The probable role of each cause of performance deterioration as a function of usage has been quantified at both the overall engine and the module level.

7.1.1 Short-Term Deterioration

Estimation of engine performance loss based on sea level PIC data indicates that significant losses occur very early, followed by a more gradual loss over the longer term. A TSFC loss of 1 percent occurs within the first 50 cycles, increasing to 2.2 percent by 1000 cycles. The rapid early loss is due to wearing-in of seals and resulting operating clearances; the longer term loss results from cold section erosion, further clearance increases, and thermal distortion.

TSFC loss in the first 50 cycles is dominated by low-pressure compressor and high-pressure turbine deterioration with smaller, but signficant, contributions from the fan and high-pressure compressor. Over the short term, TSFC losses are nearly equally split between the hot and cold sections and between the high- and low-pressure spools. No significant difference in engine deterioration trends due to wing position is apparent from the data obtained.

7.1.2 Long-Term Deterioration

The 747SP/JT9D-7A(SP) engine prerepair test-stand data "fills the gap" between the PIC data for short-term deterioration results and the airline historic test stand prerepair data for long-term deterioration. These test-stand data also represent a better controlled data source and one in which there is less uncertainty as to module age, since almost all prerepair data represents modules that have had no prior repair. The in-service engine data show an average prerepair TSFC deterioration at 1500 cycles of 3.7+0.7 percent, relative to new production engine level.

Postrepair data for in-service engines show an average TSFC deterioration at 1500 cycles of 2.7+0.7 percent, relative to new production engine level. The 1 percent average TSFC recovery during repair represents mostly high-pressure turbine performance improvement for these moderate time engines. The balance of unrecovered performance losses represents residual unrepaired module damage, particularly in the cold section modules. In some cases, modules have been "swapped" from one engine to another. In many cases where module refurbishment has been performed, previously refurbished modules from other engines have been incorporated. In some cases, postrepair TSFC for individual engines is worse than for prerepair as a result of deteriorated modules from other engines being incorporated during the repair. As a result of these practices, plus the varying levels of rework performed during repair and broader build clearances, optimum performance recovery was not achieved.

7.2 FLIGHT PERFORMANCE DATA

In-flight calibration and ECM data have proven to be of limited value in evaluating engine deterioration. ECM trend curves start at about 50 cycles, and in-flight calibration data begins at about 20 cycles, so neither type of data provides any information about short-term engine deterioration. Nor can any conclusions be drawn concerning individual engine deterioration trends over the long term because of appreciable scatter in ECM and in-flight calibration data. Deterioration averaging for the four engines on an airplane eliminates a considerable amount of scatter, suggesting that airplane systems (for example, nonuniform bleeds) may be influencing individual engine trends. Thus, the usefulness of ECM and in-flight data is limited to indicating gross average long-term deterioration trends.

An average altitude cruise deterioration trend synthesized from PIC data shows good agreement with average ECM and in-flight trends over the long-term when ECM data are referenced to a 100-cycle base line. In addition, since PIC data are collected from zero time, it shows the

absolute magnitude of deterioration which cannot be obtained from flight data alone.

7.3 PERFORMANCE RECOVERABILITY

Analysis of in-service JT9D-7A(SP) engine data indicates that a stabilized average long-term postrepair TSFC level slightly better than the historical data results is being achieved. In-service engine data at 1500 cycles show a postrepair TSFC relative to new production engine performance level of about +2.7 percent compared to a level of about +3.0 percent for the historical data study results.

Analysis conducted previously with "best" airline postrepair module historical levels suggested that average postrepair TSFC relative to new production engine performance level of something less than 2 percent could be achieved on a stabilized long-term fleet average basis. Achievement of this level of performance recovery would require that attention be given to periodic cold section rework, consistent with the performance life of cold section parts. The fan leading edge must be reworked periodically, and considerable attention must be given also to the high-pressure turbine tip clearances during rebuild. High-pressure vane class must be carefully controlled, and the second-stage vane must be reworked to control leakage.

7.4 DETERIORATION MODELS

The "average JT9D" deterioration model presented in Section 5.0 has been shown to agree well with average sea level test data trends from PIC data analyses and historical and JT9D-7A(SP) engine airline test stand data analysis. When considering individual engines of individual airlines, considerable variance from the model can be expected. Individual engine initial build clearances vary, resulting in different production performance levels and rates of deterioration. Individual engine service experience also differs. Once engine rework has begun, the extent of individual module rework varies, resulting in greater prerepair performance variations and making it difficult to project "equivalent unrepaired module cyclic age", upon which the model is based. It should be noted that the model will continue to be refined as additional information becomes available. In particular, further work with the model to reflect the results of the Simulated Aerodynamic Load Test program with respect to flight load effects and short-term deterioration trends is planned.

APPENDIX A

EFFECTS OF BLEEDS-ON VERSUS BLEEDS-OFF OPERATION
ON FLIGHT TRENDS

It has been previously indicated that airplane systems may influence the repeatability of data obtained during cruise operation on a flight-by-flight basis. This was particularly evident with airplane N536PA where wide variations in fuel flow were noted in individual engines over a given period of time while the total fuel flow being used by all four engines remained fairly constant. This is shown on Figure A-1 which presents change in fuel flow at constant EPR versus usage in flight cycles. The base fuel flow used is the average fuel flow of the four engines at 90 flight cycles. It can be seen that all four engines maintain the same relative position out to 90 cycles. By 370 cycles, shifts have occurred with the positions 1 and 2 engines exhibiting a decrease in fuel flow of approximately 1 percent while the positions 3 and 4 engines exhibited an increase of about the same amount. However, the average fuel flow across the wing does not change significantly.
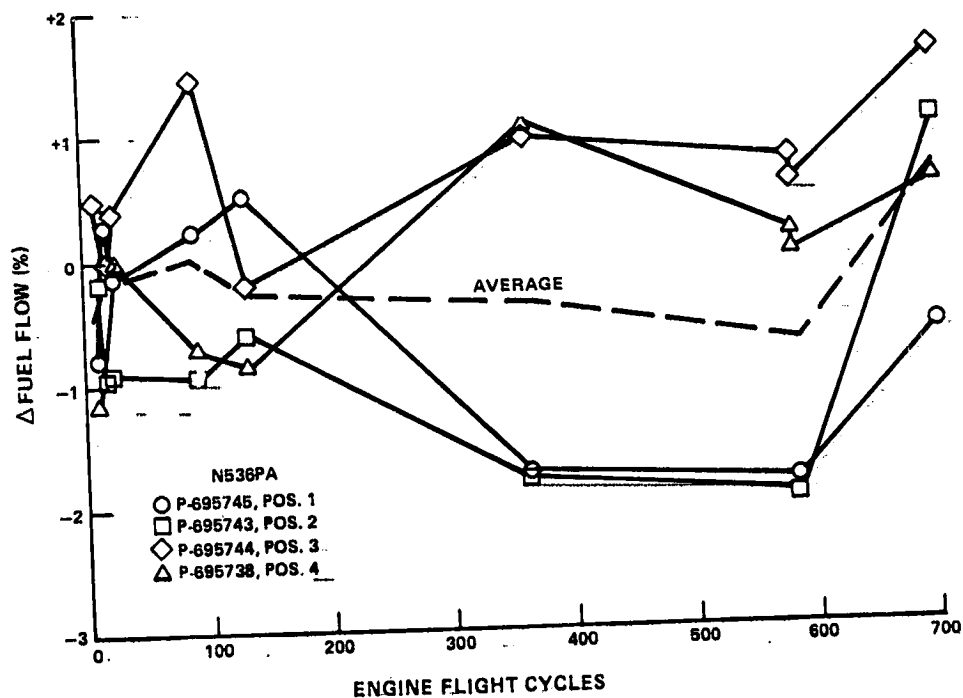
Figure A-1 In-Flight Calibration of Fuel Flow Change as a Function of Cycles at Mach 0.85, 35,000 Feet Altitude, EPR = 1.40 - Wide variations in fuel flow are shown for individual engines while the total fuel flow for all four engines remains fairly constant.

Since these large variations were not noted during the sea level PIC-testing which was accomplished with bleeds closed, one possible explanation for fuel flow variations is bleed hogging by one or two engines, that is, most or all of the service bleed air is being extracted from one or two engines with very little air being bled from the remaining engines. Bleed hogging by one engine or the engines on one side of the airplane can be caused by one or a combination of effects. These effects include:

o Differences in engine performance.

o Improper operation of one of four pylon-mounted bleed control valves.

o Improper operation of one of two wing-mounted bleed isolation valves.

o Leakage anywhere in the bleed system or pneumatic system.

The "differences in performance" effect was the only one of the above effects which we were able to investigate during this program. As part of the in-flight calibrations on both airplanes N536PA and N537PA, additional calibrations were conducted with the pylon-mounted control valve closed on one engine at a time such that it would provide no bleed air over the full power range. A typical comparative plot of fuel flow versus EPR for engine P-695760 (position 1 on airplane N537PA) for bleeds-on and bleeds-off operation is shown in Figure A-2. In the bleeds-on condition, the engine is sharing the bleed air requirement with the other three engines. As seen at low EPR values, there is no fuel penalty due to bleed, inferring that the engine is providing no bleed air. Conversely, at the high EPR settings, the fuel flow penalty due to bleed air is greater than 3 percent. During these calibrations, when the positions 1 and 4 engines operated at low EPR settings the positions 2 and 3 engines operated at high EPR and vice versa. Therefore, when the position 1 engine ran at low EPR with bleeds on, and apparently provided no bleed air, the positions 2 and 3 engines ran at high EPR and provided all of the bleed air. From this nonuniform bleed sharing effect, it can be concluded that when operating four engines, all with bleeds on, those which are developing the highest pressure at the eighth-stage bleed position are delivering the higher proportion of the bleed flow. That is, the better performing engines take the greater fuel flow penalty.

When the effects of uneven pressure drops across the two sets of valves and pressure drops caused by local leakage are added to the nonuniform bleed sharing effect described above, the wide fuel flow variations shown in Figure A-1 are understandable.

132
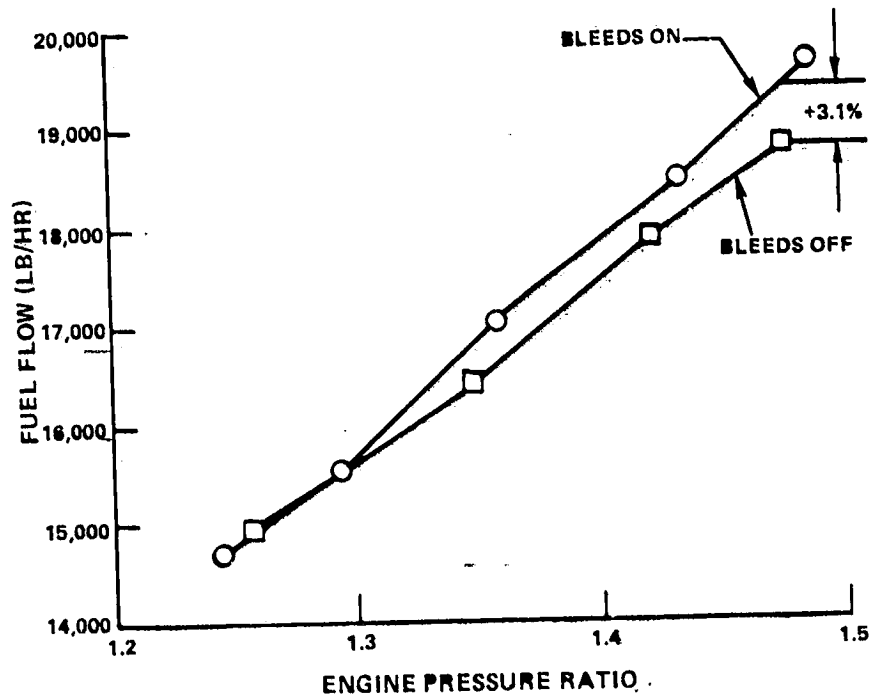
Figure A-2 Bleeds-On/Bleeds-Off Comparison for the Position 1 Engine on Airplane N537PA - Bleed flow penalty is a function of relative pressure at the eighth-stage bleed port.

APPENDIX B

EFFECTS OF FAN AND LOW-PRESSURE COMPRESSOR
FLOW CAPACITY LOSSES ON ENGINE PERFORMANCE

INTRODUCTION

This appendix presents the results of analytical studies of the effects of flow capacity losses in the fan and low-pressure compressor on engine performance losses at both sea level and altitude conditions.

FAN FLOW CAPACITY LOSSES

Early fan deterioration occurs because of increased tip clearance due to flight load-induced deflections and involves a loss in fan flow capacity and efficiency. Fan flow capacity loss is of interest because the effects on engine performance are appreciable, and these effects are considerably different between take-off and cruise conditions.

Reduction in fan flow capacity means that reduced corrected flow is available from the fan at a given corrected rotor speed. In order to match high-pressure compressor corrected flow demand, the low-pressure compressor is forced to a higher operating line. This requirement, plus the lower fan flow, results in a decreased bypass ratio (BPR). The core engine does not have to "work as hard", and turbine inlet temperature is reduced to hold constant engine pressure ratio (EPR). Reduced turbine inlet temperature results in decreased exhaust gas temperaure (EGT) and decreased fuel flow (Wf). Figure B-1 shows the changes in EGT and fuel flow at rated EPR. For a given loss in flow capacity, there is a greater EGT reduction at rated EPR at maximum cruise and maximum climb power than at take-off power. This varying EGT reduction results from a greater BPR decrease for a given flow capacity loss at cruise and climb conditions than at take-off.

At constant thrust conditions, which should be used for meaningful evaluations of thrust specific fuel consumption (TSFC), the BPR decrease which results from loss in fan flow capacity results in a slight decrease in fan airflow. At sea level static take-off, there is essentially no resulting change in fan efficiency (tip clearance increase, by itself, will cause fan efficienty loss, but this analysis considers flow capacity effects only). There is a low-pressure compressor efficiency improvement as a result of the higher operating line, and TSFC decreases slightly, as shown in Figure B-1. However, at maximum cruise and climb power (constant thrust) at altitude, the fan operates closer to choke than at take-off even in an undeteriorated condition due to higher operating corrected airflows at these conditions. When flow capacity is lost as a result of clearance increases, the fan is driven even further toward choke. The result is

a significant loss in fan efficiency. Although low-pressure compressor efficiency improves at cruise and climb power as a result of a loss in fan flow capacity, the loss in fan efficiency is much greater in importance. The result is a significant penalty in cruise and climb TSFC for a loss in fan flow capacity, as shown in the TSFC comparison of Figure B-1. For 2 percent fan flow capacity loss (typical deterioration for high-time fan blades), there is about 0.5 percent improvement in sea level take-off TSFC, about 0.6 percent TSFC penalty at maximum cruise power at altitude, and about 0.8 percent TSFC penalty at maximum climb power. For 4 percent flow capacity loss (extreme fan deterioration), the TSFC penalty at maximum cruise and maximum climb power is much greater than twice the penalty for a 2 percent loss. In other words, the penalty is nonlinear with flow capacity loss.
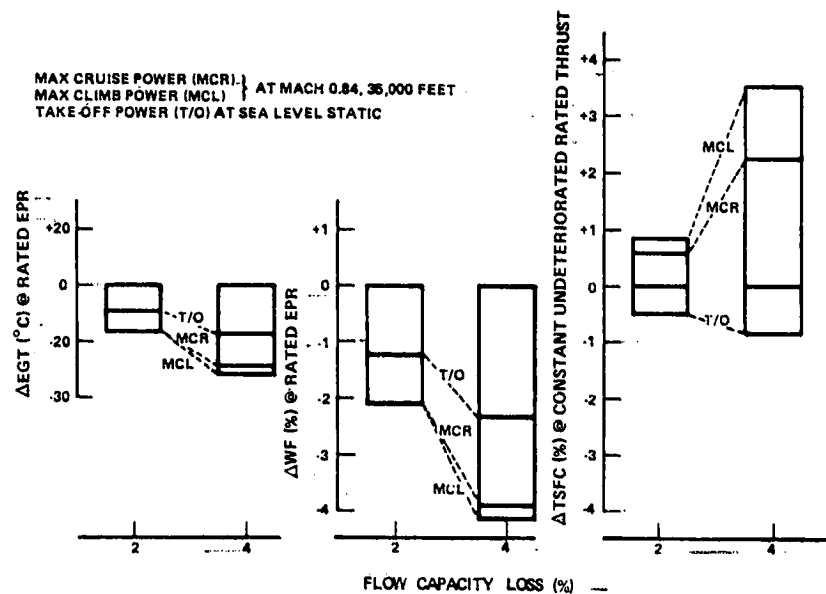
Figure B-1 Effect of Fan Flow Capacity Loss on JT9D Performance Parameters - Increasing flow capacity loss results in a significant penalty in cruise and climb TSFC, although fuel flow at constant EPR decreases.

LOW-PRESSURE COMPRESSOR FLOW CAPACITY LOSSES

Flow capacity for the low-pressure compressor of the JT9D engine has an important influence on engine performance, especially at rated power (climb/cruise) at altitude. The importance stems from the sensitivity of the low-pressure compressor operating line to flow capacity change. Low-pressure compressor flow capacity is influenced by tip clearance changes that occur during service use. Deflections and resulting rubs from the application of flight loads, together with erosion, cause

136

rub-strip wear and tip clearance increases. This condition, in turn, causes low-pressure compressor flow capacity loss. Loss in low-pressure compressor flow capacity causes the compressor operating line (pressure ratio at a given corrected flow) to drop in order to match the high-pressure compressor corrected flow demand. This lowered operating line results in less core flow, higher bypass ratio (BPR), increased exhaust gas temperature (EGT), and performance loss because of compressor efficiency loss. Efficiency loss results from unfavorable incidence angle changes and higher internal Mach numbers.

The importance of low-pressure compressor flow capacity loss is greater at altitude rated power than at take-off power because the compressor operates at higher specific flows and internal Mach numbers at altitude than at take-off. As low-pressure compressor flow capacity is lost, the compressor is driven further toward choke. The result is severe depression of the operating line and efficiency loss, particularly at climb power.

Figure B-2 shows the estimated effect of 2 and 4 percent low-pressure compressor flow capacity loss at sea level static take-off power and at Mach 0.84, 35,000 feet altitude maximum cruise and maximum climb powers. The computer simulation of the JT9D engine, which was used for all of the test stand deterioration analyses of the historical and JT9D-7A(SP) data, was used to estimate the effects of the flow capacity losses. The method of modeling the low-pressure compressor flow capacity changes is presented in Reference 1.
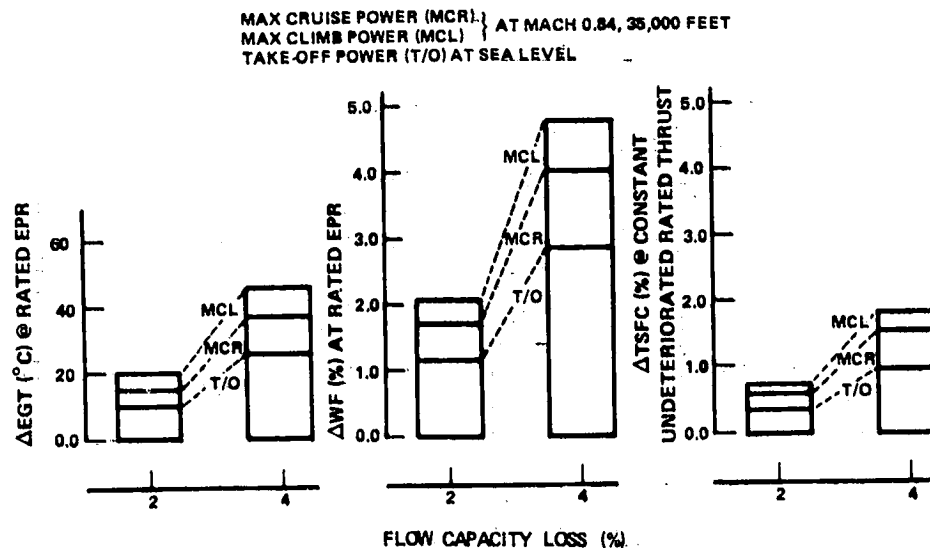
Figure B-2 Effect of Low-Pressure Compressor Flow Capacity Loss on JT9D Performance Parameters - The sensitivity of low-pressure compressor flow capacity loss is not constant but increases with the magnitude of the flow capacity loss.

As shown in Figure B-2, a 2 percent flow capacity loss (corresponding to typical low-pressure compressor tip clearance increase at about 2000 flight cycles) results in about 10°C EGT increase at take-off EPR, 0.3 percent TSFC increase at constant take-off thrust, and 0.6 percent TSFC increase at constant maximum cruise power. Note that fuel flow at maximum cruise power is up about 1.7 percent, much greater than the magnitude of the TSFC increase at maximum cruise power. The reason that the fuel flow increase is much greater than the TSFC increase is that the flow capacity loss results in a thrust increase at constant EPR. It is worthwhile noting again that altitude fuel flow measurements would be a poor indicator of engine TSFC in this case, because the fuel flow change would indicate an engine TSFC deterioration level nearly three times as great as the actual deterioration.

If the low-pressure compressor clearance increase is worse than average, as indicated by the 4 percent flow capacity loss bar in Figure B-2, the performance losses are more than twice as great as for the 2 percent flow capacity loss. In other words, the sensitivity of the low-pressure compressor to flow capacity loss is not constant, but increases with the magnitude of the flow capacity loss.

SUMMARY

It should be noted that in-flight fuel flow measurements at rated power setting are a very poor indication of changes in TSFC at constant thrust, for fan deterioration as well as for low-pressure compressor deterioration. In the case of fan flow capacity loss, not only are the magnitudes of the two parameter changes different, but the directions are reversed.

APPENDIX C

MAINTENANCE DATA COLLECTION

This appendix summarizes the maintenance data which was collected on the 22 Pan American JT9D-7A(SP) engine repairs for which prerepair and/or postrepair tests and detailed analyses were conducted. It also presents a typical description of one of these 22 repairs.

Table C-I lists the maintenance actions by engine serial number and engine removal date. It also lists the removal number, when the engine was repaired, who did the repair, and the type of repair.

These engines received either a Standard 1 or Standard 3 repair. A Standard 1 repair involves all major engine modules including the fan and diffuser/combustor. The individual modules may be refurbished per Standard 1 requirements during the repair action or may be replaced by other modules which have previously been refurbished. Module refurbishment generally includes replacement of air seals. Blades and vanes are either reinstalled as is, repaired, or replaced with new airfoils, depending on the observed condition and/or age. The reassembled modules must meet a set of build standard measurements prior to acceptance. A Standard 3 repair is essentially a hot section repair with limited inspection of the fan and low-pressure compressor.

Table C-II summarizes all of the repairs with total time on the engine, time since the last repair, and prior removal cause. It also identifies the modules in the engine at the time of repair, the type of repair, and which modules were repaired.

Attachment C-1 is a description of a typical maintenance action including a listing of pertinent build-up clearances.

TABLE C-I

PAN AMERICAN 747 SP/JT9D-7A(SP) ENGINES
WHOSE REPAIRS WERE ANALYZED

Engine Serial Number	Removal Number	Removal Date	Repair Completed	Repaired by	Repair Class
686047	1st	11-6-77	12-8-77	PA	Std. 3
686748	1st	12-21-77	2-15-78	PA	Std. 1
	2nd	8-12-78	9-15-78	PA	Std. 3
686049	1st	9-21-78	1-3-79	PA	Std. 1
686050	1st	5-17-78	8-18-78	PA	Std. 1
686053	4th	9-21-78	11-22-78	PA	Std. 1
686054	2nd	5-1-78	5-15-78	PA	Std. 3
686055	2nd	8-31-78	9-19-78	PA	Std. 3
686060	3rd	2-9-78	4-25-78	P&WA	Std. 1
	4th	8-1-78	8-15-78	PA	1st GV *
686068	2nd	9-12-78	11-13-78	PA	Std. 1
686070	2nd	5-28-78	8-18-78	PA	Std. 1
686071	3rd	10-6-78	11-8-78	PA	Std. 3
686083	1st	5-17-77	6-30-77	PA	Std. 3
	2nd	7-12-78	8-30-78	PA	Std. 3
	3rd	11-13-78	11-22-78	PA	1st GV *
686097	3rd	10-8-78	10-25-78	PA	Std. 1
695716	4th	7-6-78	9-29-78	PA	Std. 1
695722	3rd	10-23-78	1-30-79	PA	Std. 1
695727	1st	12-13-77	1-6-78	PA	Std. 3
	2nd	8-14-78	9-16-78	PA	Std. 3
695732	1st	7-10-78	8-31-78	PA	Std. 1
695745	1st	4-20-78	6-13-78	P&WA	Std. 1

* Replaced First-Stage Guide Vane.

TABLE C-II

PAN AMERICAN 747SP/JT9D-7A(SP) ENGINE PREREPAIR AND POSTREPAIR TESTING
SUMMARY OF ENGINE REPAIRS

Engine Serial No.	P-686047	P-686048	P-686048	P-686049
Removal Date	11/6/77	12/21/77	8/23/78	9/21/78
Reason for Removal	HPT distress	HPT distress	High EGT	HPT distress
Prior Removal	5/76	5/76	12/77	5/76
Reason for Prior Removal	Retrofit(1)	Retrofit(1)	HPT distress	Retrofit(1)
Total Engine Hours	7,158	7,675	10,447	11,664
Total Engine Cycles	1,083	1,242	1,642	1,823
Hours Since Last Removal	6,973	7,411	2,772	11,408
Cycles Since Last Removal	9/9	1,101	400	1,686
Engine Configuration/ TSR (2) Prior to Repair:				
LPC Module	A86047/7158	A86048/7675	A86055/2772	A86049/11663
HPC Module	B86047/7158	B86048/7675	B86048/10183	B86049/11663
Combustor Module	Mod 5/6973	Mod 5/7411	Mod 2/2772	Mod 5/11408
HPT Module	C86047/7158	C86048/7675	C95727/2772	C86049/11663
LPT Module	D86047/7158	D86048/7675	D86048/10183	D86049/11663
Repair Type & Module Change (3):				
Fan	Std. 3 Exchanged blades	Std. 1 Exchanged for fan with 1002 cycles	Std. 3 No change	Std. 1 Exchanged fan
LPC	No change	Refurb A86055	Refurb A62968	Refurb A62513
HPC	No change	No change	No change	Refurb B86068
Combustor	New Mod 5 liners and fuel nozzles	New Mod 2 Combustor and fuel nozzles	New liners	Mod 2 Combustor and new NGV
HPT	Refurb C86056(4)	Refurb C95727	Refurb C62373	Refurb C62500
LPT	No change	No change	No change	Refurb D86097
Performance Improvement:				
TSFC (%)	+0.4	-1.4	No Prerepair Test	No Prerepair Test
EGT (°C)	+5.4	+14.3		

(1) Retrofit following use in certification program.
(2) TSR = Time (hours) Since Repair.
(3) Standard 1 is a complete engine refurbishment; standard 3 is a hot section refurbishment.
(4) Refurbished C module (HPT) S/N C86056 was installed.

TABLE C-II (Cont'd)

Engine Serial No.	P-686050	P-686053	P-686054	P-686055
Removal Date	5/17/78	9/21/78	5/1/78	8/31/78
Reason for Removal	High EGT	Cracked exhaust case, high EGT	High EGT	High EGT
Prior Removal	5/76	10/77	12/77	1/78
Reason for Prior Removal	Retrofit(1)	HPT distress	HPT distress	HPT distress
Total Engine Hours	9,823	11,406	9,350	10,925
Total Engine Cycles	1,547	1,757	1,496	1,639
Hours Since Last Removal	9,559	4,580	1,130	2,992
Cycles Since Last Removal	1,406	576	179	418
Engine Configuration/TSR Prior to Repair:				
LPC Module	A86050/9823	A86053/11406	A62513/1130	A86048/2903
HPC Module	B86050/9823	B86053/11406	B86054/9210	B86055/10836
Combustor Module	Mod 5/9559	Mod 2/4580	Mod 5/1243	Mod 2/2903
HPT Module	C86050/9823	C63006/4580	C62377/1130	C62501/2903
LPT Module	D86050/9823	D86053/11406	D86054/9210	D86055/10836
Repair Type & Module Change:				
Fan	Std. 1 Rebuilt	Std. 1 Swapped blades and case	Std. 3 Replaced fan case	Std. 3 No change
LPC	Refurb A62377	Refurb A62387	No change	No change
HPC	Refurb B62473	Refurb B62309	No change	No change
Combustor	New Mod 2 Combustor, Rebuilt NGV	New liners - Refurb NGV	Mod 2 liners installed	Replaced fuel nozzles
HPT	Refurb C86070	Refurb C86040	Refurb C62321	Refurb C62469
LPT	Refurb D62533	Refurb D62400	No change	No change
Performance Improvement:				
TSFC (%)	- 4.8	No Prerepair Test	No Prerepair Test	No Prerepair Test
EGT (°C)	-67.4			

142

TABLE C-II (Cont'd)

	P-686060	P-686060	P-686068	P-686070
Engine Serial No.	P-686060	P-686060	P-686068	P-686070
Removal Date	2/9/78	8/1/78	9/12/78	5/28/78
Reason for Removal	High EGT	High EGT	HPT distress	High EGT
Prior Removal	10/76	2/78	11/77	10/77
Reason for Prior Removal	#2 bearing	High EGT	Surge	HPT distress
Total Engine Hours	6,696	7,816	11,081	10,073
Total Engine Cycles	1,101	1,283	1,670	1,448
Hours Since Last Removal	4,671	1,120	3,931	2,771
Cycles Since Last Removal	653	182	574	329
Engine Configuration/TSR Prior to Repair:				
LPC Module	A86060/6696	A86060/1120	A86068/10922	A86070/9932
HPC Module	B86060/6696	B86060/77816	B86068/10922	B86070/9932
Combustor Module	Mod 5/4671	Mod 2/1120	Mod 2/3772	Mod 2/2630
HPT Module	C86060/6696	C86060/1120	C62381/3772	C62279/2630
LPT Module	D86060/6696	D86060/1120	D86068/10922	D86070/9932
Repair Type & Module Change:				
Fan	Std. 1 Repair blades	Installed 1° open 1st stator	Std. 1 Refurb blades	Std. 1 Refurb blades New case
LPC	Repaired	No change	Refurb A62571 & 1st stator vane	Refurb 62590
HPC	No change	No change	Refurb B86056	Refurb B62469
Combustor	New Mod 2 combustor and new NGV	No change	Refurb diff. case and Mod 2 comb.	Replace liners New NGV
HPT	Rebuilt with new blades	No change	Refurb C62262	Refurb C62350
LPT	Repaired	No change	Refurb D86049	Refurb D85826
Performance Improvement:				
TSFC (%)	-1.8	Prerepair Test Only	No Prerepair Test	No Prerepair Test
EGT (°C)	-9.4			

143

TABLE C-II (Cont'd)

Engine Serial No.	P-686071	P-686083	P-686083	P-686083
Removal Date	10/6/78	5/17/77	7/10/78	11/13/78
Reason for Removal	HPT distress	High EGT	High EGT	High EGT
Prior Removal	9/77	3/76	5/77	7/78
Reason for Prior Removal	Bird strike (FOD)	Retrofit(1)	High EGT	High EGT
Total Engine Hours	8,706	5,100	9,054	10,039
Total Engine Cycles	1,258	770	1,760	1,932
Hours Since Last Removal	2,352	4,939	3,954	985
Cycles Since Last Removal	256	712	990	172
Engine Configuration/TSR Prior to Repair:				
LPC Module	A86071/8588	A86083/4939	A86083/8893	A86083/985
HPC Module	B86071/2234	B86083/5100	B86083/9054	B86050/985
Combustor Module	Mod 5 /2234	Mod 5/4939	Mod 2/3954	Mod 2/985
HPT Module	C86058/2234	C86083/5100	C62317/3954	C62968/985
LPT Module	D62400/2234	D86083/5100	D86083/9054	D62366/985
Repair Type & Module Change:				
Fan	Std. 3 No change	Std. 3 Blended blades	Std. 1 Blended blades	Install 1° open first stator
LPC	Refurb A62282	No change	Rebuilt	No change
HPC	No change	No change	Refurb B86050	No change
Combustor	New Mod 2 liners Refurb NEV, fuel nozzles replaced	New Mod 2 combustor, refurb NGV	Repair combustor new NGV	No change
HPT	Refurb C0324A	Refurb C62317	Refurb C62968	No change
LPT	Refurb D85869	No change	Refurb D62366	No change
Performance Improvement:				
TSFC (%)	No Prerepair Test	-0.4	No Prerepair Test	+ 0.9
EGT (°C)		-5.9		-30.0

TABLE C-II (Cont'd)

	P-685997	P-696715	P-695722	P-695727
Engine Serial No.				
Removal Date	10/8/78	7/3/78	10/23/78	11/14/77
Reason for Removal	High EGT	HPT distress	Combustor liner distress	High EGT
Prior Removal	11/77	12/77	10/77	None
Reason for Prior Removal	HPT distress	HPT distress	HPT distress	
Total Engine Hours	12,170	10,197	12,102	5,579
Total Engine Cycles	1,852	1,710	2,135	1,516
Hours Since Last Removal	4,785	2,454	4,768	—
Cycles Since Last Removal	653	350	243	—
Engine Configuration/TSR Prior to Repair:				
LPC Module	A86007/11954	A62246/2410	A95722/12102	A95727/5579
HPC Module	B86007/11054	B95716/10154	B95722/12102	B95727/5579
Combustor Module	Mod 2/4580	Mod 2/2410	Mod 2/4768	Mod 5/5579
HPT Module	C86053/4580	C62389/2410	C95715/4768	C95727/5579
LPT Module	D86007/11954	D-85071/8766	D95722/12102	D95727/5579
Repair Type & Module Change:				
Fan	Std. 1	Std.	Std. 1	Std. 2
LPC	Refurb blades	No change	No change	Rebuilt
HPC	Refurb A6229?	Refurb A86055 w/2700 hr TSR	Refurb A95731	No change
Combustor	No change	Refurb B62233	Refurb B86054	No change
	Replace liners, Refurb NGV, Fuel nozzles replaced	No change	Repaired inner liner, New outer liner, New fuel nozzles + fuel control	New Mod 2 combustor
HPT	Refurb C52256	Reinstalled C52389	Refurb C52952	Refurb C52294
LPT	Refurb D05727	Refurb D05732	Swapped D05738	No change
	Refurb turbine exhaust case			
Performance Improvement:				
TSFC (%)	No Prerepair Test	No Prerepair Test	-1.3	+0.1
EGT (°C)			-38	-12.8

145

TABLE C-II (Cont'd)

(page 6 of 6)

	P-695727	P-695732	P-695745	P-695743
Engine Serial No.	P-695727	P-695732	P-695745	P-695743
Removal Date	8/14/78	7/2/78	4/20/78	6/18/79 Planned
Reason for Removal	HPT distress	High EGT	High EGT	Planned
Prior Removal	11/77	None	None	7/25/77 Planned(1)
Reason for Prior Removal	High EGT			
Total Engine Hours	8,514	7,652	4,845	9,642
Total Engine Cycles	2,056	2,127	703	1,480
Hours Since Last Removal	2,935			8,561
Cycles Since Last Removal	440			1,339
Engine Configuration/TSR Prior to Repair:				
LPC Module	A95727/8514	A95732/7652	A95745/4845	A95743/9642
HPC Module	B95727/8514	B95732/7652	B95745/4845	B95743/9642
Combustor Module	Mod 2/2935	Mod 5/7652	Mod 5/4845	Mod 2/850
HPT Module	C62294/2935	C95732/7652	C95745/4845	C95743/9642
LPT Module	D95727/8514	D95732/7652	D95745/4845	D95743/9642
Repair Type & Module Change:				
Fan	Std. 3	Std. 1	Std. 1	Std. 1
	No change	Rebuilt with new blades	New OAS	Changed
LPC	Refurb A62230	Refurb A62256	Rebuilt with new seals	Changed
HPC	No change	Refurb B62559	Rebuilt with new seals	Changed
Combustor	New liners	New Mod 2 liners and rebuilt NGV	New Mod 2 combustor and rebuilt NGV	Changed
HPT	Refurb C62306	Refurb C62363	Rebuilt with new 1st stage blades and 2nd NGV	Changed
LPT	No change	Refurb D62294	No change	Changed
Performance Improvement:				
TSFC (%)	No Prerepair Test	-1.2	-1.0	Postrepair data was not analyzed
EGT (°C)		-23.5	-44.5	

(1) Planned removal - results reported in NASA CR-135431.

146

ATTACHMENT C-1

TYPICAL MAINTENENCE ACTION - ENGINE P-695722

Standard 1 Repair, November 1978
12,102 Total Hours; 2135 Cycles

INTRODUCTION

Engine P-695722 was removed from Position 3 on Pan American 747SP airplane N532PA on October 23, 1978 for combustor liner distress. It had operated 12,102 total hours and 2135 flight cycles.

HISTORY

Engine P-695722 was delivered to Pan American installed on 747SP airplane N533PA with 41 hours and 16 cycles in March 1976. In October 1977 the engine was removed due to turbine blade erosion. The Mod 5 combustor, fuel nozzles, and high-pressure turbine were replaced with a Mod 2 combustor, new fuel nozzles, and refurbished high-pressure turbine module C95715. The engine was installed on airplane N533PA where it operated 4768 hours and 848 flight cycles until this removal.

The fan, low-pressure compressor, high-pressure compressor, and low-pressure turbine were the original modules at the October 23, 1978 removal.

PREREPAIR TEST AND TEARDOWN

Before teardown, the engine was prerepair tested at the Pan American Jet Center in the partial QEC condition and, as a result, a Standard 1 repair was ordered. The engine was completely disassembled and all modules were changed.

The Mod 2 inner and outer liners exhibited burn-through of louvers. Heavy carbon deposits were noted in the air caps directly downstream of the swirl vanes.

The first-stage nozzle guide vane (NGV) assembly exhibited airfoil trailing edge cracks adjacent to the outer platform along with burning of the inner buttresses.

The high-pressure turbine was removed, and the first-stage blades were retired due to time.

147

The low-pressure turbine was in generally good condition. The third-stage nozzle guide vanes showed evidence of rub and metal buildup on six vanes.

BUILD-UP

The Standard 1 rebuild included refurbished fan, low- and high-pressure compressors, combustor, and turbines. The recorded build-up results are as follows:

Fan – Refurbished blades and new outer air seals (OAS) were installed. The blade tip/OAS clearance was 0.108 inch.

Low-Pressure Compressor - Refurbished module A95731 was installed with new OAS's. The blade and vane ages were not available, however, this module was first removed from engine P-695731 on December 8, 1978 with 9824 hours and 2239 cycles on the engine and "A" module. The blade/OAS clearances were as follows:

Stage	Clearance (inch)
2	0.086
3	0.052
4	0.042

High-Pressure Compressor - Refurbished module B86054 was installed with new OAS's and repaired blades. The blade tip/OAS clearances were:

Stage	Clearance (inch)	Stage	(Clearance (inch)
5	0.037	11	0.021
6	0.060	12	0.029
7	0.059	13	0.037
8	0.045	14	0.027
9	0.047	15	0.031
10	0.039		

Combustor - The combustor module was rebuilt with a new Mod 2 outer liner, repaired inner liner, new cokeless fuel nozzles, and new first-stage nozzle guide vanes. The inner/outer liner fit and engagement were 0.008 inch tight and 0.388 inch, respectively. The first-stage NGV NCA = 29.5. The TOBI flow was 1.319 percent.

High-Pressure Turbine - Refurbished module C62962 was installed. It had a mixture of three different part numbers in the first-stage blades whose ages were not available. It had new second-stage NGV, with NCA = 23.0, and new second-stage blades. The blade tip/OAS clearances were as follows:

Stage	Clearance (inch)
1	0.0715
2	0.030 (front)
2	0.0415 (rear)

Low-Pressure Turbine - Module D95738, which was removed from Engine P-695738 on January 2, 1979 with 8740 original hours and 1395 cycles was installed without being disassembled.

The engine was postrepair tested and failed due to a faulty fuel control. The engine was then successfully retested with a replacement fuel control on January 30, 1979 and accepted as a serviceable spare.

APPENDIX D

TEST STAND AND INSTRUMENT CALIBRATION

This appendix presents a detailed discussion of the calibration of the Pan American expanded-instrumentation test stand as to calibration standards, procedures and results. It also discusses the uncertainties in recorded data and how the uncertainty values were determined.

D.1 CALIBRATION STANDARDS

Pressures

Wallace and Tiernan, Model 65-120, 0 to 100 in. HgA calibrator for Pt7, Pt3c, and Ps3c.

Wallace and Tiernan 0 to 1000 in. HgG gage for Ps4 and Ps5i.

Wallace and Tiernan 26 to 31.5 in. HgA gage for barometer and Pcd (cell depression).

A compressed-air regulated pressure source is used for calibrations. The 30 in. water U-tubes used for Pt2 and cell static measurements are zeroed and checked prior to each engine test.

Temperatures

The chromel-alumel thermocouple system (Tt3, Tt4, Tt6, and Tt7) was calibrated with a Leeds and Northrup Model 8686 millivolt source. All temperatures were recorded through a Doric Model 400 digital indicator and Doric ten-channel select switches. The Tt2 inlet temperature resistance probes and Doric DS-100-TS indicator were calibrated with a decade box and resistance harness. The probes were also checked with a glass-bulb mercury thermometer held next to the probes.

Thrust

The Baldwin Lima Hamilton (BLH) 50,000 lb working load cell was calibrated against an identical master load cell in the thrust system. A hydraulic ram supplies the necessary force to the load cell system for calibrations. All calibrations were conducted with an engine mounted in the test stand. The master load cell is removed from the load cell system during engine testing. The master load cell and indicator were also crosscalibrated at BLH and Pratt & Whitney Aircraft.

Frequency

The N1 and N2 speed and fuel flow Hewlett Packard HP5214L varaible time base counters were calibrated using Hewlett Packard master counter frequency generators. (Note: the speed counters were changed to Digitec Model 8151 units in September 1978.)

Fuel Flow

The Cox ANC-16 flow meters were calibrated at Pan American, using the Cox Instruments Calibrator, and at Pratt & Whitney Aircraft. Pan American has two Cox flow meters available; one is normally employed in the test stand, and the second is retained as a back-up.

Fuel Density

The specific gravity measurements were obtained from an in-line hydrometer in the fuel line as well as with a second hydrometer and a fuel sample drawn from the fuel line. No calibrations of the hydrometers were available.

D.2 CALIBRATION PROCEDURES

Pan American does not employ any written procedures or calibration data recording forms for the test stand instrumentation with the exception of the Cox fuel flow meters. Typically, the calibration procedures consisted of comparing the working instrument to a reference instrument of equal accuracy and adjusting the working instrument until it is within the desired tolerance. The reference instruments are kept in the Instrumentation Laboratory and brought to the test stand when required. The master thrust load cell remains at the test stand, and the Cox Instruments Calibrator remains in the Instrumentation Laboratory.

The absence of written calibration procedures, particularly with respect to data retention, was the most difficult area of the evaluation. Pan American personnel perform the instrument calibrations and report any abnormalities for corrective action. They are very conscientious concerning the maintenance of the equipment on the test stand and in the calibration laboratory. However, the procedures involving the calibration results are essentially verbal. Written records of the calibrations are not normally retained beyond the date of calibration. Thus, developing uncertainty estimates for the performance measurements was dependent upon data recorded by Pratt & Whitney Aircraft personnel who were present during the calibration process.

152

D.3 CALIBRATION RESULTS

During the program, the Pan American test stand instrumentation was
subjected to four complete calibrations. On three occasions, Pratt &
Whitney Aircraft personnel observed the calibration procedures and
recorded the data. On one calibration by Pan American personnel, no
data were recorded. For that calibration, it was assumed that the
instrumentation was within the Pratt & Whitney Aircraft T.I.S. accuracy
limits.

The results of the calibrations are summarized on Table D-I. The errors
presented are the average deviations from the calibration standard over
the range of calibration for each instrument.

TABLE D-I

PAN AMERICAN TEST STAND CALIBRATION RESULTS

Parameter	Instrumentation, Range, or Units	May 1977	Feb. 1978	June 1978	Jan. 1979
P breather	0 to 40 in. HgG	-0.44	+0.41		-0.05
Pt7	0 to 100 in. HgA	-0.08	-0.05		+0.11
Pt3c	0 to 100 in. HgA	-0.11	-0.10		-0.31
Ps3c	0 to 70 in. HgA	-0.02	0.00	Not Recorded	+0.02
Ps5	0 to 1000 in. HgG	-0.55	+2.00		+1.00
Ps4	0 to 1000 in. HgG	-0.80	+1.00		+1.00
Barometer	26 to 31.5 in. HgA	-0.015	-0.01		-0.02

(All above pressures on Wallace & Tiernan Gages).

Parameter	Instrumentation, Range, or Units	May 1977	Feb. 1978	June 1978	Jan. 1979
Tt3, Tt4, Tt6, Tt7	Doric Model 400 Indicator, °C	-3	+1	Not Recorded	+6 *
Tt2	Resistance Sensors, Doric Indicator, °F	+1	+2	Not Recorded	+1
Thrust	BLH 50,000 lb Load Cell, lb force	— -60	-30	-50	-50
N1, N2 Speeds	Hewlett Packard Counter, rpm	+1	+1	Not Recorded	+1
Fuel Flow	Hewlett Packard Counter (only), pph	+1	+1	Not Recorded	+1

* Zero offset corrected on calibration.

Actual calibrations were not performed on the Pt2 or cell static pressures which were recorded on 30-inch water U-tubes. The U-tubes were zeroed and checked prior to engine testing. The chromel-alumel thermocouple system records all Tt3, Tt4, Tt6, and Tt7 measurements through the same Doric indicator. The individual temperature parameters can be calibrated from the engine location or at the back of the Doric unit. The Pan American procedure has generally been to apply the calibration signals at the back of the Doric unit over the range of exhaust gas temperature (EGT) (Tt6). Any adjustments are then applied on the basis of the EGT calibration. This procedure is valid, since all of the indicated parameters are recorded through one Doric unit, but can miss any errors that might be introduced by the stand wiring for each parameter.

During the period of this program, Pan American completed modifications to the test stand to accomodate RB211 engine parameters. The speed measurement systems, which had employed Hewlett Packard HP5214 counters, were changed to Digitec Model 8151 variable time base counters in September 1978. Problems were encountered with the new systems due to wiring malfunctions which caused a +60 rpm error in N1 and N2 measurements. This error existed during September to October 1978 and again in January 1979.

D.3.1 Thrust System Calibratons

The Pan American BLH 50,000 lb thrust system was calibrated versus a 60,000 lb transfer standard Interface Force Measurement System, traceable to the National Bureau of Standards. Multiple calibrations were performed during the three occasions that the thrust system was available to Pratt & Whitney Aircraft in order to assess the system's repeatability. All calibrations were performed as-is, that is, with no adjustments except for electrical checks of the system's zero and R-cal (span) values. A summary of the calibration errors (thrust system output minus applied calibration load) are presented on Table D-II. The errors are averaged at each calibration point over the total number of calibrations performed. The overall average error and the maximum observed error are also presented for each calibration period.

The last primary calibration of this thrust system performed by the manufacturer (BLH) was dated September 1976 and indicated a maximum 5 lb error. The thrust calibrations conducted at Pratt & Whitney Aircraft indicated that in March 1978 the master-load cell errors relative to the Interface Standard were negative, while the other two calibraions showed positive errors. The Interface Standard was checked for possible shifts, but none was found.

154

TABLE D-II

SUMMARY OF PAN AMERICAN THRUST SYSTEM CALIBRATIONS
BY PRATT & WHITNEY AIRCRAFT

Calibration Load (lb)	Error (lb) June 1977 (2 calibrations)	Error (lb) March 1978 (12 calibrations)	Error (lb) January 1979 (5 calibrations)
0	2	0	2
10,000	20	7	24
20,000	35	6	44
30,000	42	1	56
40,000	45	-12	61
50,000	35	-33	59
30,000	--	-18	54
10,000	--	-12	18
0	--	-7	-3
Average Error (lb)	30	-7	35
Maximum Error (lb)	50	-33	95

D.3.2 Fuel Flow Meter Calibrations

Two Pan American Cox turbine flow meters, serial numbers 23275 and 23276, were calibrated in the Pratt & Whitney Aircraft Fuel Flow Laboratory against a Cox ANC-16 11596 reference meter as a secondary standard. The calibrations were conducted with two fluids (Jet A and 9041) to compensate for viscosity effects. The calibrations produced curves of cycles per gallon (CPG) versus cycles per second divided by viscosity (CPS/) for each meter. (Pan American does not use a viscosity correction.) The average CPG values over the 120 to 1200 CPG range were used as a basis of comparison since it is the average CPG values that are used to determine the preset values for the Hewlett Packard variable time base counters in the Pan American test stand. The results of the fuel flow meter calibrations are shown on Table D-III for meter number 23275.

For meter number 23275, the calibrations at Pratt & Whitney Aircraft indicated a shift of -0.06 percent of reading for Jet-A fuel and -0.03 percent of reading for 9041 fuel. The 1977 comparison of the Pan American calibrations showed a difference of +0.065 percent of reading from the Pratt & Whitney Aircraft results. The 1978/1979 comparison indicated that the Pan American results were higher by +0.16 percent of reading. The Pan American calibrations alone showed a +0.05 percent of reading increase.

TABLE D-III

CALIBRATION RESULTS FOR COX METER NO. 23275

	Average CPG		
Calibration Date	Type II Fuel	Jet-A Fuel	9041 Fuel
April 1977 (Pan Am)	1518.4	1517.0	1517.8
May 1977 (P&WA)			
December 1978 (Pan Am)	1519.2	1516.1	1517.3
January 1979 (P&WA)			

Cox Meter number 23275 has been utilized by Pan American as the primary performance measurement instrument.

The results of the fuel flow meter calibrations for meter number 23276, which was used as a back-up fuel meter, are shown on Table D-IV.

TABLE D-IV

CALIBRATION RESULTS FOR COX METER NO. 23276

	Average CPG			
Calibration Date	Fuel Blend	Type II Fuel	Jet-A Fuel	9041 Fuel
August 1975 (Cox)*	1514.8		1513.2	
November 1975 (P&WA)*				
April 1977 (Pan Am)	1510.4			
April 1977 (P&WA)			1506.5	1507.8
March 1978 (P&WA)			1509.7	1508.5

* Conducted prior to the current program.

Comparison of the 1975 and 1977 calibrations indicates that a significant shift had occurred in this meter. The magnitude of the shift ranged from -0.29 percent of reading, based on the Pan American calibration, to -0.55 percent of reading based on the 1977 P&WA calibration versus the original Cox Instruments calibration. The shift in the average CPG introudced a corresponding incraease in the fuel flow measurements with this meter.

Comparison of the 1977 Pan American and P&WA calibrations indicated that Pan American was higher by +0.17 percent of reading in the average CPG value. The 1978 P&WA calibrations indicated a shift of

156

+0.21 percent of reading using 9041 fuel. These 1978 results were closer to the 1977 Pan American results, +0.09 peracent of reading on the average.

Differences can exist between the Pan American and Pratt & Whitney Aircraft calibrations due to the calibration standards and techniques employed. Pratt & Whitney Aircraft employs a Cox reference flow meter in series with the working meter. The calibration accuracy for this technique is +0.1 percent of reading. The Cox Instruments Calibrator employed by Pan American has a specified accuracy of +0.15 percent of reading. Evaluation of the Pan American calibrations indicates that there is more scatter in the data, +0.5 percent of reading over the 120 to 1200 CPS range, than is evident in the P&WA calibrations. The larger scatter probably is related to the calibration techniques and could result in variations in the average CPG value between calibrations.

Table D-V presents a summary of the fuel flow meter calibration results.

D.4 UNCERTAINTIES OF MEASUREMENTS AT PAN AMERICAN TEST STAND

The development of the measurement uncertainties for the Pan American test stand relied upon the periodic on-stand instrument calibrations and the laboratory calibrations at Pratt & Whitney Aircraft. The disadvantage of calibrations of these types is that instrument errors can be determined only over long time intervals. Even if the calibrations were conducted in detail, recording all pertinent data, short-term errors which could occur between calibraions would not be identifiable unless they were of extreme magnitudes. It is the short-term errors which influence the performance measurements for engines passed through the test stand between calibration intervals. The analyses of the instrument calibrations can provide an estimate of the error bounds possible but cannot account for short-term excursions beyond those bounds.

The available Pan American data, specifically the on-stand calibrations, were not generally recorded in detail. The instruments were not adjusted if they fell within the Pratt & Whitney Aircraft T.I.S. tolerances; when the deviations relative to the calibration standard were not recorded, the long-term uncertainties were assumed, based on the calibration tolerances. Where actual calibration data were available, the uncertainties were calculated. Another problem is related to the measurement of as-is errors before the instruments are adjusted to the prescribed tolerances. The as-is errors provide an indication of how much drift has occurred since the last calibration date. Not recording the as-is errors eliminates information that is useful in assessing the total measurement uncertainties.

157

TABLE D-V

SUMMARY OF FUEL FLOW METER CALIBRATION RESULTS

METER SERIAL NO. 23275:

Cycles per Gallon (CPG)

CPS	Pan Am April 1977	P&WA, May 1977 Jet-A	9041	Pan Am Dec. 1978	P&WA, January 1979 Jet-A	9041
120	1519.7	1522.3	1522.2	1517.5	1520.9	1520.1
180	1515.8	1518.9	1519.8	1515.2	1518.6	1518.5
240	1518.9	1516.1	1517.9	1519.8	1516.2	1517.6
360	1523.5	1515.8	1516.4	1519.8	1514.9	1516.6
480	1520.4	1515.4	1516.6	1519.8	1514.9	1516.4
600	1518.1	1515.3	1516.2	1521.3	1514.6	1516.2
1200	1517.4	1515.1	1515.7	1521.3	1513.8	1515.9
Average CPG	1518.4	1517.0	1517.8	1519.2	1516.1	1517.3

METER SERIAL NO. 23276:

Cycles per Gallon (CPG)

CPS	Cox Aug 1975	P&WA Nov 1975	Pan Am Apr 1977	P&WA, April 1977 Jet-A	9041	P&WA, March 1978 Jet-A	9041
120	1519.9	1514.0	1504.3	1507.2	1509.6	1512.9	1509.4
180	1514.3	1511.1	1509.9	1505.8	1508.4	1511.2	1508.2
240	1513.5	1512.6	1506.8	1504.7	1507.2	1509.3	1507.0
360	1513.1	1513.0	1512.2	1505.2	1507.1	1508.6	1507.4
480	1513.9	1512.9	1510.4	1506.3	1508.3	1508.4	1508.3
600	1514.3	1513.2	1512.2	1506.9	1509.2	1508.6	1508.9
900	1515.1	1514.1	1515.3	1507.8	1509.2	1509.3	1509.3
1200	1514.3	1514.9	1512.0	1508.1	1509.4	1509.4	1509.5
Average CPG	1514.8	1513.2	1510.4	1506.5	1507.8	1509.7	1508.5

To develop the statistical estimates of the Pan American uncertainties, the calibration performed in June 1978 was included in the analysis. Since no data were recorded, an estimate of the probable calibration error was made by calculating the mean of the three calibrations where data were

recoraded and employing that value as the June 1978 error for each instrument. This method will not alter the final bias error, but it will provide an estimate of the possible precision error over four calibraion intervals.

Bias error terms were calculated by summing the observed calibration errors and the calibration tolerances, where necessary, over the four on-stand calibrations to produce an average bias for each parameter as defined by Equation (1). Standard deviations were calculated using the calibration errors and calibration tolerances according to Equation (2). In order to obtain a precision error estimate at the 95 percent confidence level, the results from Equation (2) were multiplied by the t-statistic for a two-sided estimate (t.975) based on the degrees of freedom involved. For this analysis, the degrees of freedom equalled the number of calibrations (4) minus one.

$$\text{average bias } (\overline{x}) = \sum_{i=1}^{n} \frac{(x_i)}{n} \qquad \text{Equation (1)}$$

$$\text{standard deviation (s)} = \sum_{i=1}^{n} \frac{(x_i - \overline{x})^2}{n-1} \qquad \text{Equation (2)}$$

where: n = number of on-stand calibrations, and
   x_i = calibration error (observed error or tolerance).

The total uncertainty for each parameter is the arithmetic sum of the average bias and precision errors. The uncertainties for the measured parameters are then: $\overline{x}$ + ts, where t is the t.975 statistic for the degrees of freedom involved. (For four stand calibrations, the t statistic for n - 1 = 3 degrees of freedom is 3.182.)

The Pan American uncertainties are presented in the following sections. Calibrations where no data were recorded are so indicated.

D.2.1 Pressures

Parameter	May 1977	Feb. 1978	June* 1978	Jan. 1979	Uncertainty Bias	Uncertainty Precision
P breather (0 - 40"HgG)	-0.44	+0.41	-0.027	-0.05	-0.027	+1.10
Pt7 (0 - 100"HgA)	-0.08	-0.05	-0.07	+0.11	-0.07	∓0.28
Pt3 (0 - 100"HgA)	-0.11	-0.10	-0.17	-0.31	-0.17	∓0.31
Ps3 (0 - 70"HgA)	-0.02	0.00	0.00	+0.02	0.00	+0.052
Ps5 (0 1000"HgG)	-0.55	+2.00	+0.81	+1.00	+0.81	∓3.34
Ps4 (0 - 1000"HgG)	-0.80	+1.00	+0.40	+1.00	+0.40	∓2.70
Barometer (26 - 31.5"HgA)	-0.015	-0.01	-0.015	-0.02	-0.015	±0.013

* No data recorded. The estimated error is the mean of the three remaining calibrations where data were available.

D4.2 Temperatures

Parameter	May 1977	Feb. 1978	June* 1978	Jan. 1979	Uncertainty Bias	Uncertainty Precision
Tt3, Tt4, Tt6, Tt7 (^oC)	-3	+1	+1.33	+6	+1.33	+11.7
Tt2 (^oC)	+1	+2	+1.33	+1	+1.33	∓ 1.5

* No data were recorded. The June 1978 error is the mean of the three available calibration errors.

The high precision error of the Tt3, Tt4, Tt6, Tt7 temperature system is due primarily to the +6^oC error exhibited during the January 1979 calibration. The error was a zero shift, that is, a constant error from 0 to 1300^oC. However, the temperature system was calibrated for a Rolls Royce RB211 engine correlation program in December 1978, and, although the data were not supplied to Pratt & Whitney Aircraft, it was indicated that the system was within +1^oC at that time. The zero shift thus occurred within one month and should have affected relatively few engines. The precision error of about +12^oC is therefore a pessimistic estimate of the systems performance. Using only the May 1977 error, based on the average of the two available calibrations, the errors for the Tt3, Tt4, Tt6, and Tt7 measurements would be:

Bias = -2^oC
Precision = ±4.3^oC

160

D4.3 Thrust

The thrust uncertainties were derived from the results of the on-stand calibrations of the working thrust system and laboratory calibrations of the master thrust system. The on-stand calibrations indicate the deviation of the working system from the master, and the laboratory calibrations indicate the deviation of the master from a reference standard. The thrust system calibrations are analyzed separately, and the resulting bias and precision error terms are combined to yield the total thrust uncertainty.

Thrust System	May 1977	Feb. 1978	June 1978	Dec. 1978	Uncertainty	
					Bias	Precision
Working System (1b)	-60	-30	-50	-50	-48	+40

	June 1977	March 1978	Jan. 1979	Uncertainty	
				Bias	Precision
Master System (1b)	+30	-7	+34	+19	+99

Uncertainty	Bias	Precision	Total
Total Thrust Measurement Error (1b)	29	+107	+136

The total uncertainty also contains an additional +5 lb precision error due to the resolution of the thrust system indicator.

The uncertainties were calculated based on the average errors recorded during each calibration period. Also, the precision error of the master system was calculated using a t.975 statistic of 4.30 bacause only three calibrations, (degrees of freedom = 2), were involved.

D4.4 Speeds

The on-stand calibrations performed on the N1 and N2 speed counters have consistently shown them to be within +1 rpm of the input calibration signals. Based on the specifications for the Leeds and Northrup frequency generator used for calibrations, the Hewlett Packard Model 5214L counter, and the engine rpm transmitters, a more realistic estimate of the speed uncertainties would be:

Instrument	N1 Speed		N2 Speed	
	Bias	Precision	Bias	Precision
Leeds and Northrup Generator (rpm)	±1		±1	
Hewlett Packard Counter (rpm)	±4		±6	
Speed Transmitters (rpm)		±1		±4
Total (rpm)	±4 *	±1	±6 *	±4

* Total bias and precision errors are each determined by the root-sum-square (RSS) approach.

Pan American has changed to Digitec 8151 counters, and no accuracy specifications for these units have been received.

D4.5 Fuel Flow

The fuel flow uncertainty is a function of the Cox meter, the frequency counter, and fuel specific gravity measurements. On-stand calibrations have checked only the response of the frequency counter. The specific gravity measurements were obtained from the on-line hydrometer and were cross-checked by Pan American on several occasions using a separate fuel sample and hydrometer.

The laboratory calibrations of the two Cox meters did identify a 0.55 percent of reading shift in the serial number 23276 meter at the beginning of the program. However, this meter is the back-up meter, and serial number 23275 meter was used as the primary performance measurement instrument. Calibrations of meter 23275 have shown it to be very stable throughout the engine testing conducted under this program.

Based on the available calibration data and observations of the Pan American fuel flow system, the estimated uncertainty in fuel flow measurements is as follows:

	Bias	Precision
Working Meter (% Reading)	±0.10	±0.25
Pan American Cox Calibrator (% Reading)	±0.15	
Specific Gravity (% Reading)		±0.15
Total (% Reading)	±0.18	±0.28

Total Uncertainty (% Reading) = ±0.46

162

The error contribution of the frequency counter is assumed to be negligible.

The fuel flow uncertainty, as compared to the other parameters, was not developed from calibration data. Only two calibrations per meter were performed at Pratt & Whitney Aircraft which was not considered to be adequate for development of rigorous statistical conclusions. However, even considering the differences between Pan American and Pratt & Whitney Aircraft in calibration techniques and fuel types, the results were in good agreement. Therefore, the fuel flow uncertainties were based on Pan American's ability to calibrate and utilize their fuel flow system.

D4.6 Parameter Total Uncertainties

Table 3.2-I. is a summary of the total uncertainties derived for each performance parameter. The total uncertainties for the Tt3, Tt4, Tt6, and Tt7 measurements of +6 to $\pm13^{\circ}C$ reflects the error contribution of the January 1979 calibration of $6^{\circ}C$. The lower uncertainty does not include that $6^{\circ}C$ error, and the higher uncertainty does include that error.

D4.7 Comments

The uncertainties quoted in Section 3.2.4 are based on the calibration data acquired from the Pan American test stand over a period of approximately two years. As such, the uncertainties in this document should not be compared to those in the report on the historical data analyses, CR-135448 (Ref. 1), of the JT9D Jet Engine Diagnostics Program which utilized instrument specifications as estimates for the measurement uncertainties. One test stand instrument calibration was available for those historical studies, but it was not used to estimate the total uncertainties. The uncertainties presented in this document represent the long-term bias and precision errors exhibited by the Pan American instrumentation. They are intended to provide realistic error bounds for estimating the most probable error of a given parameter at any point in time with 95 percent confidence.

APPENDIX E

QUALITY ASSURANCE

Individual and joint Pan American and Pratt & Whitney Aircraft quality assurance programs provided the policy and methodology for achieving validity in all the data gathering efforts in this in-service engine performance deterioration study. These programs included correlation of the Pan American test stand, calibration of performance instrumentation, and measurement of assembled gas-path clearances.

Pan American standard procedures were used for the following tasks:

o Recording of flight performance data;

o Calibration of installed aircraft instrumentation;

o Measuring and recording data relevant to engine repairs at the Pan American Jet Center including: part and module histories; part, module, and engine repair; part replacement; and pertinent engine build-up dimensions and clearances.

These procedures are all part of the Federal Aviation Administration (FAA) approved Pan American Maintenance Program.

Pratt & Whitney Aircraft standard quality assurance programs were used for the following tasks:

o Measuring and recording engine initial production performance levels;

o Measuring and recording data relevent to engine repairs at Pratt & Whitney Aircraft including: part, module, and engine repair; part replacement; and pertient engine build-up dimensions and clearances;

o The Plug-In Console (PIC) installed engine performance measurement system and the periodic calibration of all components of this system (the PIC data components were calibrated to instrument standards six times over the period of this program);

o Correction of Engine Condition Monitoring (ECM) data to standardized values of change in performance.

o Reduction of in-flight calibration data to a standard set of conditions.

Pratt & Whitney Aircraft and Pan American jointly conducted measurement and calibration of systems in the following areas that were unique to this program:

o Calibration of the expanded test stand instrumentation (three sets of calibrations of the Pan American test stand were conducted during the period of this program);

o Back-to-back (Pratt & Whitney Aircraft, Middletown/Pan American Jet Center) engine testing to establish corrections between the different test stands used in the program (Test Stand Correlation Testing).

The above combination of quality assurance procedures were used to obtain high quality input data required to detect the changes in engine and engine-module performance with usage.

APPENDIX F

ACRONYMS AND SYMBOLS

ACRONYMS (Organizations)

AA	American Airlines
BCAC	Boeing Commercial Airplane Company
DAC	Douglas Aircraft Company
NASA	National Aeronautics and Space Administration
NW	Northwest Airlines
PA	Pan American World Airways
P&WA	Pratt & Whitney Aircraft
TBC	The Boeing Company
TW	Trans World Airlines
UA	United Airlines

SYMBOLS

A	Area (square feet)
ASG	Axial skewed groove
ATM	Assumed temperature method
BLH	Baldwin Lima Hamilton (thrust cell)
BPR	Bypass ratio
CDX	Control differential transformer
CPG	Cycles per gallon
ECM	Engine condition monitoring
Eff	Efficiency (percent)
EGT	Exhaust gas temperature (^{o}C)
EPR	Engine pressure ratio
F	Engine thrust (pounds)
FC	Flow capacity
FOD	Foreign object damage
FP	Flow parameter
HPC	High-pressure compressor
HPT	High-pressure turbine
IAS	Inner air seal
ID	Inside diameter
K	Kilo (10^3)
LE	Leading edge
LHV	Lower heating value
LPC	Low-pressure compressor
LPT	Low-pressure turbine
Mn	Mach number

SYMBOLS (Cont'd.)

Mod	Modification
N	Rotor speed (rpm)
NASTRAN	NAsa STRuctural ANalysis computer program
NCA	Nozzle equivalent (flow) area
NGV	Nozzle guide vane
OAS	Outer air seal
OD	Outside diameter
P	Pressure (lb/in^2) (psia)
PIC	Plug-In Console (test system)
PLA	Power lever angle (degrees)
PR	Pressure ratio
QEC	Quick engine change (built-up engine/nacelle)
SLS	Sea level static
SP	Special Performance (Boeing 747SP airplane)
T	Temperature (^oF) (^oC)
TE	Trailing edge
TIS	Test Information Sheets
T/O	Take-off
TOBI	Tangential onboard injection system
TOGW	Take-off gross weight (pounds)
TSFC	Thrust specific fuel consumption (lb/hr-lb)
TSR	Time since repair
W	Mass flow (lbm/sec)
W	Flow rate (fuel) (pounds/hour) (%)
WC	Flow capacity
β	Vane angle (degree)
Δ	Change
δ	Pressure correction (in. Hg/29.92)
η	Efficiency (percent)
θ	Temperature correction $(^oR/519)$
μ	Micro (10^{-6})

SUBSCRIPTS *

1	Undisturbed inlet (pressure and temperatures)
1	Low-pressure rotor (rotor speeds)
2	Fan inlet (pressures and temperatures)
2	High-pressure rotor (rotor speeds)
2.4	Fan blade discharge

* For simplicity, subscripts may be written "on the line" of type, especially in text.

SUBSCRIPTS (Cont'd.) *

2.6	Fan exit guide vane discharge
3	LPC discharge
4	HPC discharge
5	HPT inlet
6	HPT discharge
7	LPT discharge
amb	Ambient
b	Burner
bar	Barometric
F, f	Fuel
JE	Jet (primary stream)
N, n__	Net
s	Static
T, t	Stagnation (total)

* For simplicity, subscripts may be written "on the line" of type, especially in text.

REFERENCES

1   Sallee, G. P.: Performance Deterioration Based on Existing (Historical) Data. NASA CR-135448, 1978.

2   Bouchard, R. J., Beyerly, W. R., and Sallee, G. P.: Short-Term Performance Deterioration in JT9D-7A(SP) Engine 695743. NASA CR-135431, 1978.

3   Jay, A and Todd, E. S.: Effect of Steady Flight Loads on JT9D-7 Performance Deterioration. NASA CR-135407, 1978.

4   Sallee, G. P. and Martin, R. L.: Expanded Study of Feasibility of Measuring In-Flight 747/JT9D Loads, Performance, Clearance, and Thermal Data. NASA CR-159717, 1979.

PRECEDING PAGE BLANK NOT FILMED